Master's thesis

NTNU
Norwegian University of Science and Technology
Faculty of Information Technology and Electrical Engineering
Department of Electric Power Engineering

Martin Gulleik Teigenes

Provision of Primary Frequency Control from Electric Vehicles in the Nordic Power System

Master's thesis in Electric Power Engineering
Supervisor: Kjetil Obstfelder Uhlen
June 2023

NTNU
Norwegian University of
Science and Technology

Martin Gulleik Teigenes

Provision of Primary Frequency Control from Electric Vehicles in the Nordic Power System

Master's thesis in Electric Power Engineering
Supervisor: Kjetil Obstfelder Uhlen
June 2023

Norwegian University of Science and Technology
Faculty of Information Technology and Electrical Engineering
Department of Electric Power Engineering

NTNU
Norwegian University of
Science and Technology

Preface

This thesis concludes my master's degree in Electric Power Engineering at the Norwegian University of Science and Technology.

I would like to thank my supervisor, Kjetil Uhlen, for his continuous guidance and help throughout my last year at NTNU. He has provided some great pointers and insights regarding my work and has been an excellent discussion partner who has helped form the direction that the thesis has taken. I would also like to thank Aldrich Zeno, who has provided some great comments and feedback regarding the construction of the N45 model. Additionally, I would like to thank Hallvar Haugdal who has helped me out of several errors which I ran into during the process of performing dynamic simulations in DynPSSimpy.

Finally, I would like to thank my girlfriend and my 1-year-old daughter for their continuous love and support throughout the work of this master's thesis.

Trondheim, 05.06.2023

Martin Gulleik Teigenes

Abstract

In the coming years and decades, as the green transition moves forward, intermittent renewable energy sources (IRES) such as solar and wind will take over as the dominating source of energy in large parts of the world. These energy sources do not provide inertia to the electrical power system (EPS), making it more challenging to maintain a stable frequency in the EPS at the occurrence of faults or disturbances. Additionally, the green transition involves phasing out coal and gas-powered plants, which leads to a further deterioration of the power system's ability to maintain its frequency stability. However, with a total of 600,000 Electric Vehicles (EVs) in Norway as of December 2022 [1], there is an enormous untapped potential of providing large amounts of frequency containment reserves (FCR) and fast frequency reserves (FFR) in the Nordic EPS. This thesis will therefore analyze the use of EVs for provision of frequency containment reserves for disturbances (FCR-D) and FFR in the Nordic power system.

In order to lay some theoretical background for the simulations and results of the thesis, the most important theory regarding the provision of primary frequency control in an EPS is covered. Additionally, the current rules and regulations regarding the provision of FCR and FFR in the Nordic EPS are summarized, and some interesting findings from a project which analyzed the provision of FCR in the Nordic EPS are discussed.

An EV fleet is modeled both as a provider of FCR-D upwards and FFR, following the current rules and regulations for providers of such services. An updated and improved version of the Nordic 44 test model (N44) is constructed, called the Nordic 45 test model, which enables more precise simulations to be performed on the Nordic power system. 10 simulation cases are made, which are designed to highlight the different aspects of the performance of EVs as providers of frequency reserves in both the Kundur's two-area power system model (K2A) and the new Nordic 45 test model (N45).

The results of these cases are represented and discussed, and a conclusion is drawn as to whether or not EVs have sufficient performance as providers of frequency reserves in the Nordic power system as of today. It was concluded that using EVs as providers of FCR-D and FFR is currently not a viable option. The reason for this is the inherent time delay of the charging equipment and measurement devices associated with the use of EVs as providers of such services. However, it was found that if the time delay of charging equipment and measurement devices is sufficiently reduced, making it possible to activate the frequency response of the EVs almost instantaneously after the occurrence of a fault, the EVs could potentially perform just as well as the hydro-powered generators which are currently used for these types of services, if not better.

Sammendrag

Etterhvert som det grønne skiftet fortsetter vil fornybare energikilder som sol og vind ta over som den dominerende energikilden i store deler av verden. Disse energikildene bidrar ikke med treghet til kraftsystemet, noe som gjør det mer utfordrende å opprettholde en stabil frekvens ved forekomster av større feil eller forstyrrelser i nettet. I tillegg vil det grønne skiftet føre til at kull- og gassdrevne kraftverk fases ut, noe som ytterligere svekker kraftsystemets evne til å opprettholde frekvensstabiliteten. I desember 2022 [1] var det totalt 600 000 elbiler i Norge. Disse utgjør til sammen et enormt potensiale ved at de kan tilby store mengder primærreserver (FCR) og raske frekvensreserver (FFR) i det nordiske kraftsystemet. Denne oppgaven analyserer derfor bruken av elbiler som leverandører av driftsforstyrrelsesreserver (FCR-D) og FFR i det nordiske kraftsystemet.

Den teoretiske bakgrunnen som legger grunnlaget for simuleringene og resultatene i oppgaven gjennomgås sammen med de gjeldende reglene og forskriftene som omhandler leveranse av FCR og FFR i det nordiske kraftsystemet. I tillegg diskuteres noen interessante funn fra et prosjekt som analyserte leveranse av FCR i Danmark.

En elbilflåte modelleres både som en leverandør av FCR-D upwards og FFR etter gjeldende regler og forskrifter for leverandører av slike tjenester. Nordic 45 modellen utvikles, som er en oppdatert og forbedret versjon av den eldre Nordic 44 modellen. Denne modellen gjør det mulig å utføre mer presise simuleringer på det nordiske kraftsystemet. Det lages 10 simuleringsscenarioer som brukes for å vise frem flere aspekter ved ytelsen til elbiler som leverandører av frekvensreserver i både K2A modellen og den nye Nordic 45 modellen.

Resultatene fra disse scenarioene brukes for å konkludere om elbiler per dags dato har en tilstrekkelig ytelse som leverandører av frekvensreserver i det nordiske kraftsystemet eller ikke. Det konkluderes til slutt med at elbiler foreløpig ikke ville egnet seg som leverandører av FCR-D og FFR. Årsaken til dette er tidsforsinkelsen som ligger i elbilens ladeutstyr og i eksternt måleutstyr. Det ble imidlertid også konkludert med at dersom denne tidsforsinkelsen reduseres tilstrekkelig, noe som gjør det mulig å aktivere frekvensresponsen til elbilene nesten umiddelbart etter en feil oppstår, kan elbilene potensielt yte vel så godt som dagens vannkraftgeneratorer, om ikke bedre.

Table of Contents

List of Figures

List of Tables

Abbreviations

AEM Alert State Energy Management

EPS Electrical Power System

EV Electric Vehicle

EVSE Electric Vehicle Supply Equipment

FCR Frequency Containment Reserves

FFR Fast Frequency Response

FRR Frequency Restoration Reserves

HVDC High Voltage Direct Current

IRES Intermittent Renewable Energy Sources

K2A Kundur’s two area power system model

LFDD Low-Frequency Demand Disconnection

LER Limited Energy Reservoir

N44 Nordic 44

N45 Nordic 45

NEM Normal State Energy Management

ROCOF Rate Of Change Of Frequency

SAM Synchronous Area Monitor

SOC State Of Charge

SOA System Operation Agreement

TSO Transmission System Operator

V2G Vehicle-to-Grid

VSC Voltage Source Converter

1 Introduction

1.1 Background and objective

With a total of 600,000 EVs in Norway as of December 2022 [1], there is an enormous untapped potential of providing large amounts of frequency containment reserves and fast frequency reserves in the Nordic power system. The number of EVs and their combined battery capacity will only increase during the green transition, while most providers of traditional inertia will be phased out.

In the coming years and decades, IRES will take over as the dominating source of energy in large parts of the world. In most countries, the green transition to renewable energy does not involve the construction of large, stable, and reliable hydropower plants. Instead, wind and solar power will become the leading source of energy in most countries.

Even though the introduction of more wind and solar power is good for the environment, it also brings certain challenges, particularly challenges related to maintaining a stable grid frequency. Both wind and solar power are IRES, which means that their power production is almost solely dependent on how the sun shines and how the wind blows. On top of that, IRES does not provide inertia to the power system, which further complicates the challenge of maintaining frequency stability.

Inertia, explained simply, is the physical property of the rotating mass of turbines in traditional power plants (such as hydro, gas and coal plants) which resists changes in speed. Having more inertia in the power system makes it more resistant to frequency changes following disturbances and faults.

As the green transition to solar and wind continues, and the need for inertia in the power system increases, coal- and gas-powered plants will be phased out from production, leading to a further deterioration of the power system's ability to maintain its frequency stability. This is the background that leads to the objective of this thesis, which is to analyze whether or not EVs can be used as providers of FCR-D and FFR as an alternative to having large amounts of inertia in a power system. Since EVs are already widely used in the Nordic countries, this thesis will specifically analyze the use of EVs for provision of FCR-D and FFR in the Nordic power system.

1.2 Scope of work

The scope of work for this thesis is to:

- Create a new and improved version of the Nordic 44 test model in order to perform more realistic simulations on the Nordic power system.
- Make a realistic model of an EV fleet as a provider of FCR-D upwards and FFR by following the current rules and regulations for such providers.
- Analyze, discuss and identify different aspects of the performance of the EV fleet as a provider of FCR-D upwards and FFR, and compare it with the current providers of such services.

- Make a realistic case in the Nordic power system where EVs are used as providers of both FCR-D upwards and FFR.
- Conclude whether or not EVs have a sufficient performance as providers of FCR-D upwards and FFR. If not, find out what needs to be done in order to make their performance sufficient.

1.3 Outline

This thesis consists of 6 chapters:

Chapter 1 introduces the background and objective, the scope of work, and the outline of the thesis.

Chapter 2 contains theory on the frequency stability and control of a power system, the frequency reserve services of the Nordic power system, and the vehicle-to-grid technology used in today's EVs. It also goes through the findings and results of a project where, amongst other things, FCR-D was provided by EVs in Denmark.

Chapter 3 presents the methods used for modeling the EV fleet as a provider of FCR-D upwards and FFR. It also goes through the construction process of the new Nordic 45 test model and the simulation cases which are used to analyze the performance of the EV fleets.

Chapter 4 presents the results of the simulation cases of Chapter 3.

Chapter 5 discusses the results from Chapter 4 and shortly touches upon some thoughts regarding the viability of using EVs as providers of FCR-D upwards and FFR

Chapter 6 concludes the thesis and specifies some further work that could be done in order to investigate the objective of this thesis further.

2 Theory

2.1 Frequency stability and control

The project preceding this master thesis reviewed some key aspects of the theory behind frequency stability and control, which is also of importance in this master thesis. Therefore, this chapter is an improved and expanded upon version of the theory on frequency stability and control taken from the specialization project [2] leading up to this master thesis.

When assessing the overall stability of an EPS, the rotor angle stability, voltage stability and frequency stability are the traditional indicators of the overall stability of the system, while converter-driven stability and resonance stability have recently been included as important indicators. As one can see from Figure 1, these make up the five main classes of power system stability. For this thesis, only the frequency stability of the EPS will be looked upon in detail.

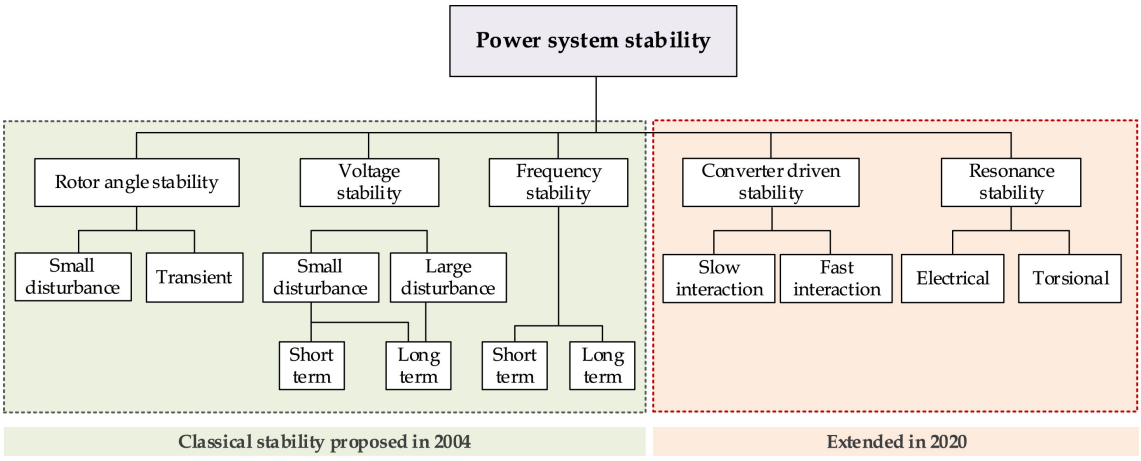

Figure 1: Classification of power system stability [3]

Whenever there is a difference between the production and the consumption of active power in an EPS, the frequency in the grid will either increase or decrease. Seen from the generator side, if the mechanical torque applied to the shaft of the rotor is larger or smaller than the electrical torque applied from the stator windings onto the rotor, the rotor will accelerate or decelerate accordingly. The speed of the rotor is directly linked to the frequency of the grid as shown in the following equation:

$$f = \frac{P \cdot n}{f_s \cdot 2} \tag{1}$$

f : Electrical frequency $[Hz]$ P : Number of poles
n : Rotational speed $[rpm]$ f_s : Synchronous frequency $[Hz]$

This means that if there is a long-term disturbance in the grid, for example an outage of a power plant, the electrical torque of the connected generators will decrease. Such a fault will cause a drop in frequency in the grid before the balance of production and consumption in the grid is regained. Figure 2 shows an example of how the frequency can change following a disturbance.

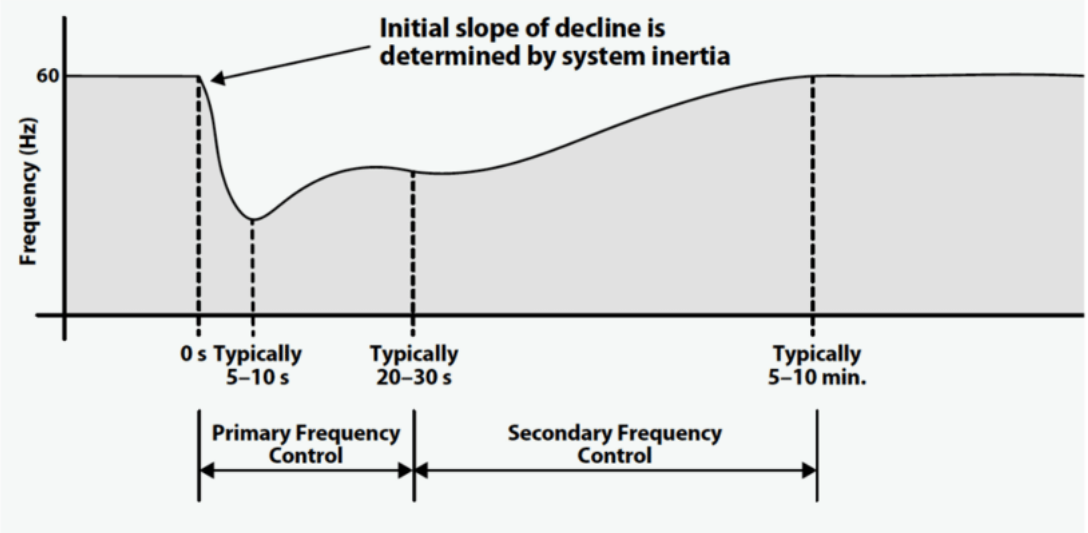

Figure 2: Frequency change in a grid disturbance event [4]

As one can see from the figure, a frequency drop event such as this one can be divided into two main stages. Initially, the kinetic energy stored in the total inertia of all connected generators will brake the frequency drop. During these first few seconds, the primary frequency control kicks in, where power plants providing frequency containment reserves (FCR) increase their power output according to their droop settings. After half a minute or so, when the primary frequency control has regained a balance between production and consumption in the grid, the secondary frequency control kicks in. Here, power plants providing frequency restoration reserves (FRR) will bring the frequency back to its nominal value while also freeing up primary reserves so that they are ready to be deployed again in the case of a new disturbance.

2.1.1 Inertia

In the first few seconds after a load event occurs, the inertia of all traditional rotating turbines in an EPS will oppose any change in their rotational speed, which also means they will oppose any change in the frequency of the grid. Inertia is the term given to the kinetic energy that is stored in the rotating masses of the traditional turbines in an EPS [5].

Using Newton's equation for rotating masses, the angular acceleration of an electrical machine depends on the mechanical and electrical torque applied to the machine as well as the moment of inertia of the turbine.

$$\frac{d\omega_m}{dt} = \frac{T_m - T_e}{J} \tag{2}$$

ω_m : Angular velocity $[rad/s]$ T_m : Mechanical torque $[Nm]$
J : Inertia $[kgm^2]$ T_e : Electrical torque $[Nm]$

In an EPS, the total moment of inertia in the system is described through the inertia constants of the connected generator-turbine units. The inertia constant (H) of a generator describes the ratio of kinetic energy stored in the rotating masses of the

generator to its MVA rating [5].

$$H = \frac{E_k}{S_n} = \frac{\frac{1}{2} J \left(\omega_n\right)^2}{S_n} \tag{3}$$

H : Inertia constant $[s]$
E_k : Kinetic energy $[Ws]$
w_n : Rated angular velocity $[rad/s]$
S_n : Rated apparent power $[MVA]$

In order to explain the inertia constant more intuitively, one could say that it corresponds to the time it would take to accelerate the turbine to the rated speed using the generator's full rated power. This is not completely precise as it would mean that the MVA rating of the machine could be output purely as active power (MW), which is not completely true, but it gives an idea of how much it takes to alter the speed of the turbine. In short, it requires a lot to alter the speed of a machine with a high inertia constant, which is positive from a stability point of view.

Table 1: Typical inertia constants of some power plant types [6]

Production type	$H[s]$
Nuclear	6
Combined cycle gas turbine	5.5
Single-shaft gas turbine	4.5
Large-scale hydro	3
Diesel genset	2
Converter-based units	0

Table 1 shows the typical inertia constants of some power plant types. Some loads in the EPS also supply inertia, but they are usually ignored as they typically have way less inertia than the combined inertia of the production units. Table 2 shows the typical inertia constants of some consumers.

Table 2: Typical inertia constants of certain consumers [6]

Consumer type	$H[s]$
Direct-on-line induction motor and compressor	1
Direct-on-line synchronous motor and compressor	1
Direct-on-line induction motor and conveyor belt	0.6
Variable speed drive	0
Lighting	0

As one can see from Table 1, converted-based production units do not provide inertia. This means that having large amounts of IRES in an EPS, such as wind and solar power, makes it challenging to maintain frequency stability at the occurrence of a disturbance. Voltage source converters and line commutated converters are used in order to run wind turbines at variable wind speeds while still maintaining rated power production. When using converters between the generator and the grid, there is no electromagnetic coupling between the machine and the power system. This means that any disturbances on the grid side of the converter can not be transformed into mechanical torque on the generator side of the converter [5], which removes the generator's ability to provide inertia.

When the amount of converter-based production units increases as the green transition to wind and solar power continues, the total inertia in the EPS will decrease. What this means is that the rate of change of frequency (ROCOF) will increase, and the frequency might drop so low that under-frequency load shedding is activated before secondary and tertiary frequency control has a chance to reestablish stability. One method which can dampen the ROCOF is the fast injection of active power known as the fast frequency response (FFR). The FFR in the Nordic EPS will be explained in further detail in Chapter 2.2.1.

2.1.2 Primary frequency control

This chapter goes through and summarizes the theory behind the primary frequency control of an EPS, which has mostly been obtained from [7].

Turbine governors increasing or decreasing their power output because of changes in the system frequency is the primary frequency control of the EPS. The action of the turbine governors in the EPS is dictated by their droop settings and their spinning reserves. The droop can be interpreted as the percentage of change in generator speed required to increase the power input on the turbine from zero to max [7] while the total amount of power in the EPS available to participate in primary frequency control is referred to as the spinning reserves. So, for example, with a droop setting of 5%, a generator would go from zero production to full production if the speed of the generator decreased by 5% from synchronous frequency. Some generation units can also have droop characteristics with dead zones where they keep their power production constant even though there are small frequency deviations of some 10s to 100s of mHz [7]. The relation of generator speed, mechanical power input and droop of the generator can be shown by the following formula:

$$\frac{\Delta\omega}{\omega_n} = -\rho\frac{\Delta P_m}{P_n} \tag{4}$$

ρ : Droop [%] P : Active power [MW]

As the rotational speed of the generator is proportional to the electrical frequency in the system, Eq. (4) can be written as:

$$\frac{\Delta f}{f_n} = -\rho\frac{\Delta P_m}{P_n} \tag{5}$$

So, when a large disturbance occurs in an EPS, causing a change in frequency, the total change of generated power in the system (caused by primary frequency control) will be:

$$\Delta P_T = \sum_{i=1}^{N_g} \Delta P_{mi} = -\Delta f \sum_{i=1}^{N_g} \frac{P_{ni}}{\rho \cdot f_n} \tag{6}$$

where N_g is the number of connected generators in the EPS.

The generation characteristic (droop characteristic) of the entire EPS will in reality be a sum of the droop characteristics of all generation units. This means that in a large EPS,

the droop characteristic will be almost horizontal around the operating point. Figure 3 shows how the combined generation characteristic in an EPS with many generation units becomes more horizontal the more units there are in the system.

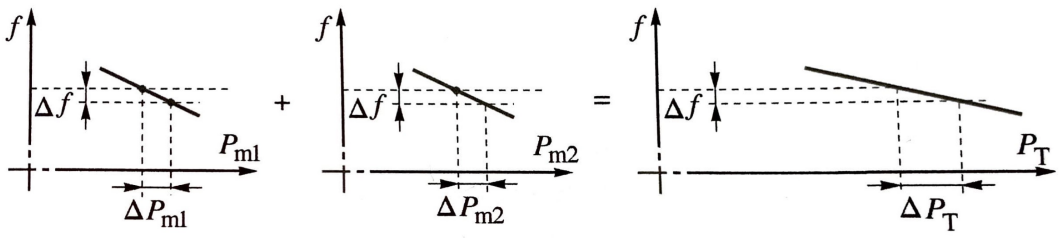

Figure 3: Generation characteristic as a sum of the speed-droop characteristic of all generation units [7]

However, as different generation units have different technical capabilities and varying amounts of spinning reserves, the generation characteristic is not linear. Figure 4 shows the influence of the upper turbine limit and the amount of available spinning reserves on the generation characteristic of the EPS.

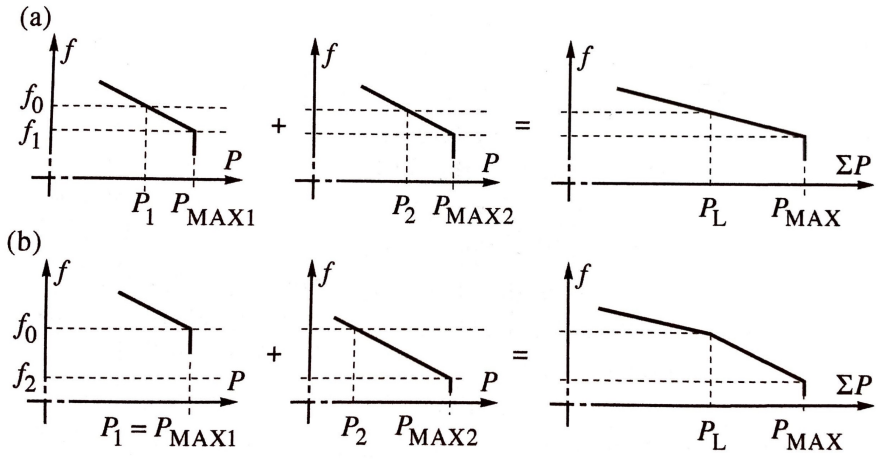

Figure 4: Influence of upper turbine power limit and spinning reserve allocation [7]

When the spinning reserves of the generating units are depleted and the maximal amount of generation is reached, the generation characteristic drops vertically. Figure 5 shows a typical generation characteristic of a large EPS.

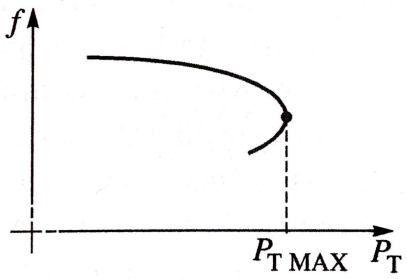

Figure 5: Realistic nonlinear generation characteristic [7]

When looking at the generation characteristic in close vicinity of the operating point, which encompasses a large range of possible power deviations, it can be considered linear with a local droop value. In order to find the local droop value of an EPS, one must calculate the droop of the system with respect to the total demand and production at the operating point instead of the power rating of the generators. The local droop value depends on how the spinning reserves of the generation units are allocated.

By dividing Eq. 6 by the total power demand in the EPS (P_L), which in a stable system is equal to the total power production in the system (P_T), one will find the following relation:

$$\frac{\Delta f}{f_n} = -\rho_T \frac{\Delta P_T}{P_L} \tag{7}$$

ρ_T : Local droop value [%]

$$K_T = \frac{1}{\rho_T} \tag{8}$$

K_T, which is the inverse of the local droop value, describes how the total production in the EPS responds to a change in frequency (around the operating point). The load in an EPS is inherently sensitive to frequency changes, and it can be described in a similar way to how K_T is described. The relation between the change in electrical load caused by a change in frequency is known as the frequency sensitivity coefficient of the power demand (K_L), and is shown in Eq. 9.

$$\frac{\Delta P_L}{P_L} = K_L \frac{\Delta f}{f_n} \tag{9}$$

While K_T typically has a value of around 20, as the droop settings typically can have values around 0.05, K_L only has values of around 0.5 to 3 [7], which means that the generation characteristic of the EPS is way more frequency-dependent than the load characteristic. Since K_T and K_L in Eqs. 7 and 9 have opposite signs, a decrease in frequency corresponds to an increase in generation and a decrease in load. A change in demand of power can then be calculated as follows:

$$\Delta P_{demand} = \Delta P_T - \Delta P_L = -(K_T + K_L) P_L \frac{\Delta f}{f_n} = -K_s P_L \frac{\Delta f}{f_n} \tag{10}$$

where K_s is referred to as the stiffness of the system.

In Figure 6 one can see that the intersection between the generation characteristic and the load characteristic defines the system equilibrium point and the system frequency. So, when there is an increase in the power demand ΔP_{demand}, the load characteristic moves from point 1 to point 3. The point where the load characteristic and the generation characteristic then meets (point 2) is the new system equilibrium point, and the demand in power (ΔP_{demand}) is met by the increase in generation from the turbines (ΔP_T) and the decrease in load caused by its inherent frequency sensitivity (ΔP_L).

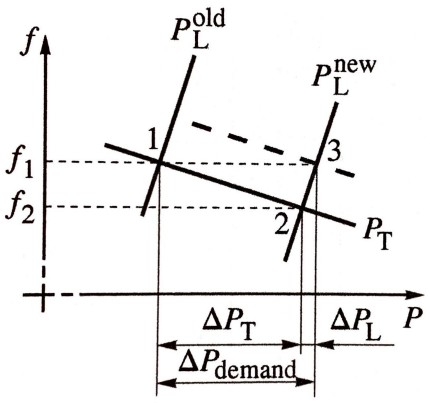

Figure 6: Equilibrium points for an increase in the power demand [7]

So, when the power demand in the EPS changes, the primary reserves are activated wherever there are spinning reserves available. In order to have a safe operation of the EPS, there must be adequate amounts of spinning reserves distributed among several locations. If the spinning reserves are concentrated within only one area of the EPS, the transmission lines from this area might get overloaded as a result of the primary frequency control, and the disturbance might spread to other parts of the EPS.

The response time for primary frequency control is typically around 15-30 seconds [8]. After this, the balance between total production and consumption of power in the EPS is re-established. However, the frequency will not be balanced at synchronous frequency without further action. Rebalancing the generation scheme in order to restore the frequency to its initial value is the purpose of the secondary frequency control.

2.1.3 Secondary frequency control

Looking at the situation in Figure 6, one can see that in order to reestablish nominal frequency in the EPS (f_1 in the figure) after the primary frequency control has reestablished system equilibrium and a stable frequency, the generation characteristic must be shifted to the position of the dashed line. In order to do this the load reference set points in the turbine governors are changed, which enforces a shift in the position of the generation characteristic as illustrated in Figure 7.

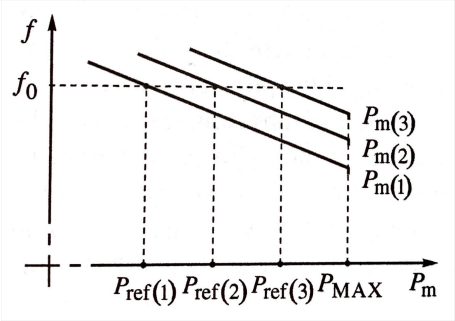

Figure 7: Speed-droop characteristics for various values of P_{ref} [7]

When enough governors have increased the power output from the generator as a result of increasing their load reference set points, the nominal system frequency will be restored. This control of the turbine governing systems is what is referred to as secondary frequency control, also known as Automatic Generation Control (AGC) or Load Frequency Control (LFC). In the Nordic EPS, automatic Frequency Restoration Reserves (aFRR) are the automatically deployed power reserves used in secondary frequency control.

In a large interconnected power system, one must take into account the fact that there are different areas in the EPS with limited power transfer capabilities between them. This means that each power plant contributing to secondary frequency control can't act independently as they won't know where the power imbalance in the EPS occurs. Therefore, in order to reestablish synchronous frequency in the EPS, while also maintaining the set tie-line power transfer capabilities of the EPS, a centralized secondary control system is needed.

The secondary frequency control works in such a way that each area of the EPS has its own central regulator. The EPS is said to be in equilibrium for each area if the following condition is satisfied:

$$P_T - (P_L + P_{tie}) = 0 \tag{11}$$

where P_{tie} is the net power transfer out of the area.

The regulator in each area of the EPS is tasked with maintaining a power balance according to Eq. 11. This is known as the "non-intervention rule" [7]. If the non-intervention rule is followed correctly in all subsystems after a disturbance, the power balance will be restored in the whole EPS, while also restoring synchronous frequency.

In practice, the required change in power generation needed for a single area to reach nominal frequency while also following the non-intervention rule can be calculated by amplifying the frequency deviation with a frequency bias factor λ_R, as shown in Eq. 12.

$$\Delta P_f = \lambda_R \Delta f \tag{12}$$

λ_R : Frequency bias factor $[MW/Hz]$

For a single generator, the nominal frequency bias can be calculated as follows:

$$K_{fg} = \frac{\Delta P}{\Delta f} = \frac{P_n}{\rho \cdot f_n} \tag{13}$$

The demand of power generation in the EPS following a disturbance can be calculated as shown in Eq. 10, while the increased generation of ΔP_f enforced by the central regulator in a subsystem is shown in Eq. 12. $\Delta P_f = -\Delta P_{demand}$ as the central regulator must cover the total demand. The frequency bias factor can then be expressed as follows:

$$\begin{aligned} \Delta P_f &= -\Delta P_{demand} \\ \lambda_R \Delta f &= -(-K_s P_L \frac{\Delta f}{f_n}) \\ \lambda_R &= \frac{K_s P_L}{f_n} = K_f \end{aligned} \tag{14}$$

Where K_f is referred to as the frequency stiffness of the entire EPS, K_s is the frequency stiffness of the subsystem and P_L is the total demand in that subsystem.

2.2 Frequency reserves in the Nordic EPS

2.2.1 Fast Frequency Response - FFR

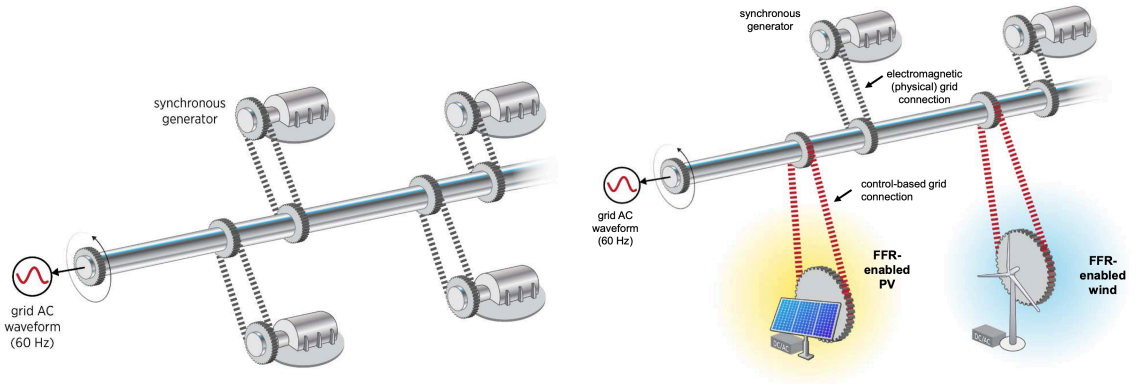

(a) Illustration of EPS with traditional provision of inertia

(b) Illustration of EPS with FFR in addition to traditional provision of inertia

Figure 8: EPS with and without FFR

In the Nordic EPS, low inertia is causing issues with maintaining the transient frequency stability in the grid [9]. This is especially an issue in the summer months when there is low consumption and low production of power combined with a high penetration of wind power and high import from HVDC cables. FFR has now taken over as the first mitigation measure during large faults with low levels of system inertia, and acts as a complement to the primary reserve for disturbances, which is the provision of FCR-D [10]. Fast frequency reserves are only procured for underfrequency events, and are rapidly deployed following a drop in frequency in order to keep the frequency from falling below 49.0Hz [9]. Figure 8 illustrates how FFR-enabled power sources are connected to an EPS, where they can contribute to primary frequency control in a similar way to traditional sources of inertia. Explained simply, FFR acts as a power reserve which can be injected into the EPS in about 1 second after the system frequency passes a certain value [9]. In Norway, one can activate FFR at a set frequency between 49.5Hz and 49.7Hz. When choosing a low activation frequency, the response must act faster in order to provide the desired effect.

In 2017, Nordic TSOs (EnergiNet (Denmark), Fingrid (Finland), Statnett (Norway) and Svenska Kraftnät (Sweden)) did a study on the issues related to the decreasing levels of inertia in the EPS, as well as potential ways of resolving these issues [9]. The implementation of a fast frequency response was found to be the most cost-effective solution, and they expected a demand of 300MW of fast frequency reserves from May to September of 2020. Each TSO is responsible for providing a given share of the demand of FFR based on a distribution key (Figure 10) which can be changed from year to year. Currently, the demand for FFR is estimated by a forecasting tool that can calculate the demand for the upcoming few days and hours.

A commercial market for the acquisition of FFR in the Nordic EPS was established in 2022, and it's divided into two products: a seasonal profile where a limited amount of reserves are made available for weekends and nights ("FFR Profil"), and a flexible profile where reserves are made available based on the predicted demand of FFR calculated by the forecasting tool ("FFR Flex") [9]. Statnett, the Norwegian TSO, is

procuring 150MW of FFR capacity in the period from 29.04.23 to 30.10.23 [9], where 100MW of FFR Profil and 50MW of FFR Flex will be procured.

The activation frequency of the FFR is set so low that in some years, the fast frequency response is never activated. The activation of FFR is therefore not expected to occur frequently, making the acquisition of FFR more attractive for potential providers.

Current rules and methodologies

This subchapter summarizes the technical requirements, rules and regulations regarding the provision of FFR in the Nordic EPS found in the Nordic System Operation Agreement (SOA) [11]. Ultimately, the goal of FFR is to prevent the system frequency to fall so far that low-frequency demand disconnection (LFDD) is activated. FFR is therefore procured only when the total inertia in the system is so low and the reference incident is so high that the FCR-D reserves will not be able to prevent the frequency drop from activating LFDD.

Definition of the reference incident in the Nordic EPS

According to the Nordic synchronous area proposal for the dimensioning rules for FCR [12], the reference incident shall be defined as the largest imbalance that may result from an instantaneous change of active power of:

a. A single power-generating module
b. A single demand facility
c. A single HVDC interconnector
d. Tripping of an AC-line: This may result in i) system protection scheme (SPS) activation which may trip one or more power generating units or ii) loss of a regional part of the system.
e. Single failure on a busbar tripping more than one generation module or demand facility.

Currently, all Nordic TSOs are responsible for defining the FFR dimensioning. The synchronous area monitor (SAM) monitors the level of inertia in the power system and the frequency stability in real-time, and helps the TSOs by coordinating which measures are required in case of insufficient FFR. The TSOs are also held responsible when it comes to procuring the required amount of FFR reserves (and the prequalification process of their FFR providers) given information from the FFR forecast and the FFR sharing key. In case there is a shortage of FFR, the TSO with the FFR deficit is held responsible and must take ownership of the issue. All TSOs are however responsible to take action in case there is a shortage of FFR in the Nordic EPS.

Requirements for FFR providing entities

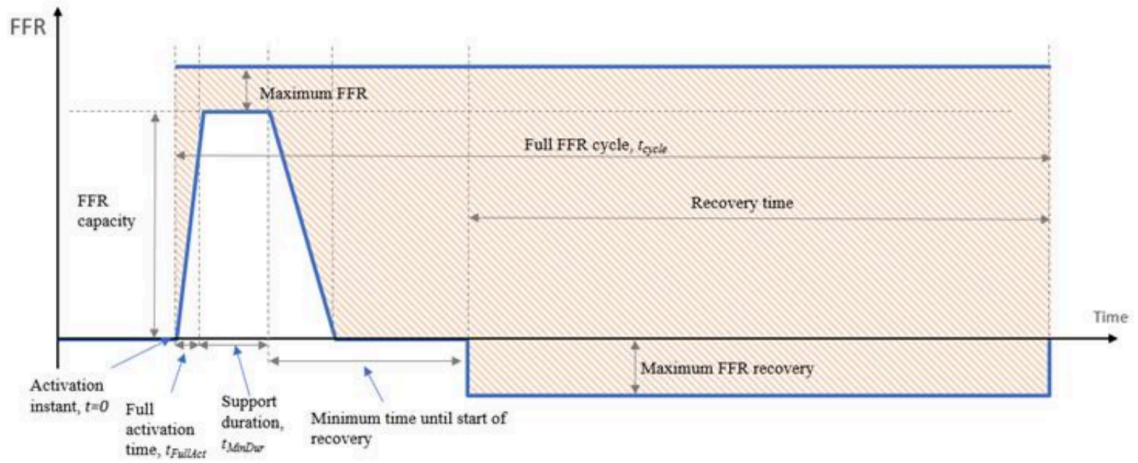

Figure 9: Sequential diagram of FFR provision [11]

Figure 9 shows a sequential diagram for the activation of FFR reserves. The following requirements apply to the provision of FFR:

- The activation instant is at time = 0
- Different combinations of frequency activation level and full activation times are allowed: The maximum time for full activation is 0.70 s (for the activation level 49.5 Hz), 1.00 s (for the activation level 49.6 Hz), and 1.30 s (for the activation level 49.7 Hz);
- Different minimum support duration is allowed: 5.0 s (for short support duration) and 30 s (for long support duration);

The prequalified FFR capacity (in MW) from an FFR-providing entity is the minimum support power that must be delivered in the support duration. The maximum allowed support power is 20% over the prequalified FFR capacity, but the TSO may allow up to 35% over-delivery depending on the national procurement process.

There is no limitation in the rate of deactivation of supporting power for an entity that provides FFR with a long support duration (over 30 seconds). The deactivation may also be step-wise and non-linear. For an entity providing FFR with a short support duration, the rate of deactivation is limited to a maximum of 20% of the prequalified FFR capacity per second (as an average over any integration time of one second). Also, no single step can be over 20% of the prequalified FFR capacity.

In order to recover FFR reserves as quickly as possible, all FFR-providing entities must be ready for a new activation cycle within 15 minutes after the previous activation instant. There are no requirements on the shape of recovery and it may be stepwise. The recovery must however not exceed 25% of the prequalified FFR capacity and it must not start before a time corresponding to the activation time, plus the support duration, plus the deactivation time, plus 10 seconds after the activation instant.

The TSO that connects the FFR provider must make sure that the entity is prequalified and fulfills the requirements mentioned above. Prequalification tests must also be

performed.

FFR need

The TSOs must forecast the need for FFR seven days ahead based on inertia forecasts. One day before operation, the FFR demand for the following day is specified on an hourly resolution. The distribution key between the Nordic TSOs shall be agreed upon annually.

The SAM monitors the frequency stability in the EPS in real-time by using a tool that is implemented in the Supervisory Control And Data Acquisition (SCADA) systems of the TSOs. An alarm is generated whenever the instantaneous frequency deviation caused by one or more contingencies exceeds the maximum instantaneous frequency deviation. The tool uses real-time kinetic energy in the EPS, the power of each incident in the list of contingencies and the available FFR volume as inputs. The TSOs are tasked with providing the most actual information as the input data to the tool.

If the tool finds that there are insufficient volumes of FFR capacity, the SAM coordinates the required measures that must be taken in order to restore a sufficient volume. This is done by assessing which possible actions can increase FFR provision from all TSOs and initiating actions that could increase FFR. If none of the TSOs are able to increase their FFR capacity, they would have to evaluate whether or not they can reduce the reference incident instead. As explained earlier, the reference incident is defined as the largest imbalance that may result from an instantaneous change of active power from an entity in the EPS. However, there is no point in trying to reduce the reference incident if it would take more time than the duration of the FFR deficit.

Distribution key - FFR

Parameter	Value	Validity period	Approved by, on
Dimensioning of FFR		Updated daily	
Sharing key for FFR			
- **Denmark/East (DK2)**	**8%**	Until changed by new RGN decision	RGN on 10-12-2020
- **Finland**	**18%**		
- **Norway**	**39%**		
- **Sweden**	**35%**		

Figure 10: Dimensioning of FFR and initial distribution of FFR [13]

Synthetic inertia

Synthetic inertia can be defined as ”the contribution of additional electrical power from a source which does not inherently release energy as its terminal frequency varies, but which mimics the release of kinetic energy from a rotating mass” [14]. A wind power plant providing synthetic inertia will provide an electrical torque proportional to the ROCOF measured from the main grid when a load event occurs. This is an already widely implemented and used technology in the wind power plants in ERCOT,

which is the main transmission grid of Texas, USA [14]. ERCOT is a relatively small independent EPS, and by using synthetic inertia to cope with the problem of maintaining primary frequency control in a grid with a high penetration of IRES, they are able to achieve 58% instantaneous penetration of wind and are expected to allow even greater penetration levels in the future [14].

Many consider synthetic inertia to be a form of fast frequency response, and they use the terms interchangeably. One could however say that synthetic inertia is the inertial response of a generator where torque is released in direct proportion to the ROCOF measured in the grid [15], as this mimics the inertial response of a traditional rotating machine. All other forms of fast deliverance of power in response to a large ROCOF or the frequency reaching a set value can be defined as FFR, and one could look at synthetic inertia as a subset of FFR.

2.2.2 Frequency Containment Reserves - FCR

Any imbalance between production and consumption in the Nordic EPS is primarily taken care of by the automatic deployment of FCR. Recently, the Nordic TSOs concluded that the current guidelines and regulations regarding FCR in the Nordic EPS must be audited [16]. The reason behind this conclusion is that with a decreasing amount of inertia and changing patterns of production and consumption in the EPS, increasingly frequent and large frequency changes occur, which requires an improvement of the frequency containment reserves. The quality of the FCR is defined by its ability to activate and deactivate the reserves. Therefore, the current function of the FCR as a power reserve which is deployed proportionally with the deviation of system frequency is retained, but the revised technical specifications of FCR sets stricter requirements as to how the reserves are activated and deactivated. It also sets stricter requirements for the testing and prequalification of the reserves. These revised technical requirements were published in June 2022 [17] and were approved by the Nordic Regulatory Authorities (RME) on the 3rd of April 2023. In Norway, these new technical requirements will be taken into effect on the 1st of January 2024 [18].

Three FCR products are defined in the technical requirements [17]:

- FCR-N, in the range of 49.9 - 50.1Hz
- FCR-D upwards, in the range of 49.9 - 49.5Hz
- FCR-D downwards, in the range of 50.1 - 50.5Hz

It is specified that each product can be provided either as a linear function of the frequency deviation or as an approximation of a linear function of the frequency deviation.

In the event of a frequency drop to 49.5Hz, 50% of the FCR-D upwards capacity shall be activated within 5 seconds and 100% shall be activated within 30 seconds [19]. Similarly, in the event of a frequency change to 50.5 Hz, 50% of the FCR-D downwards capacity shall be activated within 5 seconds and 100% shall be activated within 30 seconds.

Chapter 2 of the requirements contains information on the prequalification process for providers of FCR, which is simplified compared to earlier requirements in order to

make the provision of FCR available for more potential providers [20].

In Chapter 3, the technical requirements for potential providers of FCR are listed. The purpose behind these requirements is to guarantee that the resources taking part in frequency control have sufficient static and dynamic performance and that they do not destabilize the EPS. These requirements are the same for generating entities, load entities and energy storage entities. Some important requirements from the technical requirements [17] include:

- ”FCR shall remain activated as long as the frequency deviation persists.”
- ”The FCR response shall not be artificially delayed and should begin as soon as possible after a frequency deviation.”
- ”FCR providers shall disable their FCR contribution when not procured.”
- ”Voltage control using frequency-voltage droop is allowed”.
- ”Static FCR-D shall be deactivated and ready for reactivation within a grace period of a maximum of 15 minutes from the frequency return to the standard frequency range.”
- ”The maximal provision per single point of failure is limited to 5 % of the nominal reference incident in the Nordic EPS. Currently, the maximal provision of FCR-N or FCR-D per single point of failure is 70 MW in the upward direction and 70 MW in the downward direction. In addition, when providing both FCR-N and FCR-D at the same time, the combined maximal provision is 100 MW in the upwards direction and 100 MW in the downwards direction respectively.”

This last point refers to the nominal reference incident in the Nordic EPS (typically 1450MW), meaning that a maximum of 5% of this (about 70MW) can be delivered through a single point in the grid when providing either FCR-N or FCR-D, while a maximum of 100MW can be delivered when providing both.

Static or non-continuously controlled resources must activate their FCR contribution based on the monotonic piecewise power-frequency characteristic shown in Figure 11 and 12. The black line in the figure represents the target response of the resource providing FCR (in % of available power), while the blue field marks the allowed out-come of the deviations from the line.

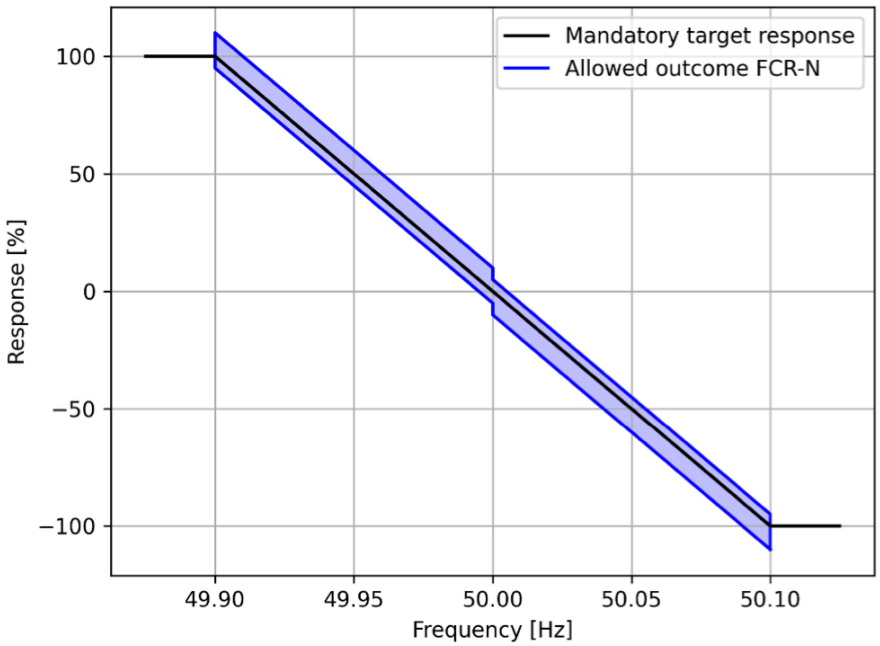

Figure 11: Activation [%] of linear FCR-N resources [17]

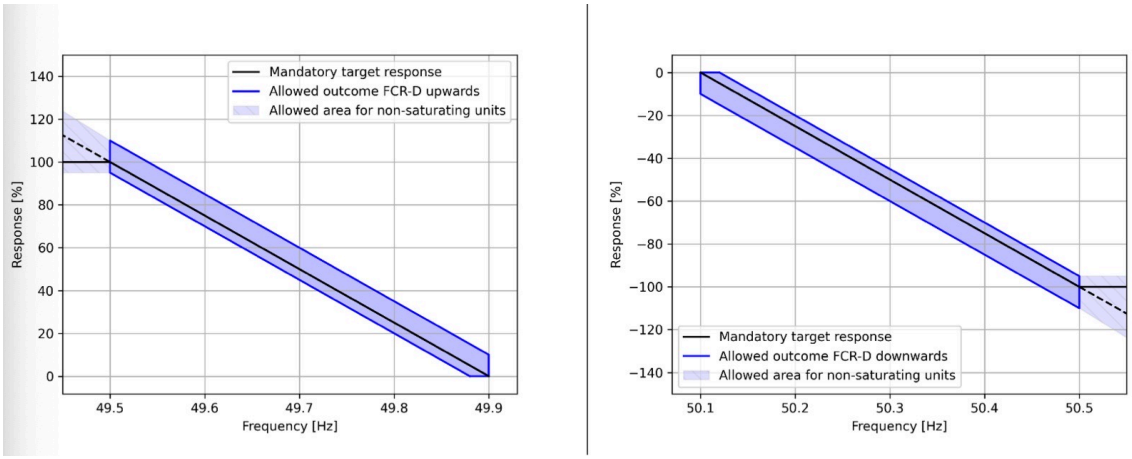

Figure 12: Activation [%] of linear FCR-D resources [17]

Dimensioning of FCR capacity

In 2023, 600MW of FCR-N shall be procured at all times [13]. Regarding FCR-D, there are several dimensioning rules (all obtained from [12]):

Firstly, the required FCR-D capacity must be dimensioned daily. FCR-D upwards and FCR-D downwards is also dimensioned separately.

The input to the dimensioning process of FCR-D shall be:

a. Planned network topology

b. Estimated production of large generation modules

c. Estimated demand of large connected consumers

d. Estimated flows on HVDC interconnectors.

The total reserve capacity for FCR-D upwards shall be dimensioned at least equal to the imbalance caused by the reference incident in the negative direction. The total reserve capacity for FCR-D downwards shall be dimensioned at least equal to the imbalance caused by the reference incident in the positive direction. The imbalance volume of the reference incident shall be determined by the net change of active power in the grid. For example, one must take into account that the auxiliary load of generation modules may still consume power even when the generator is tripped.

Dimensioning of initial FCR capacity per TSO

The initial distribution key for FCR capacity is dimensioned per year.

The inputs to the calculation of the initial distribution key are:

a. The net generation per control area for calendar year y-2 in which net generation of a unit is defined as the generation level less than the total gross power generation of a unit, due to internal auxiliary power consumption of the unit.

b. The net consumption per control area for calendar year y-2 in which 'net' means that the consumption of power plants' auxiliaries is excluded, but network losses are included.

Further, the initial distribution share for each TSO shall be based on the sum of the net generation and consumption of its control area divided by the sum of net generation and consumption of the entire Nordic EPS over a period of 1 year.

Distribution key - FCR

Parameter	Value	Validity period	Approved by, on
Dimensioning Nordic FCR-N	**600 MW**	2023	RGN on 15-08-2019
Dimensioning Nordic FCR-D		Updated daily	
Initial distribution of FCR (both FCR-N and FCR-D)			
- **Denmark/East (DK2)**	**3,06%**	2023	RGN on 31-08-2022
- **Finland**	**20,11%**		
- **Norway**	**38,38%**		
- **Sweden**	**38,45%**		

Figure 13: Dimensioning of FCR and initial distribution of FCR [13]

Limited Energy Reservoirs (LER) as providers of FCR

This subchapter summarizes some of the requirements and definitions from the revised technical requirements revolving around LER entities providing FCR [17], which is the source of all information in this subchapter.

An FCR-providing entity is classified as a limited energy reservoir (LER) if it has an energy reservoir smaller than the equivalent of a continuous full activation of the prequalified FCR capacity for two hours. LER entities must reserve power in both directions for energy management.

Regardless of the type of FCR-providing entity, it is required that the FCR response shall remain activated for the total duration of the frequency deviation. Therefore, the LER entity must specify the limitations of its energy reservoir in the application document in accordance with instructions from the reserve connection TSO. Also, the implementation of an energy management solution including the recovery process must be described. The ability to provide FCR shall remain intact during the use of energy management functions.

For LER entities, the prequalification application shall contain the following power resource-dependent documentation:

- Rated apparent power [MVA]
- Rated energy capacity of the energy storage [MWh]
- Energy storage maximum and minimum state of charge [MWh]
- Technical description of the controller including controller settings
- Description of energy management

The technical requirements [17] specify that the prequalification requirements for LER concerning minimum energy storage, additional capacity to activate the energy management states, and the functioning of the energy management states for FCR-N and FCR-D are still under development. The reason for this is that the requirements are based on the principles from continental Europe, which may not be directly implementable in the Nordic EPS. The main goal of these requirements is to ensure the reliable provision of FCR with a low risk of depleting the energy reservoir.

Figure 14 shows the required power and energy reserve for FCR-N and FCR-D where C_{FCR} is the FCR capacity. As mentioned above, these values are subject to change as the requirements may be updated later on.

	FCR-N[9]	FCR-D upwards	FCR-D downwards
Required power upwards [MW]	$+1.34 \cdot C_{FCR-N}$	$+C_{FCR-Dupwards}$	$+0.20 \cdot C_{FCR-Ddownwards}$
Required power downwards [MW]	$-1.34 \cdot C_{FCR-N}$	$-0.20 \cdot C_{FCR-Dupwards}$	$-C_{FCR-Ddownwards}$
Required energy upwards [MWh]	$1\text{h} \cdot C_{FCR-N}$	$\frac{1}{3}\text{h} \cdot C_{FCR-Dupwards}$	0
Required energy downwards [MWh]	$1\text{h} \cdot C_{FCR-N}$	0	$-\frac{1}{3}\text{h} \cdot C_{FCR-Ddownwards}$

Figure 14: Required power and energy reserves for FCR-N and FCR-D [17]

FCR-N provision from an LER entity shall be continuously available during the whole contractually agreed delivery period of increments of 1 hour. For full activation of FCR-N, there is a minimum endurance requirement of 60 minutes in both directions.

FCR-D provision from an LER entity shall be continuously available in normal state operation. From the triggering of the alert state and during the alert state, the LER entity shall be able to fully activate FCR-D continuously for a time period of 15 minutes. Since FCR-D can be fully activated in both normal and alert states, the total endurance requirement for full activation of FCR-D becomes 20 minutes.

Normal state energy management (NEM) is an energy management scheme for LER entities providing FCR-N or FCR-D. The purpose of this scheme is to ensure that there is enough energy stored in order to activate FCR, while also reducing any potential imbalances due to the State of Charge (SOC) management. The LER entity enters the alert state energy management (AEM) when the SOC goes outside of the allowed range for NEM. The range for the SOC is chosen such that the LER entity is able to smoothly deactivate its steady-state response over a period of 5 minutes.

2.3 Vehicle-to-grid technology

EVs can contribute to frequency recovery services both if they use unidirectional or bidirectional charging. Unidirectional charging, however, only allows the EV to act as a controllable load, which limits its usefulness greatly compared to an EV with bidirectional charging.

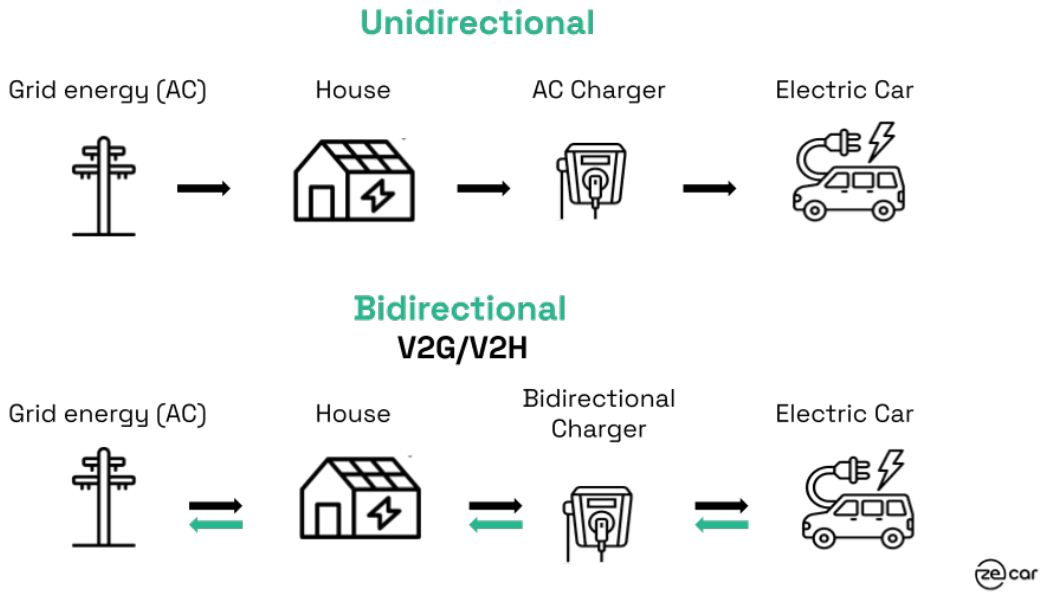

Figure 15: Unidirectional vs. bidirectional charging [21]

Today, technologies like Tesla's Powerwall act as a battery buffer that can be charged when the price of electricity is high and be discharged when the cost of electricity increases. Some EVs with bidirectional charging have the same ability, which is categorized as vehicle-to-home charging. vehicle-to-grid (V2G) charging, on the other hand, is a charging scheme where the vehicle is treated as part of a virtual power plant, and its charging/discharging is controlled after a specific energy management system from the local regulations of the TSO [21].

Currently, there are only a few commercially available V2G compatible cars, some of which include:

- Nissan Leaf
- Mitsubishi Outlander PHEV
- Ford F-150 Lightning

This is a technology that will most likely become a mainstream functionality in the future. For example, in an interview performed by Handelsblatt with the Volkswagen Group in 2021 [22], VW stated the following: "From 2022 onwards, every electric car from the Volkswagen Group that is developed on the basis of the MEB electric platform ("modular electrification kit") will not only be able to charge the electricity, but also feed it back into the grid. In addition to VW, the sister brands Audi, Skoda and Seat-Cupra also use the MEB." In the same interview, Handelsblatt states that

around 6.5 TWh of electrical energy produced from wind farms in the North and Baltic seas is wasted each year as there is no place to store the energy. This corresponds to about 1 percent of the annual electricity consumption in Germany [22], and according to Volkswagen, this is enough energy for 2.7 million fully battery-powered cars to be driven for a year.

2.3.1 The Parker Project

The Parker project [23] was a Danish demonstration project aimed at showcasing the potential of utilizing contemporary EVs in advanced smart grid services, including V2G technologies. It builds on two previous projects which laid the foundation for understanding the EVs' potential for providing support for the EPS. It used EVs and V2G DC chargers to carry out tests and demonstrations in PowerLabDK, which is an experimental platform for power system research. The project also partnered with the Frederiksberg Forsyning V2G hub in Copenhagen, which is an actual operational customer site consisting of 10 Nissan e-NV200 EVs and 10 Enel V2G chargers controlled by a Nuvve aggregator providing Frequency Regulation to the Danish DK2 grid. At this test site, they were able to test the quality of EVs as FCR providers. The main focus revolved around the grid applications, grid readiness and scalability of EVs as a grid-balancing service. The project was concluded in January 2019 and resulted in a final report which summarized their findings [23].

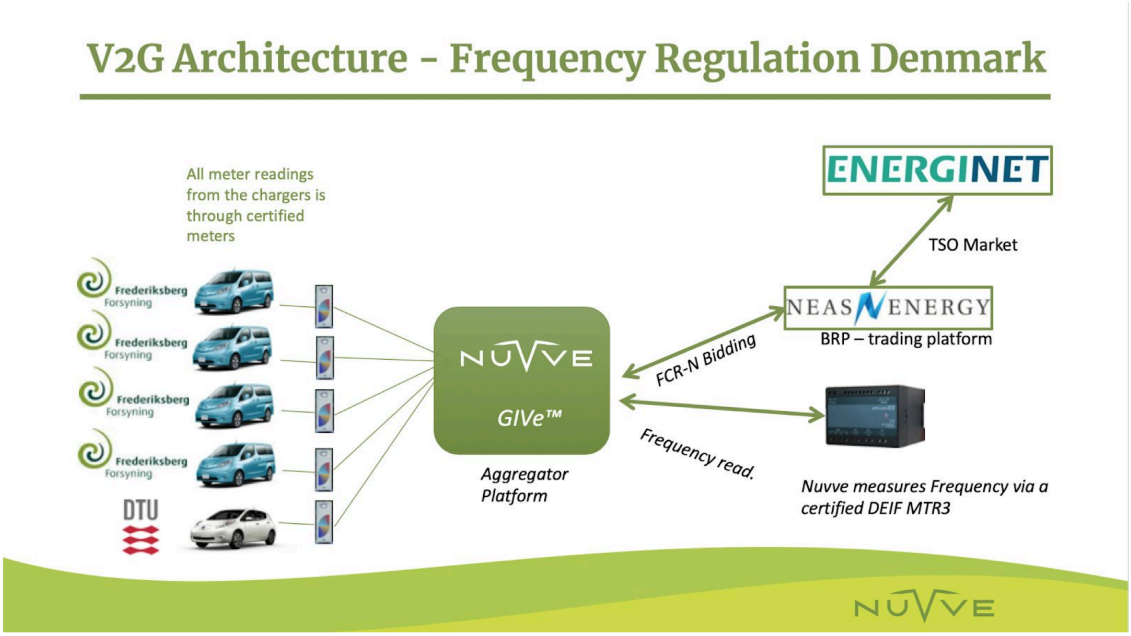

Figure 16: Project V2G architecture for FCR-N in DK2 [23]

In Figure 16, one can see the V2G setup used at Frederiksborg Forsyning V2G Hub.

The project proved that commercial EVs with V2G technology and presently available charging infrastructure are technically able to provide all types of frequency regulation services used in Denmark. They also concluded that the V2G technology is scalable both in terms of the number of EVs, type of FCR service, TSO regions, battery sizes and duration of service. At Frederiksberg Forsyning V2G hub, FCR-N was found to

be ”by far the most demanding service of the ones investigated” [23]. The reason for this was the intensive battery usage that follows this type of service. Although battery usage is high when providing FCR-N, this is also a rather profitable service to be providing. The project used the Nissan eNV200 EV in their tests, and each car used in the project provided FCR-N services for two years under temporarily relaxed market terms, which amounted to 13 000 hours for each car with an average revenue of 1860 Euro for each car per year.

A test protocol was developed in order to analyze whether the technical capabilities of EVs and charging infrastructure were good enough to support V2G and other grid-supporting services. A grid key was made in order to summarize a list of requirements for controllability, observability, and performance of the power exchange between the EVs and the grid. The requirements in the grid key were compared with frequently used standards and protocols regarding EVs and Electric Vehicle Supply Equipment (EVSE). These standards include IEC 61851, ISO 15118 and CHAdeMO (fast charging technology [24]), which are all standards and protocols regarding EVs, EVSE, and fast charging. CHAdeMO was the only standard that supported V2G at the time, and all standards and protocols needed to be updated and extended in order to make them fully capable of supporting vehicle-grid integration. The test protocol was performed on all EV models included in the project (Nissan Leaf, Nissan Evalia, Peugeot iOn, Mitsubishi Outlander PHEV). The tests evaluated the activation time, accuracy and precision of power exchange among some other aspects of the FCR provision of the vehicles. The activation time was measured to be around 5-6 seconds when including communications delay down to about 3 seconds when controlling the charger and car directly. They found that ultimately, the performance depends on the power electronics and the software and protocols used to control it.

The project concludes that V2G capability works well when using a DC V2G charger and the CHAdeMO standard. However, in order to make the technology behind vehicle-grid integration universal and to potentially introduce new services such as reactive power provision and sub-second response, further work on the subject is needed.

Finally, the project explored the business case of providing FCR with EVs, which was found to be very sensitive to a number of factors with an expected profit ranging from -955 Euro per car/year to 2304 Euro per car/year. This suggests that it may take some time for businesses to see this as a viable business case, with further development of V2G-enabled EVs and charger infrastructure being some of the most important factors to encourage further growth of the technology. When analyzing the barriers of providing FCR using EVs, the project found that most countries are battling barriers regarding few V2G capable EVs, market structures not ready for EV aggregation, and market frameworks not developed for the new decentralized energy market. When analyzing Norway, Sweden, Denmark and Germany, Denmark was found to have the lowest barriers, followed by Sweden. Norway, Sweden and France were found to be some of the most interesting markets in Europe to consider for EV aggregators providing FCR-type services. A subtopic of vehicle-grid integration called distribution system services was also investigated. This involves services such as congestion management, load shifting, peak shaving and voltage control. Through case studies and investigations, the project argued that the provision of reactive power from EVs could minimize grid losses and allow for 50% more EVs in a grid without any additional investments.

The Parker Project - Test Results

As previously mentioned, the Parker project used the Frederiksberg Forsyning V2G Hub as a test site, which is located in DK2 and is, therefore, a part of the Nordic synchronous area. So, since the test results consist of real-life measurements from EVs providing FCR in the Nordic synchronous area, it is highly relevant for this thesis.

In order to test the provision of FCR-D from EVs, a canned (measured and stored) frequency signal from when the frequency fell below 49.9Hz was tested on the FF test site. The frequency in DK2 was measured over a period of 452 days, where the longest time spent between 49.9 and 49.5Hz was found to be 998 seconds. The canned signal from this time period was used to test the FCR-D service.

Figure 17 shows the resulting power response from the test site. Only one charger (with a Mitsubishi Outlander PHEV using it) was working during the test. This vehicle had a battery size of 12kWh while the charger had a rating of +-10kW. The energy content is quite low with only 0.4 kWh being delivered for the 998-second interval.

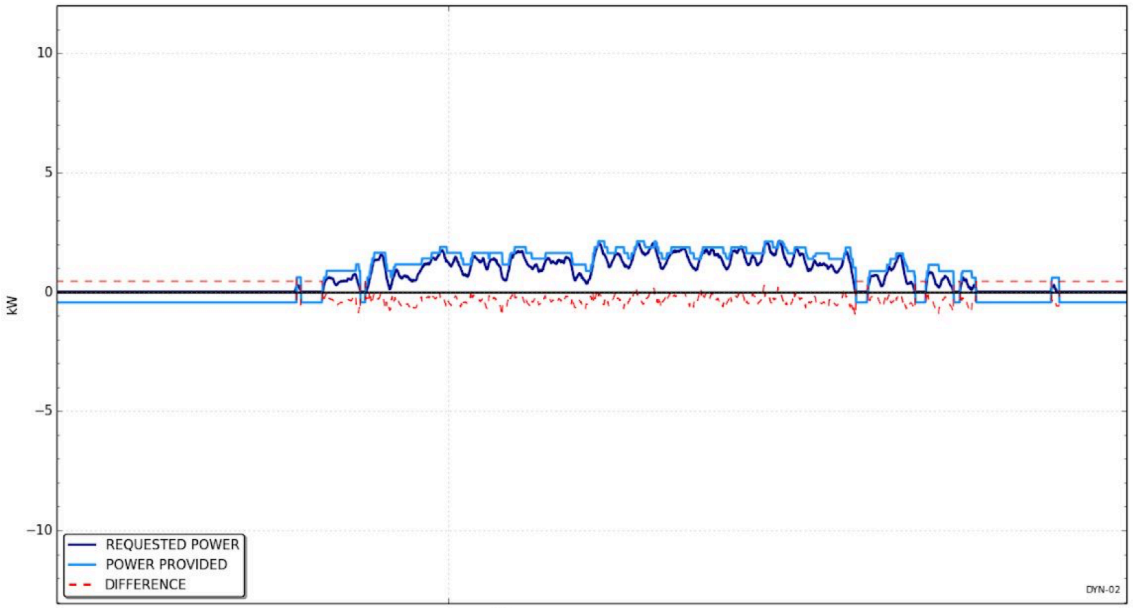

Figure 17: FCR-D provision from an EV [23]

One can assume that the frequency did not fall far below 49.9Hz, since the peak output delivered from the EV to the grid was only about 2kW, while the charger was rated at 10kW.

Regarding the viability of EVs providing FCR-D as a business case, Figure 18 shows the projected availability payments for FCR-D providers in some periods of 2017 and 2018 in DK2.

DK2			
Period	**FCR-D DK2 Price/MWh-h**	**Weekly Revenue/car@9.25 kW**	**Projected Yearly Revenue per car**
Feb 06-13, 2017	€4.02	€4.39	€228.17
May 22-29, 2017	€12.30	€13.43	€698.12
Aug 07-14, 2017	€8.27	€9.03	€469.39
Nov 06-13, 2017	€3.99	€4.36	€226.46
Jan 01 - Dec 31, 2017	€7.45		€457.13
Jan 01 - Oct 11, 2018	€19.56		€1,200.20

Figure 18: Projected FCR-D DK2 availability payments per year (2017-2018) [23]

According to the Parker project [23], the revenues for FCR-D were significantly lower than for FCR-N in 2017. However, as can be seen in the time period between January and October of 2018, in periods of extreme weather conditions, FCR-D availability becomes rather profitable. Additionally, FCR-D is very rarely activated, so for most of the time, providers of FCR-D will be able to charge their cars as usual, reducing wear and tear on their batteries. Also, with larger batteries in EVs both presently and in the future, the bidding capacity of each vehicle can increase greatly compared to EVs from 2017. With less inertia in future power systems, large frequency deviations will occur more often, and the importance and price of FCR-D availability will probably increase quite a bit.

3 Method

3.1 Modelling of an EV fleet

In reality, an EV fleet at a charging station will act as a load before the occurrence of a fault, since the EVs are charging. This means that the total EV fleet capacity is different for FFR and FCR-D upwards than for FCR-D downwards. In case of a decrease in frequency, the EV fleet as a provider of FFR/FCR-D upwards will go from charging to discharging, which means that it will increase its production by 2 times its charging/discharging capacity. In case of an increase in frequency, however, the EV fleet will not be able to provide FCR-D downwards unless there are EVs that are not charging at the occurrence of the fault or if the EVs are able to increase their charging speed/battery capacity usage. Therefore, the provision of FCR-D downwards will not be investigated in this thesis. Further, since the main challenge related to the reduced total system inertia of future power systems is the primary frequency control services, the provision of FCR-N from EVs will not be investigated either.

3.1.1 EV fleet capacity

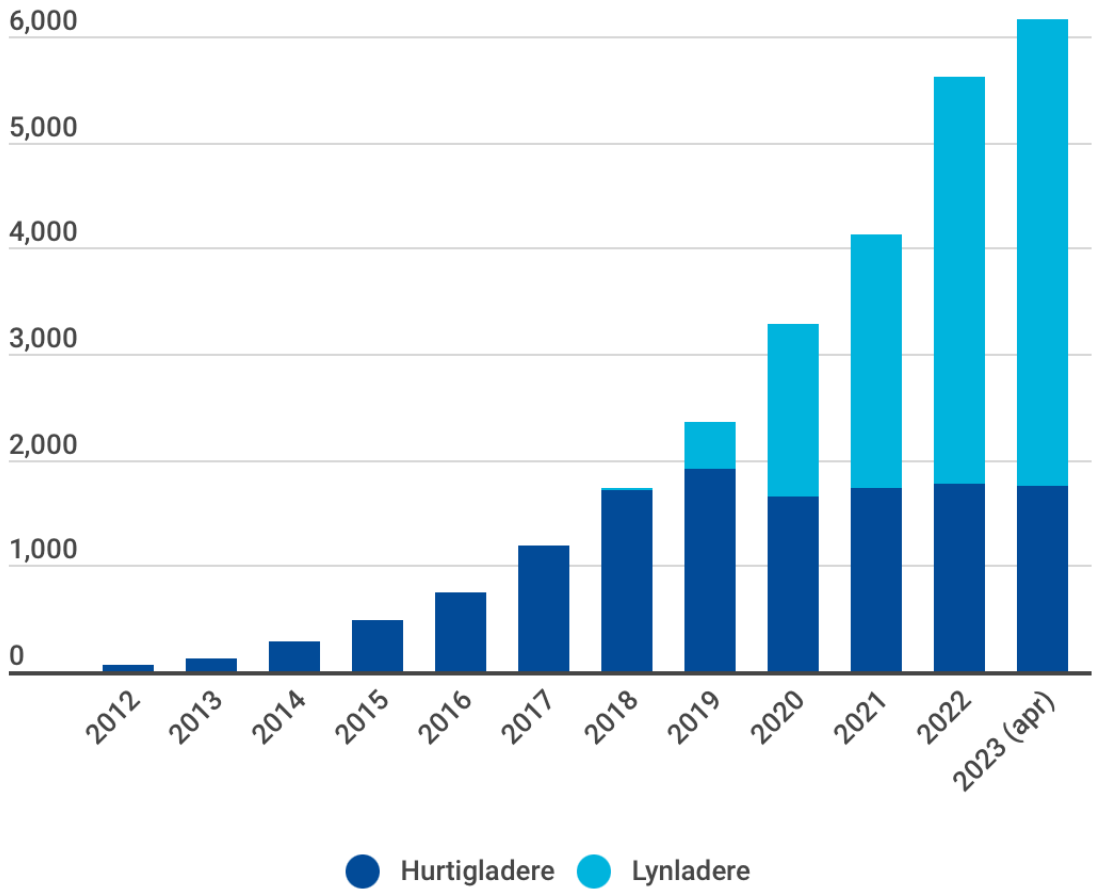

Figure 19: Number of high-speed EV chargers in Norway [25]

Figure 19 shows the number of high-speed EV chargers in Norway as of April 2023. There is a total of 4408 ”lightning-speed chargers” and 1749 ”high-speed chargers. Lightning-speed chargers are classified as chargers with a rated output of over 150kW while high-speed EV chargers have a rated output of 50kW - 150kW [25]. Based on Figure 19 and the assumptions that the average lightning-speed charger has an output of 200kW while the average high-speed charger has an output of 100kW, one can assume that the average rated output of a charger is as follows:

$$P_{EV} = \frac{4408 \cdot 200kW + 1749 \cdot 100kW}{6157} = 172kW$$

Further, by assuming that only 30% of an EV charging station is being used at any point in time, one can calculate the total capacity in Norwegian charging stations as follows:

$$P_{Fleet} = 172kW \cdot 6157 \cdot 0.3 \approx 300MW$$

Sweden, Denmark and Finland have fewer EVs than Norway. For the case of this thesis, it is assumed that Swedish EVs can provide 150MW, Finnish EVs can provide 100MW and Eastern Danish EVs can provide 50MW. This gives a total EV fleet capacity in the Nordic EPS of 600MW. However, if assuming that an EV fleet providing FFR or FCR-D will be able to go from charging to discharging, one could say that it is able to provide twice its rated charging/discharging power output relative to its power output before the fault occurred. Therefore one can assume a total EV fleet capacity in the Nordic EPS of 1200MW.

3.1.2 Modelling of an EV fleet as a provider of FCR-D upwards

When modeling an EV fleet as a provider of FCR-D, one must take into account the previously mentioned technical requirements of an FCR provider listed in Chapter 2.2.2. The most important points to take from these technical requirements revolves around the delay of the FCR provider and the total endurance requirement for full activation of FCR-D (20 minutes). Firstly, the delay of the FCR provided by an EV fleet can be estimated to be around 3 seconds according to the Parker project [23]. Secondly, it will be assumed that the total endurance requirement will be fulfilled. The reason for this is the fact that if an FCR-D event lasts for 20 minutes or longer, which is a highly unlikely scenario as secondary frequency reserves typically take over for the primary frequency reserves after only 30 seconds, the TSOs and the local system operators of the Nordic countries could potentially have fully charged EVs drive out to charging stations in order to maintain a sufficient total battery capacity in the EV fleet when other EV batteries become depleted.

The technical requirements regarding the provision of FCR [17] specify the following activation rates:

Product	100 % negative activation	0 % activation	100 % positive activation
FCR-D upward	N.A.	$f \geq 49.9$ Hz	$f \leq 49.5$ Hz
FCR-N	$f \geq 50.1$ Hz	$f = 50$ Hz	$f \leq 49.9$ Hz
FCR-D downward	$f \geq 50.5$ Hz	$f \leq 50.1$ Hz	N.A.

Figure 20: Activation rate [%] for FCR providers for deviation in frequency [17]

As previously mentioned, they also specify that each product can be provided either as a linear function of the frequency deviation or as an approximation of a linear function of the frequency deviation.

Regarding the procurement of FCR-D capacity in the Nordic EPS, one could assume a reference incident in the power system of 1500MW in both the negative and the positive direction. With this reference incident, the procured FCR-D reserves must be dimensioned to at least 1500MW. With the given initial distribution key of FCR (Figure 13), the Nordic countries must procure (approximately) the following amounts of FCR-D reserves:

- Norway: 575MW
- Sweden: 575MW
- Finland: 300MW
- Denmark: 50MW
- Total: 1500MW

So, when modeling an EV fleet as a provider of FCR-D upwards in DynPSSimpy, one could use a simple linear function of delivered power as a function of frequency deviation:

$$P(f) = P_{Fleet}[MW] \cdot \frac{f(t - t_{delay}) - 49.9Hz}{-0.4Hz}, \text{if } 49.9Hz \geq f \geq 49.5Hz \tag{15}$$

Where $t = 0$ at the instant of the occurrence of the fault, $t_{delay} = 3s$ and P_{Fleet} is twice the rated charging/discharging power of the EV fleet.

3.1.3 Modelling of an EV fleet as a provider of FFR

One of the most important and challenging aspects of providing FFR in an EPS is the requirements regarding activiation time. As previously mentioned, the Parker project [23] found a delay of about 3 seconds for EVs providing FCR-D. However, in order to be able to assess the performance of an EV fleet as a provider of FFR, it will be assumed that the EV charging stations providing FFR will have a full activation time of 0.7 seconds and no time delay.

With a full activation time of 0.7 seconds, the EV fleet is able to have a frequency activation level of 49.7Hz. As FFR is only provided for very small amounts of time

(minimum 5 seconds), the battery capacity and charging/discharging of the fleet will not have to be assessed. Therefore, long support duration (minimum 30s) can be provided. As previously mentioned, there is no limit in the rate of deactivation for entities providing long support duration. Further, the requirements regarding recovery of FFR reserves does not need to be assessed because of the large battery capacity of an EV fleet.

As mentioned in Chapter 2.2.1, Statnett has procured 150MW of FFR reserves in 2023. Taking the distribution key for the initial distribution of FFR reserves (Figure 10) into consideration, one will find that the Nordic countries must procure (approximately) the following amounts of FFR reserves:

- Norway: 150MW
- Sweden: 135MW
- Finland: 70MW
- Denmark: 30MW
- Total: 385MW

Since the total EV fleet capacity in the Nordic EPS is assumed to be around 600MW, all FFR reserves could in theory be procured from EV fleets. It will be assumed that the fleet will have a deactivation time of half its activation time.

$$P(f) = \begin{cases} \frac{P_{Fleet}[MW]}{0.7s} \cdot t, & \text{if } f \leq 49.7Hz \text{ and } t \leq 0.7s, \text{ (Activation time)} \\ P_{Fleet}[MW], & \text{if } f \leq 49.7Hz, \text{ (Support duration)} \\ \frac{-P_{Fleet}[MW]}{0.35s} \cdot t, & \text{if } f \leq 49.7Hz \text{ and } t_d \geq 0.35s, \text{ (Deactivation time)} \end{cases} \tag{16}$$

Where $t = 0$ at the instant of the occurrence of the fault, $t_d = 0$ at the instant when the frequency reaches 49.7Hz after having reached the point of the frequency nadir and P_{Fleet} is twice the rated charging/discharging power of the EV fleet.

3.2 Construction of the Nordic 45 test model

For several years, the Nordic EPS has been modelled as a 44 bus power system model called the Nordic 44 test model (N44). The current version of the N44 model has not been updated in several years. Therefore, in order to be able to run more precise simulations when evaluating whether or not EV Fleets could be used as FCR-D providers in the Nordic EPS, a new model has been made using the N44 model as a foundation. Having one bus more than N44, the new model is hereby called the Nordic 45 model (N45). The construction of the N45 model will be documented through this chapter, which also lays a foundation of information which could be useful when assessing the simulation results of Chapter 4.2.

Firstly, the motivation behind updating the N44 model will be discussed, before presenting the new and updated N45 model.

3.2.1 The Nordic 44 test model (old version)

The N44 model, shown in Figure 21, is an ”aggregated dynamic power system simulation model designed for analysis of dynamic phenomena in the Nordic power grid” [26]. It represents the connected EPS of Norway, Sweden, Finland and the eastern part of Denmark (DK2). The Danish part of the system is represented as loads/generators in the southern part of Sweden (Bus 8500, 8600 and 8700 of zone SE4).

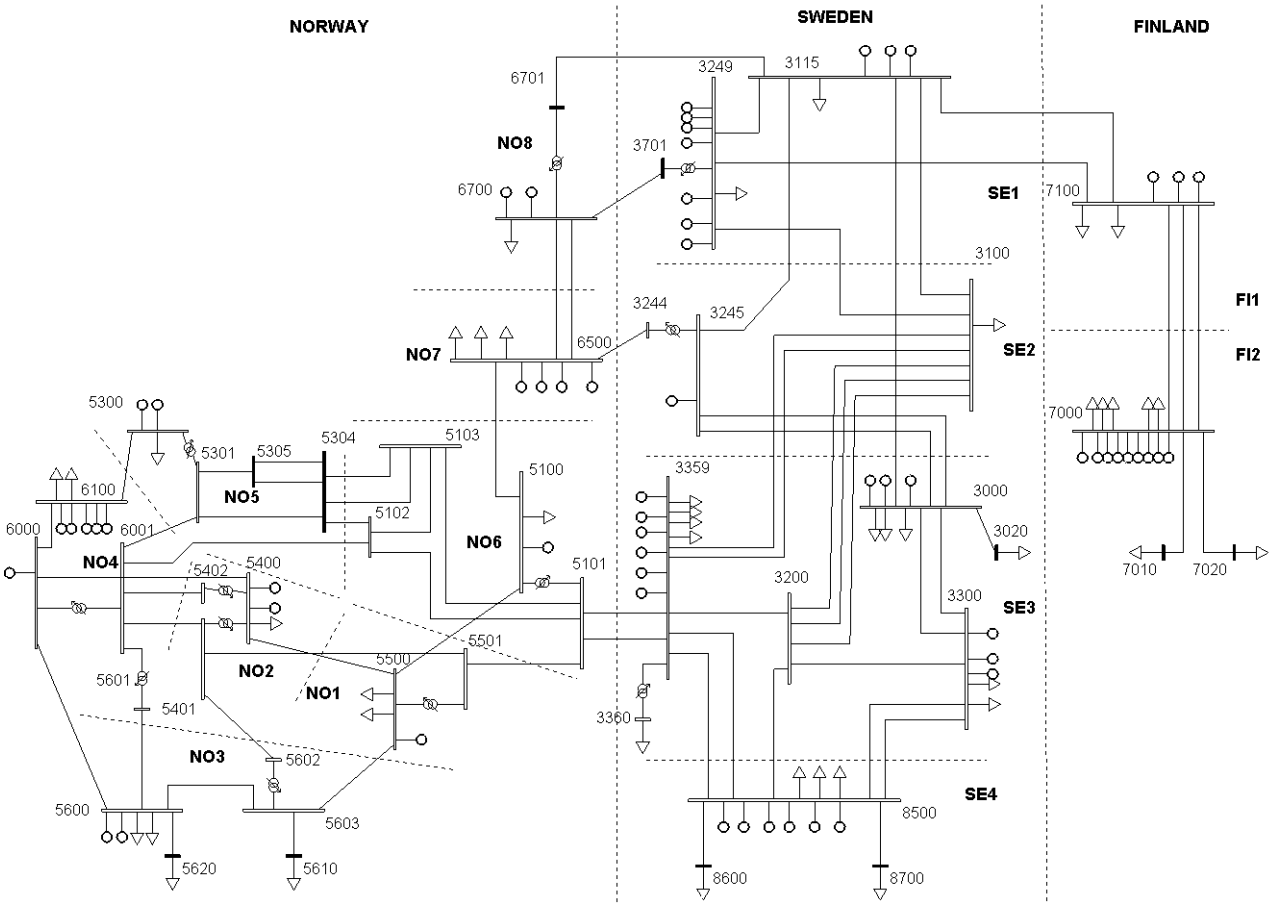

Figure 21: The Nordic 44 test model [27]

Figure 22 shows the voltage levels and the current topology of the Norwegian part of the N44 model. The first major issue with this model was the fact that many transmission lines which are now upgraded to 420kV were modelled as 300kV lines. The second major issue was the fact that a 420kV transmission line connecting the southern and northern parts of the Norwegian grid were not included in the model. This line connects Trondheim (Bus 6500 in Figure 22) to the major hydro power clusters of the western part of Norway, which greatly improves the transmission capacity between southern and northern Norway. Finally, the Norwegian Elspot areas have been updated since the construction of the N44 model, which means that Nordpool data (which uses the updated Elspot areas) will not be mapped correctly with the areas of the model.

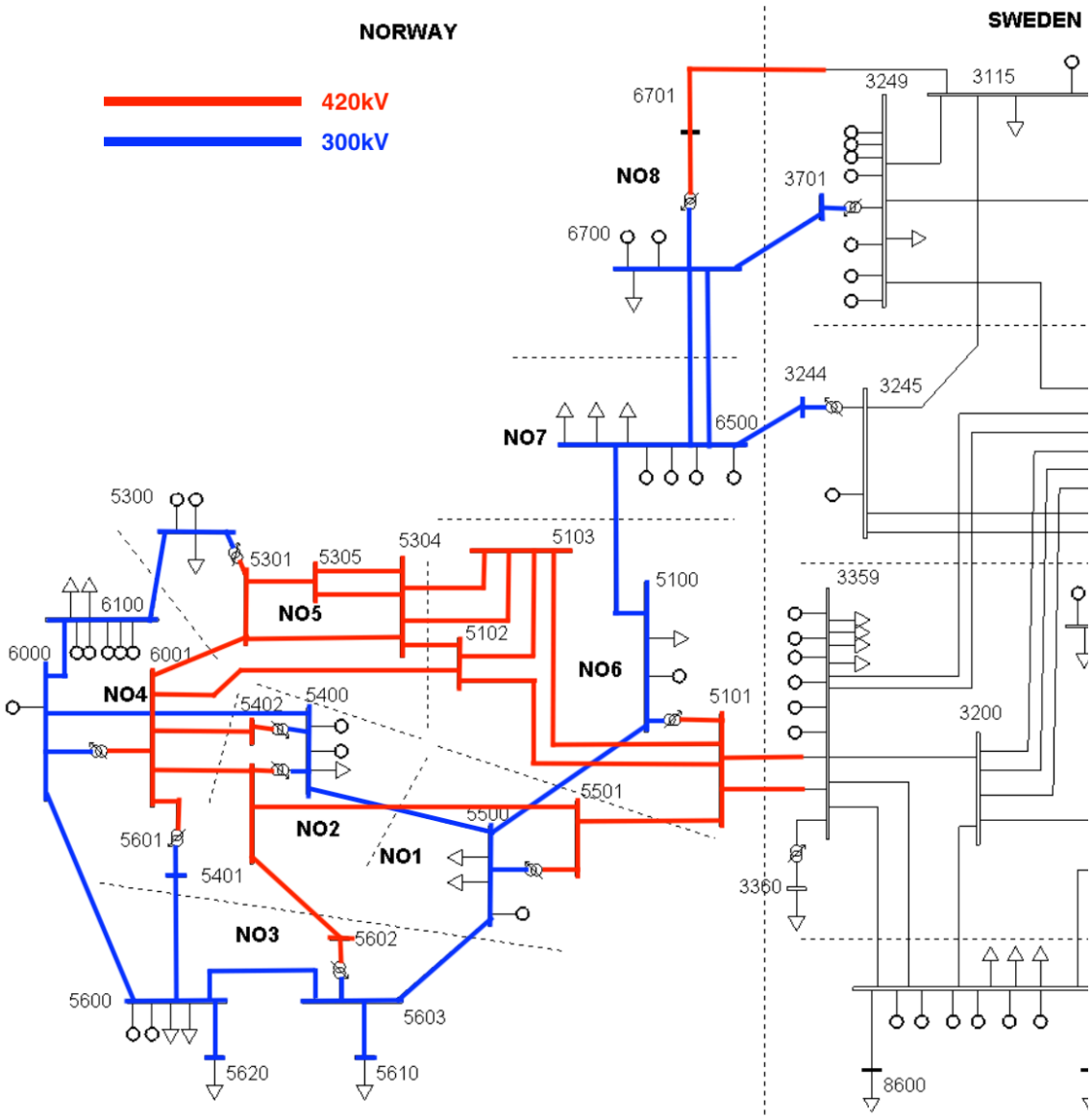

Figure 22: The Norwegian part of the Nordic 44 system [28]

3.2.2 The Nordic 45 test model (new version)

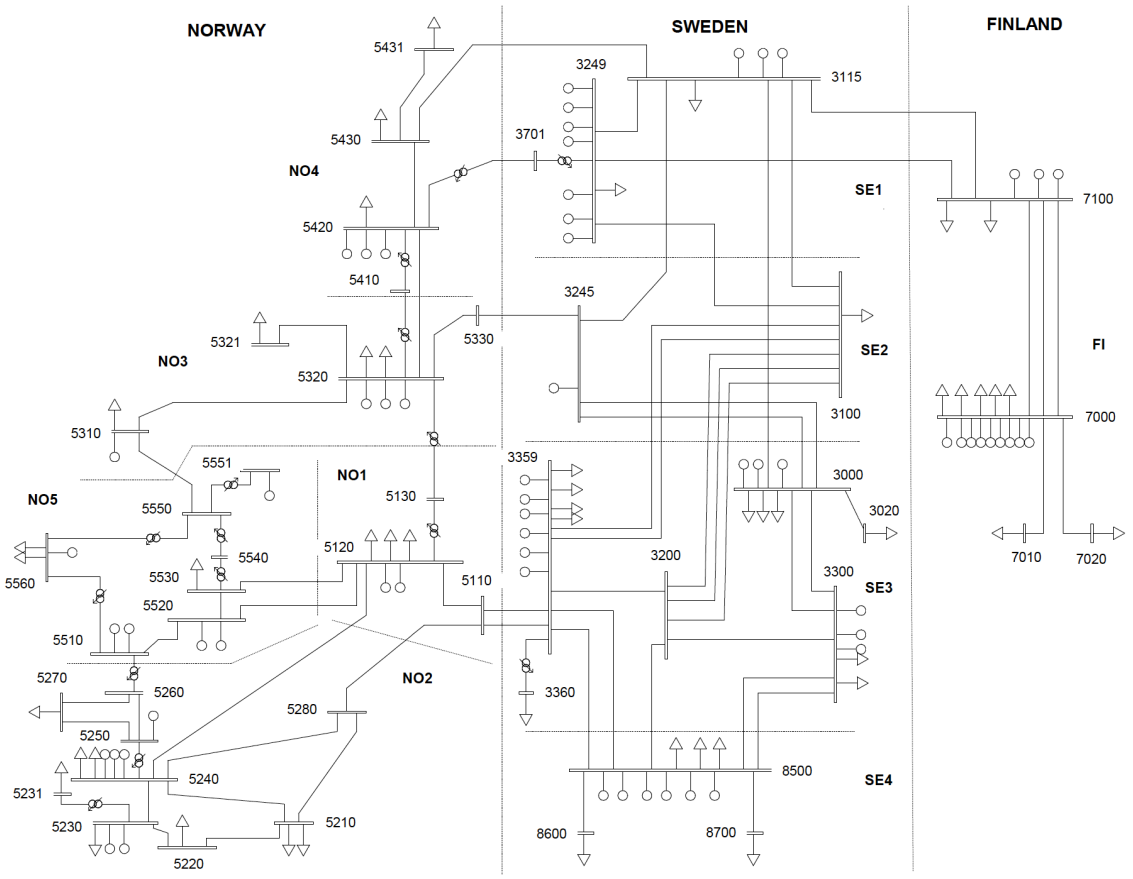

Figure 23: The Nordic 45 test model

The new model, depicted in Figure 23, uses the updated Elspot areas as well as an entirely reconstructed system topology in line with the Norwegian grid topology of 2021 [29]. As rebuilding the entire Nordic power system model from scratch would demand more time than a master thesis could provide, and as this thesis is mostly focused around analyzing the provision of FCR/FFR, only the Norwegian part of the grid has been rebuilt. As a consequence of the power system data from the chosen date and time in Nordpool, all generators and loads in the Swedish, Danish and Finnish parts of the system have been updated with new ratings and values. Additionally, due to low voltage magnitudes in the new model during the first power flow simulations, the line reactance of all transmission lines were lowered, which also affected lines in the Swedish, Finnish and Danish areas. Finally, all HVDC-connections in the Nordic EPS which was not included in N44 have been included in N45, while the other HVDC connections have had their ratings updated according to current values.

The loads and generation in the new model is updated and set according to data from Nord Pool [30] at the chosen date and time of 01.06.2022 between hours 11:00 - 12:00. These base-case parameters of the model can be found in Appendix C. Most of the export and import of the EPS is sent through HVDC connections, which are modelled as positive loads (import) or negative loads (export). An overview of all HVDC connections in the Nordic EPS is shown in Table 3. The AC transmission line connections from SE4 to DK2 and FI to RU are also modelled as loads.

Table 3: Overview of HVDC-connections in the Nordic EPS

HVDC Connection	Zones	From bus	Capacity	01.06.2022 [MW]
NordLink	NO2-DE	5230 (Tonstad)	1400MW	1436
North Sea Link	NO2-GB	5240 (Kvilldal/Holen)	1400MW	637
Skagerrak 1-4	NO2-DK1	5210 (Kristiansand)	1700MW	990
NorNed	NO2-NL	5220 (Feda)	700MW	0
Konti-Skan	SE3-DK1	3360 (Lindome)	550MW	714
SE4-DK2 (not HVDC)	SE4-DK2	8600 (Söderåsen)		449
FI-RU (not HVDC)	FI-RU	7020 (Yllikkälä)		0
SwePol	SE4-PL	8700 (Kruseberg)	600MW	344
Baltic Cable	SE4-DE	8600 (Stärnö)	600MW	175
NordBalt	SE4-LT	8700 (Nybro)	700MW	413
Fenno-Skan 1 & 2	SE3-FI	3020 / 7010	1300MW	450
Estlink 1 & 2	FI-EE	7020	1000MW	514

With a new model representing the Norwegian part of the EPS, the production and consumption in each area must be allocated to new generators and loads. In the previous version of N44, there was a total of 20 generators and 15 loads in Norway. In the new model there is a total of 21 generators and 21 loads. Most of the loads are located at buses representing large cities, such as Oslo, Bergen and Trondheim. The generation is located at buses representing areas with large amounts of hydro power. The loads and the generation in the Swedish and Finnish parts of the model have simply been scaled up or down according to the consumption and generation values in each area as specified in the data from Nord Pool at the chosen date and time.

A couple of changes were made to the Swedish and Finnish parts of the system. The SE4-DK2 transmission line and the Baltic Cable was set to bus 8600 while the HVDC lines NordBalt and SwePol was set to bus 8700. Also, Finland was previously divided into two zones (FI1 and FI2). Currently however, Finland consists of only one zone (FI), so this has been updated in the model.

After having built the new system in PSSE, the power flow between the Elspot areas was far from similar to the actual power flow recorded in Nordpool. One reason for this was the fact that losses in transmission lines and transformers had not been taken account of when assigning load values in the model. Therefore, the first load values were lowered in order to take account of transmission losses. Secondly, and most importantly, the power flow between the systems were incorrect. In order to make the power flow in the model similar to the power flow recorded in Nordpool, the transmission line reactances throughout the model was changed. The new line reactances are probably not very realistic as they were only changed for the sake of achieving the specific power flow from Nordpool, but they do provide the correct power flow which gives a good snapshot of the state of the Nordic EPS in that instant. Tables 4 and 5 shows the power flow in PSSE compared to the actual power flow from Nordpool before and after altering the transmission line reactances of the model.

Table 4: Power flow before updated line reactances

[MW]	Nordpool	PSSE	Difference
SE1-FI	1175	1198	-23
SE3-FI	450	450	0
SE1-SE2	1629	1486,3	142,7
SE2-SE3	6283	5234,5	1048,5
SE3-SE4	3061	3111	-50
NO4-SE1	257	98,5	158,5
NO3-SE2	369	-414	783
NO1-SE3	50	765,1	-715,1
NO4-NO3	649	726,3	-77,3
NO3-NO1	369	958	-589
NO3-NO5	523	790,5	-267,5
NO1-NO2	988	85,1	902,9
NO5-NO2	654	1612,6	-958,6
NO5-NO1	2026	1316,7	709,3

Table 5: Power flow after updated line reactances

[MW]	Nordpool	PSSE	Difference
SE1-FI	1175	1176	-1
SE3-FI	450	450	0
SE1-SE2	1629	1639	-10
SE2-SE3	6283	6267	16
SE3-SE4	3061	3061	0
NO4-SE1	257	265	-8
NO3-SE2	369	345	24
NO1-SE3	50	64	-14
NO4-NO3	649	643	6
NO3-NO1	369	377	-8
NO3-NO5	523	528	-5
NO1-NO2	988	987	1
NO5-NO2	654	653	1
NO5-NO1	2026	2032	-6

After the model was complete and the power flow was as desired, the model was incorporated into DynPSSimpy in order to perform dynamic simulations. It is possible to perform dynamic simulation in PSSE as well, but DynPSSimpy offers more flexibility in the sense that it is possible to very easily access and tune all elements of the system. Further, since DynPSSimpy is a software which runs directly in Python, both the model data and the simulation cases are run within the same program, making it possible to set up highly specific simulation cases while also having access to all types of component properties and dynamic data of the system.

3.2.3 Tuning

In order for the model to better represent the production scenario at the given time and date of 01.06.2022 between hours 11:00 - 12:00, some modifications was made after moving the model to DynPSSimpy.

As explained in Chapter 2.1.1, the inertia constant (H) of a generator describes the ratio of kinetic energy stored in the rotating masses of the generator to its MVA rating (Eq. 3). This means that the total amount of kinetic energy in the system, which breaks the initial drop of a frequency decrease, is a product of the total amount of inertia in the system. The dynamics of the system following an outage of production or load can be expressed as the dynamics of a lumped machine with an inertia constant H_{sys} which is the weighted sum of the inertia constants of all generators in the EPS [14]:

$$H_{sys} = \frac{\sum_{i=1}^{N_g} H_i S_{ni}}{\sum_{i=1}^{N_g} S_{ni}} \tag{17}$$

where N_g is the number of connected generators in the EPS.

According to an ENTSO-E project which analyzed the frequency behaviour in the Nordic

EPS [31], the kinetic energy in the Nordic EPS in 2025 will stay above 150GWs for 90% of the time. Also, according to data from Fingrid (the Finnish TSO), the kinetic energy in the Nordic EPS between hours 11:00 - 12:00 on 01.06.2022 was about 180GWs [32].

Therefore, in order to reduce the total kinetic energy (inertia) of the N45 model to this level, the inertia constant of all governors were reduced by 1. Previously, the inertia constants were set according to the values in Table 1. This means that the inertia constant of nuclear power plants went from 6 to 5 and the inertia constants of the hydro power plants went from 3 to 2. This led to a total of 183.5GWs of kinetic energy in the system.

The total frequency bias of the N45 system can be calculated in two ways. Firstly, the nominal frequency bias of all generation units can be calculated (using Eq. 13) before being summed up into one value representing the frequency bias of the whole EPS. Alternatively, a load event can be simulated in order to find the deviation in frequency after the primary frequency control is finished [2].

Nominal frequency bias

There are a total of 46 generators in the N45 system distributed among the 45 buses. Table 6 is an overview of where the generators are located as well as their rated power and droop.

Table 6: Generator overview

Bus	Area	Rated Power [MW]	Droop	Frequency bias [MW/Hz]
3000	Sweden	2200	0.35	126
3115	Sweden	2800	0.12	467
3245	Sweden	7000	0.12	1167
3249	Sweden	3200	0.12	533
3300	Sweden	5100	0.35	291
3359	Sweden	6000	0.12	1000
5120	Norway	3000	0.12	500
5230	Norway	2600	0.12	433
5240	Norway	3900	0.12	650
5250	Norway	1300	0.12	217
5310	Norway	1400	0.12	233
5320	Norway	4200	0.12	700
5420	Norway	4800	0.12	800
5510	Norway	2000	0.12	333
5520	Norway	2000	0.12	333
5551	Norway	1000	0.12	167
5560	Norway	1000	0.12	167
7000	Finland	8400	0.35	480
7100	Finland	1800	0.12	300
8500	Denmark	1800	0.35	103
-	Whole EPS	-	-	**9000**

Typically, the hydro power plants in Norway and Sweden are the main contributors to primary frequency control in the Nordic EPS as they represent the largest share of

the power mix. Thermal generators, on the other hand, will typically not be part of the primary frequency control. This is the reason why the thermal generators have a rather high droop setting, so that they take less part in the provision of frequency reserves.

Buses 3300 and 3359 represent nuclear power plants in the south of Sweden (Forsmark and Ringhals), bus 7000 represents nuclear power plants in the south of Finland (Loviisa and Olkiluoto) and bus 8500 is an equivalent of the EPS of Sjelland in Denmark [2].

Simulated frequency bias

In order to find the frequency bias of the EPS through simulation, a load of 1000MW was added to bus 3359, which is located near the border separating NO1 from SE3.

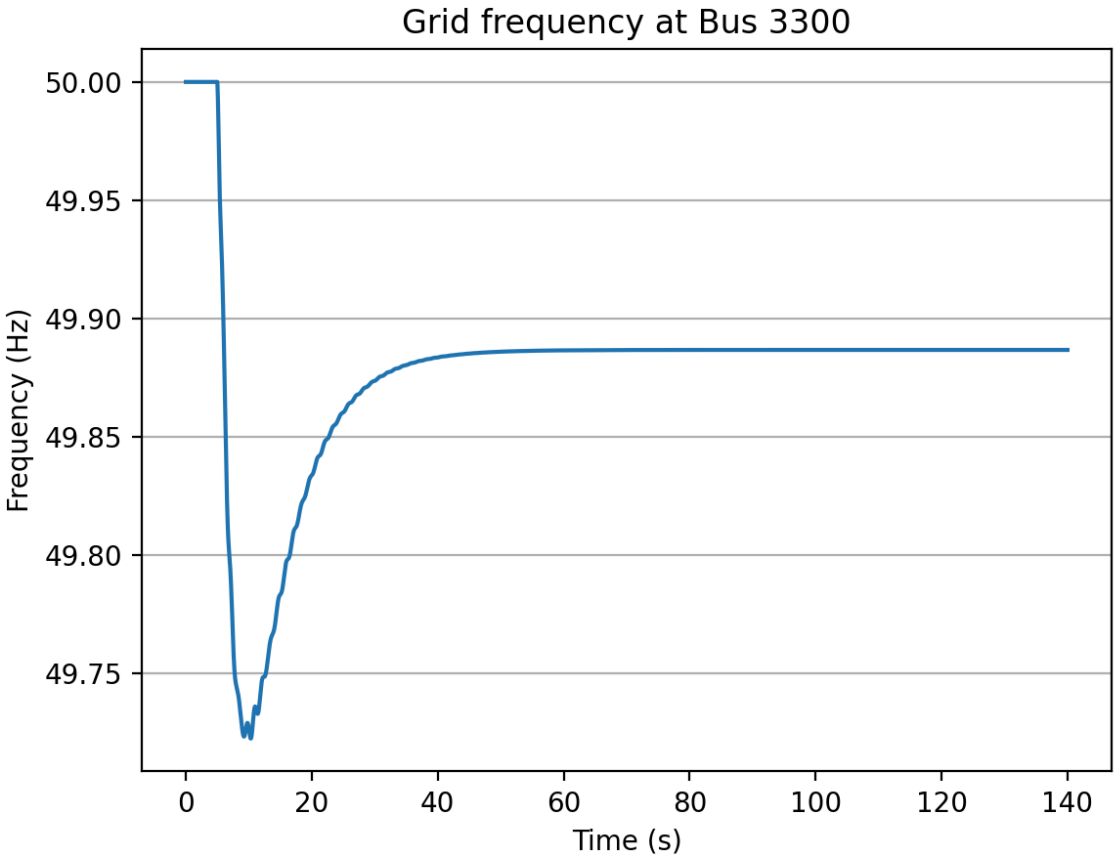

Figure 24: Frequency after fault

The simulation resulted in a decrease in frequency as shown in Figure 24. The increased load of 1000MW led to an increased total production of 989.5MW after the primary frequency control was finished, and the frequency decreased by 0.113Hz. This gives a simulated frequency bias of (using Eq. 13):

$$K_f = \frac{\Delta P}{\Delta f} = \frac{989.53266MW}{0.11323} = 8739MW/Hz \tag{18}$$

The simulated and nominal frequency bias are rather similar, which to a certain degree validates the dynamics of the simulated system.

3.2.4 Construction process

This chapter will go through the construction process of the Nordic 45 model. This is done both in order to provide some sort of a guide for anyone wanting to perform further updates on the model, but also in order to provide transparency regarding the methods behind this process. As part of the work on this thesis, a considerable amount of time was spent building the Nordic 45 model in PSSE, which could certainly have been shortened had there been some documentation regarding the construction process of the Nordic 44 model. Of course, there may be some documentation regarding this somewhere, but in that case it was simply not found.

Firstly, the PSSE file of the Nordic 44 model was used as a blueprint. This was a fully functional model with a converged load flow, meaning that the provided data of generators, loads, lines and system topology was good enough that PSSE was able to produce a load flow scenario within acceptable limits.

A general recommendation regarding the process of adjusting or building models in PSSE is to continuously run load flows and check that they converge after having performed any alteration of the model. By doing this, any errors in the system can be identified and isolated when they occur, making them much easier to handle compared to when there are multiple errors without any known cause. Whenever the load flow does not converge, there could be an error in the system, and it can be solved if needed. It must be kept in mind, however, that even though the load flow does not converge, there isn't necessarily any mistakes in the alteration that was performed. For example, if the load flow converged at the previous step of the building process, where there were 500MW of export to the area which is being built upon, that volume of export should be kept intact in the following step as well. Therefore, by keeping track of the export and import between areas, which keeps the power balance of the system at bay, the load flow is much more likely to converge. Load flows were run continuously throughout the construction of the N45 model, which ”approved” the new system topology step-by-step until it was finished.

Step 1 - Drawing the Norwegian part of the model

Before launching PSSE, the first step of reconstructing the Norwegian part of the N44 model was to draw a new and updated system topology. As mentioned earlier, this drawing was heavily inspired by Statnett's (the Norwegian TSO) drawing of the Norwegian grid topology of 2021 [29]. However, the topology could not be too detailed, as it would strain the performance of PSSE as well as leading to an increased complexity which would make it more difficult for the users of the program to interpret the results of their simulations. Further, the most important characteristics of the Norwegian EPS had to be identified and brought in to the model. This included elements like the major 420kV transmission line corridors, the hydro power clusters of the western part of Norway, the location of the HVDC lines in southern parts of Norway and the transmission lines connecting Norway and Sweden.

While the Norwegian buses had previously been given numbers such as 5xxx (for example 5401) or 6xxx (for example 6100), no pattern was found regarding the naming, so a new naming scheme was made (only for the Norwegian buses). For the first digit, the number 5 was used since it was used for most of the Norwegian buses in the N44

model. The second digit refers to the Elspot area where the bus is located, which is a number from 1 to 5. The third and fourth digit are just used for pure numbering of the buses. So, for example, the first bus in Elspot area 3 is called 5310, while the second bus is called 5320 and so on. For smaller satellite buses, they use the fourth digit, so a satellite bus connected to bus 5310 gets the name 5311.

All buses were also given the name of their real-life location in addition to their bus number in PSSE in order to make it easier for other users to be able to understand the system topology. This could for example be valuable in case the transmission line values of the model is to be updated later on, where the distance between the locations of the buses is important.

Step 2 - Removing the Norwegian part of the model

After launching PSSE, the first step of updating the model was quite simply to remove the part which was to be updated. This was done by deleting all PSSE data of the Norwegian part of the system, while the Swedish, Finnish and Danish parts of the system remained unchanged. Then, after incorporating the updated HVDC lines into the model, the production and consumption of the Swedish, Finnish and Danish parts of the system was updated according to the data from Nord Pool. This was mainly done in Excel, as the previous generator- and load data was just scaled up or down by a given factor which made the total production and consumption of each area equal to the one found in Nord Pool.

Luckily, after having removed the Norwegian part of the system and having updated the Swedish, Danish and Finnish parts, the load flow converged. One of the reasons it converged so easily without the Norwegian part was probably the fact that there were previously very little transmission of power between Norway and Sweden, causing little change to the power balance and system dynamics after this alteration.

As a side note, in case an entire PSSE model is to be updated, it is recommended that the different parts of the model is removed and rebuilt part by part, so that there is always an intact part of the model where the load flow converges. This could be easier than rebuilding the entire model from scratch without knowing whether the load flow of the complete model will converge or not.

Step 3 - Constructing the Norwegian part of the model

The Norwegian part of the model was rebuilt step by step, by adding a transmission line, adding a bus, adding generation and/or consumption on the bus and performing a load flow. Here are some notes regarding the modelling choices that were made:

The reactive load at each bus was set so that the total reactive load in each Norwegian zone in N45 was equal to the total reactive load in each Norwegian zone in N44. For this thesis, where the dynamics of primary frequency control is analyzed, the dynamics surrounding the reactive production and consumption of the model is not very important, hence it has not been put a lot of effort into.

The choice of generator settings were performed using the following strategy:

P_{gen} was set to the desired value (from Nordpool data).

P_{max} was set to $P_{gen}/0.85$.
M_{base} (S_n) was set to $P_{max}/0.8$.
Q_{max} was set to $0.6 \cdot M_{base}$.

Hence, the active power generation of each generator determined all the other generation data.

Initially, the transmission line resistance, reactance and susceptance was based on one of the already existing transmission lines which length was approximately known. Then, depending on the rated voltage of the transmission line and its approximate length, the values were scaled up or down. However, in order to obtain the desired power flow in the system, most of the transmission lines between the different areas in the model had their reactance changed.

Later on, it was discovered that some of the voltage levels at the buses in the N45 system were so low that it affected the stability of the system. Therefore, in order to increase the voltage levels, all transmission line resistances, reactances and susceptances were multiplied by a factor of 0.6.

Step 4 - Initiating dynamic simulation

Finally, after having obtained the desired power flow in the system, the dynamic simulation had to be initialized before moving the model over to DynPSSimpy. Being able to initialize the dynamic simulation in PSSE meant that the model would be more likely to successfully run in DynPSSimpy. Since DynPSSimpy does not have any graphical interface, it is much easier to identify errors and faults in the model when using PSSE.

In PSSE, in order to initialize a dynamic simulation, the initial conditions must be within acceptable limits. For example, this means that the speed of a generator must not be accelerating when there is a power balance in the system, as this indicates that something is wrong in the model data. When trying to initialize a dynamic simulation on the N45 model, there were many initial conditions which were not within acceptable limits. It was very challenging to find out what caused these issues, but after some days of trial and error, the problem was identified. Apparently, the source reactance of the generators in the model were not set to the same value as the subtransient reactances in the generator models of the dynamic simulation. After having fixed this, all initial conditions were within limits, and the dynamic simulation was initialized. This meant that the model could be transferred over to DynPSSimpy.

Step 5 - Moving the Nordic 45 model from PSSE to DynPSSimpy

When constructing the Nordic 45 model in DynPSSimpy, an Excel sheet was made in order to be able to efficiently transform PSSE data into DynPSSimpy data. This data included information such as the base MVA rating of the system, the system frequency, the name of the slack bus and component data for all buses, lines, transformers, loads and generators.

Generators which were inactive ($P = 0$) in the PSSE version of the model were removed in the DynPSSimpy version. All generators in Norway, Northern Sweden and North-

ern Finland were given HYGOV governors, made to represent the governors of hydro power generators. All generators in Southern Sweden (including Eastern Denmark) and Southern Finland were given TGOV governors, made to represent the governors of thermal generation units. Also, all generators with governors were given AVRs.

3.3 Kundur's two-area power system model (K2A)

In order to showcase the benefits of providing FCR-D upwards and FFR in an EPS, the K2A system will be used. The K2A system is a simple two-area power system model which has one heavily loaded area and one lightly loaded area with a weak tie between the two areas. The transmission system nominal voltage is 230kV while the distribution system nominal voltage is 20kV.

All relevant data for generators, loads, transformers and lines can be found in Appendix A.

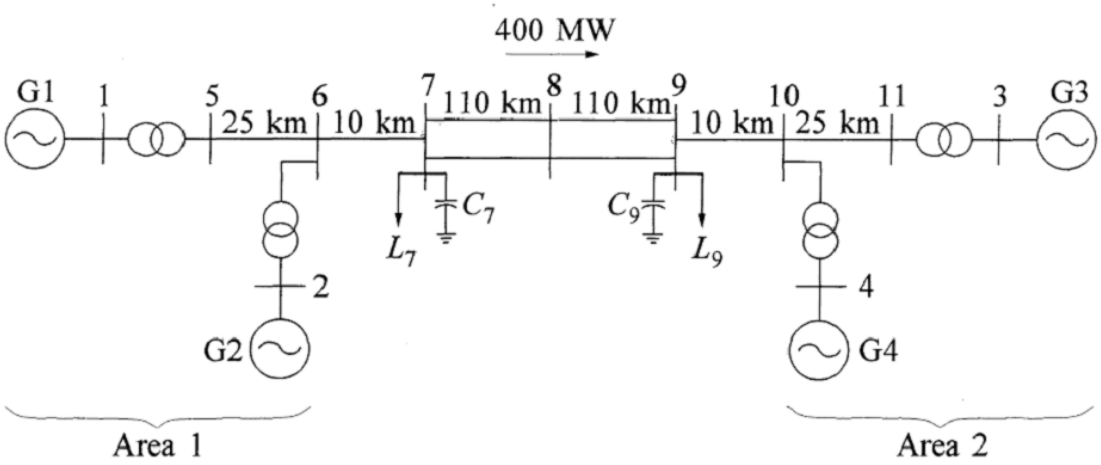

Figure 25: Kundur's two-area power system model [33]

Modified K2A

A modified version of the K2A model has been made in order to better highlight the effect of the EV fleets providing FCR-D and FFR.

Firstly, the base version of the K2A model, with no governors, automatic voltage regulators or power system stabilizers, was almost voltage instable. Therefore, the modified version uses shorter transmission lines in order to increase the robustness of the model. Additionally, two extra buses were made in order to represent the EV fleets in each area. These buses (6_{EV} and 10_{EV}) have a nominal voltage of 110kV and are connected to bus 6 (Area 1) and bus 10 (Area 2) via transformers (110kV/230kV).

The EV fleets are represented by a voltage source converter (VSC) model which is found in the model library of DynPSSimpy. This model imitates a VSC-controlled power source, such as an HVDC-line or a battery.

In order to better showcase the effect of the EV fleets, the total inertia in the system has been reduced. This has been done by decreasing the nominal power of the generators by a factor of 0.8, which leads to a drop in their production by 563.8 MW. The loads in the system have not been decreased, so in order to maintain the power balance in normal system operation, an HVDC-cable importing 563.8 MW has been simulated by adding a constant power input from the VSC model at bus 8. This also makes the model a better representation of future power systems, where a higher penetration of IRES and days with large import from HVDC-cables in the system leads

to lower amounts of traditionally provided inertia.

The governors of generators 1 and 2 are modelled as HYGOV governors with a droop of 6%, while generators 3 and 4 use TGOV1 models with a droop of 12%. All generators also have automatic voltage regulators modelled as simple excitation systems (SEXS).

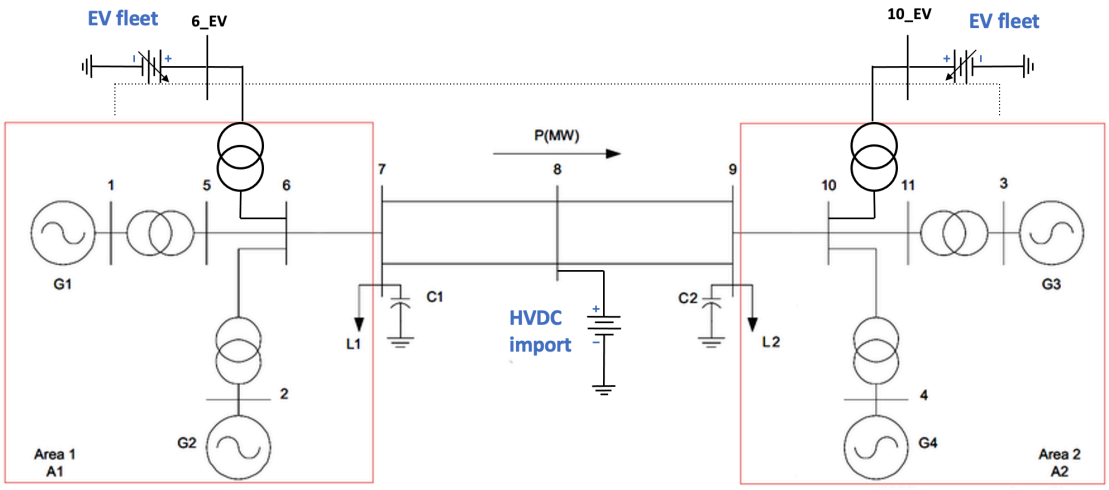

Figure 26: Modified K2A model (base figure taken from [34])

All relevant data for generators, loads, transformers and lines can be found in Appendix B.

Modelling of the EV fleet

Finally, the EV fleet as a provider of FCR-D upwards uses Eq. 19 as its power output control function with a P_{Fleet} value of 70MW (5 % of the nominal reference incident) and different time delays. Similarly, the EV fleet as a provider of FFR uses Eq. 16 as its power output control function with a P_{Fleet} value of 70MW.

$$P(f) = 70[MW] \cdot \frac{f(t - t_{delay}) - 49.9Hz}{-0.4Hz}, \text{if } 49.9Hz \geq f \geq 49.5Hz \tag{19}$$

$$P(f) = \begin{cases} \frac{70[MW]}{0.7s} \cdot t, & \text{if } f \leq 49.7Hz \text{ and } t \leq 0.7s, \text{ (Activation time)} \\ 70[MW], & \text{if } f \leq 49.7Hz, \text{ (Support duration)} \\ \frac{-70[MW]}{0.35s} \cdot t, & \text{if } f \leq 49.7Hz \text{ and } t_d \geq 0.35s, \text{ (Deactivation time)} \end{cases} \tag{20}$$

As mentioned earlier, an EV fleet providing FFR or FCR-D upwards will be able to go from charging to discharging, which in practice means that its power output will be twice as large as its rated power of charging/discharging (relative to its power output before the fault). In these simulations, the P_{Fleet} value of 70MW can therefore be seen as twice the charging/discharging capability of the fleet (35MW).

Scenario Topologies

The simulations on the K2A model will be performed in three different scenarios:

- Scenario 1: EV fleet placed in Area 1.
- Scenario 2: EV fleet placed in Area 2.
- Scenario 3: EV fleets placed in both Area 1 and Area 2.

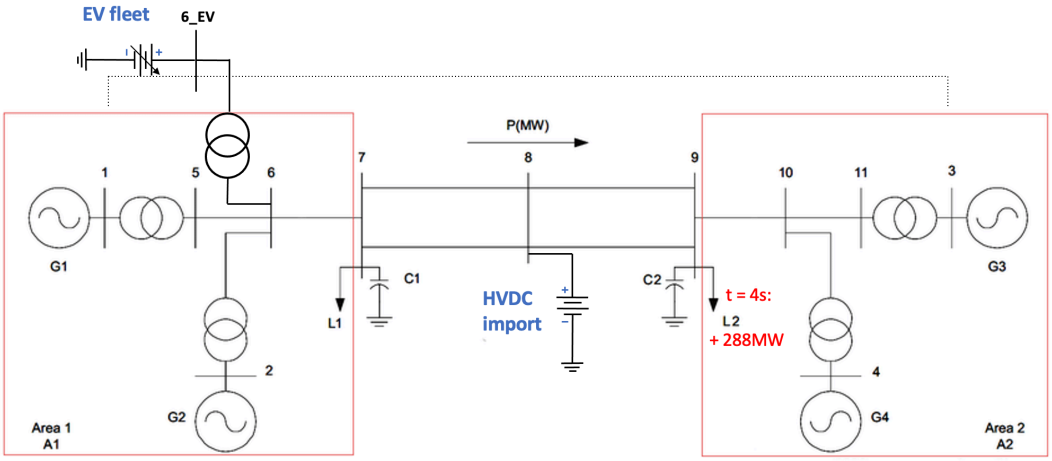

Figure 27: Scenario 1 - EV fleet in Area 1

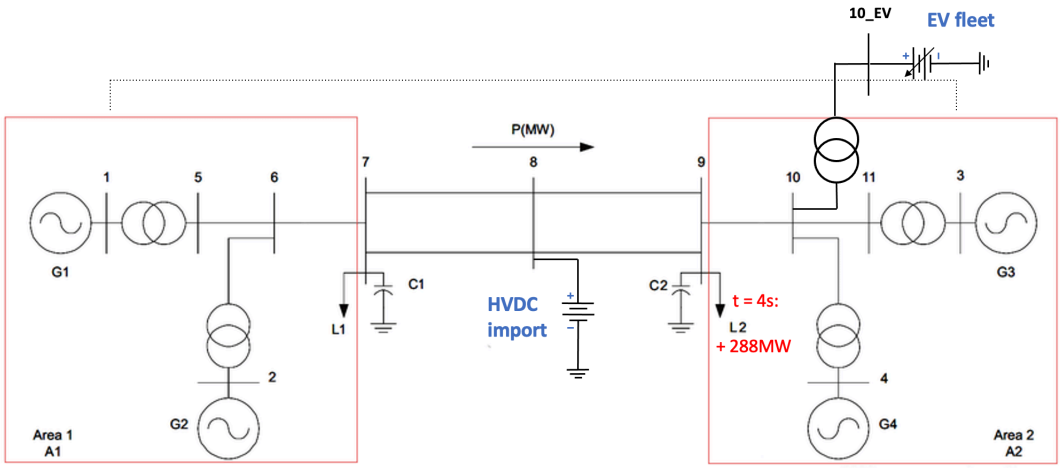

Figure 28: Scenario 2 - EV fleet in Area 2

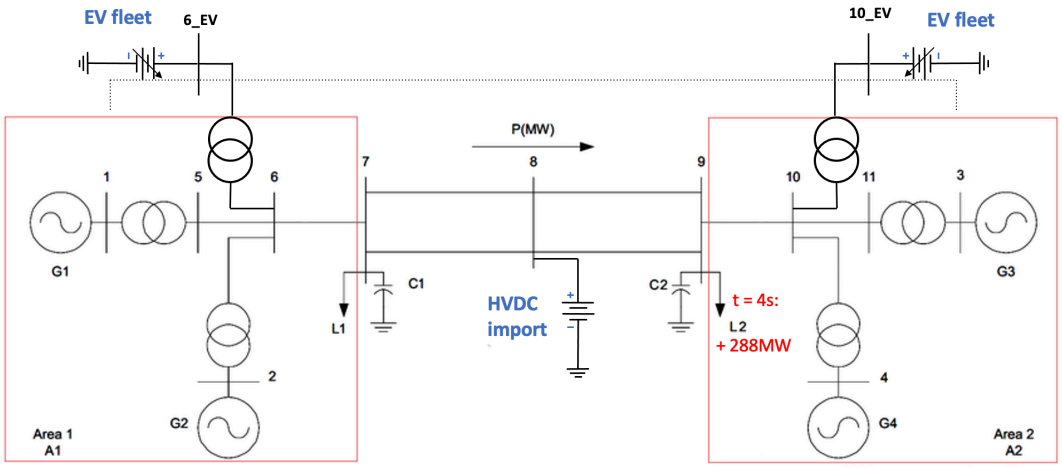

Figure 29: Scenario 3 - EV fleet in both Area 1 and Area 2

3.3.1 Cases

For each case, a load of 288MW will be added at bus 9 at $t = 4s$.

Case 1 - FCR-D without time delay

In order to get a good idea of how the location of the EV fleets affects their performance as providers of FCR-D upwards, they are modelled as simply as possible without having any time delay. Additionally, this case shows how the provision of FCR-D upwards in an EPS helps reduce the frequency drop.

Case 2 - FCR-D with time delay

Realistically, the EV fleet as a provider of FCR-D upwards would have a time delay, which in this simulation is set to 3 seconds. Only the results from Scenario 3 will be shown here as this scenario is best at showing the effects that an increased time delay has on the frequency response of the EPS.

Case 3 - FFR with short deactivation time

When simulating the provision of FFR from EV fleets, the fault was increased from 288MW to 504MW. This was done in order to cause the frequency to drop further than 49.5Hz, which makes it easier to see the effect of the deployment of FFR provision. In order to show the deactivation dynamics of the FFR reserves, the minimum support duration for the provision of FFR was not assessed in these simulations.

Case 4 - FFR with long deactivation time

In this case, the effect of increasing the deactivation time of the EV fleet from 0.35 seconds to 10 seconds is analyzed.

Case 5 - FFR with step-wise deactivation

As the EV fleet in this simulation is modelled as a 35MW EV fleet which is charging at rated power at the occurence of the fault, it is able to ”provide” 70MW of FFR reserves by going from 35MW of charging to 35MW of discharging. Therefore, this case will analyze the effect of using a step-wise deactivation of the EV fleet where the fleet goes from charging, to not charging, to discharging. This means that in order to reduce the frequency drop after deactivation, the following power output control function will be used:

$$P(f) = \begin{cases} \frac{P_{Fleet}[MW]}{0.7s} \cdot t, & \text{if } f \leq 49.7Hz \text{ and } t \leq 0.7s, \text{ (Activation time)} \\ P_{Fleet}[MW], & \text{if } f \leq 49.7Hz, \text{ (1st support duration)} \\ P_{Fleet} - \frac{P_{Fleet}[MW]}{10s} \cdot t_{d1}, & \text{if } f \leq 49.7Hz \text{ and } t_{d1} \leq 5s, \text{ (1st deactivation time)} \\ \frac{P_{Fleet}}{2}[MW], & \text{if } f \leq 49.7Hz, \text{ (2nd support duration)} \\ \frac{P_{Fleet}}{2} - \frac{P_{Fleet}[MW]}{10s} \cdot t_{d2}, & \text{if } f \leq 49.7Hz \text{ and } t_{d2} \leq 5s, \text{ (2nd deactivation time)} \end{cases} \tag{21}$$

Where $t = 0$ at the instant of the occurrence of the fault, $t_{d1} = 0$ at the instant when the frequency reaches 49.7Hz the first time (when rising) and $t_{d2} = 0$ at the instant when the frequency reaches 49.7Hz the second time (when rising). P_{Fleet} is twice the rated charging/discharging power of the EV fleet.

3.4 The Nordic 45 test model (N45)

In order to analyze the use of EV fleets as providers of FCR-D upwards and FFR in the Nordic EPS, the N45 model as presented in Chapter 3.2.2 will be used. Additionally, by setting up an extreme scenario within the Nordic EPS, the effects of providing frequency reserves from distributed reserves such as EV fleets versus centralized reserves such as large generators or large industrial consumers may be analyzed. Chapter 3.4.1 will go through some aspects and details about the scenario.

3.4.1 Extreme scenario

Arguably, the largest advantage of using distributed reserves instead of centralized reserves is the fact that bottlenecks in the power flow of the transmission system could be avoided. Therefore, simulating an extreme, but still realistic, scenario in the Nordic EPS could highlight how big of an advantage this potentially is.

In short, the extreme scenario will have maximum export of power from Norway to Sweden before a fault in the Northern part of Finland occurs. With power reserves located in Norway, Sweden, Finland and Denmark, this will lead to an overload of the transmission lines between Norway and Sweden. 15 seconds after the occurrence of the fault in Finland, one of the two lines connecting Southern-Norway to Southern-Sweden will trip, leading to a further overload of the remaining transmission lines connecting the two countries. The following subchapters will provide further details regarding the scenario.

Transmission capacity from Norway to Sweden

The transmission capacities at the chosen date and time of 01.06.2022 between hours 11:00 and 12:00, according to data from Nord Pool [30], are listed in Table 7.

Table 7: Transmission capacities from Norway to Sweden - 01.06.2022, 11:00-12:00 [30]

Transmission line	Zones	Equivalent Bus Nordic 45	Transmission capacity [MW]
Ofoten - Ritsem	NO4 - SE1	5430 - 3115	500
Nedre Røssåga - Ajaure	NO4 - SE1	5420 - 3701	150
Nea - Järpstrømmen	NO3 - SE2	5330 - 3245	600
Hasle - Borgvik	NO1 - SE3	5110 - 3359 (1)	725
Hasle - Loviseholm	NO1 - SE3	5110 - 3359 (2)	725
Total	NO - SE	-	2700

In order to be able to measure the line flow between buses 5420 and 3701, a new bus (bus 3702) was added right next to bus 3701. The measured line flows in the base-case scenario were as shown in Table 8.

Table 8: Transmitted power from Norway to Sweden - DynPSSimpy (Base case)

Transmission line	Zones	Equivalent Bus Nordic 45	Transmitted power [MW]
Ofoten - Ritsem	NO4 - SE1	5430 - 3115	192.85
Nedre Røssåga - Ajaure	NO4 - SE1	3701 - 3702	123.09
Nea - Järpstrømmen	NO3 - SE2	5330 - 3245	510.72
Hasle - Borgvik	NO1 - SE3	5110 - 3359 (1)	-25.55
Hasle - Loviseholm	NO1 - SE3	5110 - 3359 (2)	-22.85
Total	NO - SE	-	778.26

In order to make an extreme scenario with maximum export from Norway to Sweden, some loads were increased in Sweden and Finland and some generation was increased in Norway. A load of 200MW was added to one bus in SE1 and one bus in SE2 while a load of 750MW was added to one bus in SE3 and one bus in SE4. Further, the generators in NO1, NO2 and NO5 (southern parts of Norway) had their power generation increased by a total of 1500MW while the generators in NO3 and NO4 (northern parts of Norway) had their power generation increased by a total of 400MW. After this, the power flow from NO1 to SE3 were close to its limit at about 1450MW, but the power flows from Northern Norway to Northern Sweden needed some adjustments. After having increased the reactance of the line connecting NO3 to SE2 by 111% (reducing its power flow) and decreasing the reactance of one of the lines connecting NO4 to SE1 by 24% (increasing its power flow), the power flows ended up giving a correct representation of an extreme situation of high export from Norway to Sweden. The resulting power flows are shown in Table 9.

Table 9: Transmission from Norway to Sweden - DynPSSimpy (Extreme scenario)

Zones	Transmission capacity [MW]	DynPSSimpy transmitted power [MW]
NO4 - SE1	650	651.74
NO3 - SE2	600	599.88
NO1 - SE3	1450	1446.7
NO - SE	2700	2698.34

Disturbance in Finland

According to an ENTSO-E report from 2021 [35], the reference incident then and in the near future was the outage of the Oskarshamn 3 unit (Swedish nuclear power station) at a total production of 1450MW. Olkiluoto 3 is a Finnish nuclear power station with a total production of 1600MW which started its production on the 16th of April 2023 [36]. In order to keep the reference incident at 1450MW, 300MW of load will automatically be disconnected if Olkiluoto 3 is tripped, leaving a total loss of power of 1300MW.

The extreme simulation scenario will therefore simulate the disconnection of Olkiluoto 3, at a total rated power of 1300MW, which will be located at bus 7000 (Southwestern part of Finland). This disturbance will take place 5 seconds into the simulation.

N-1 criteria, line disconnection

In order to further stress the system, the N-1 criteria will be tested shortly after the disturbance in Finland takes place. The ”N-1” criteria says that the grid shall be capable of handling an outage of a single transmission line, transformer or generator without causing losses in the supply of power in the system.

One of the two lines connecting Bus 5110 (NO1) to Bus 3359 (SE3) will be disconnected 15 seconds after the occurrence of the disturbance in Finland. As can be seen from Table 9, these two lines combined deliver about half of the total transmitted power from Norway to Sweden. The line with the lowest resistance will be disconnected, causing larger line losses when an increased power flow passes through the other of the two lines.

In order to maintain stability in the system after disconnection of the line, the gains of the AVRs had to be reduced from 100 to 50.

3.4.2 Classification of reserves

In the following simulations, there will be two types of centralized reserves and one type of distributed reserve:

- **Centralized reserve:** Industrial consumer - An industrial consumer of power, a large factory, for example, can be used as a power reserve in the case of a large disturbance. One could assume that a factory would only cover the minimum requirements from Chapter 2.2.2.
- **Centralized reserve:** Centralized generator - Generators which sole purpose is to provide frequency reserves will be referred to as ”centralized generators” in order to differentiate them from all other generators in the EPS. These generators will be modeled as hydro power generators.
- **Distributed reserve:** EV fleet - Large EV fleets charging all around the Nordic EPS can act as distributed reserves in the case of a large disturbance as has previously been simulated using the K2A system.

The centralized reserves will be located at Buses 5220 (NO2), 3300 (SE2), 7100 (FI) and 8500 (DK/SE4). The power rating (P_{IndCon} and P_{Gen}) of the centralized reserves in each country is equal to the FCR-D procurement level for each country as specified in Chap. 3.4.3.

Centralized reserves - Industrial consumers

It will be assumed that large industrial consumers representing centralized reserves will only decrease their consumption in line with the minimum technical requirements from Chapter 2.2.2. This means that they will decrease their consumption by 50% in 5 seconds and by 100% in 30 seconds. It will also be assumed that these large industrial consumers will be able to decrease their production without any time delay. For the sake of simplicity, they are modeled as VSCs generating power instead of loads having their consumption decreased.

The industrial consumers as providers of FCR-D upwards will have their power production modeled as shown in Eq. 22.

$$P(f) = \begin{cases} 50\% \cdot P_{IndCon}[MW] \cdot \frac{t_0}{5s} \cdot \frac{f(t) - 49.9Hz}{-0.4Hz}, & \text{if } 49.9Hz \geq f(t) \text{ and } t_0 \leq 5s \\ 50\% \cdot P_{IndCon}[MW] \cdot (1 + \frac{t_0 - 5s}{25s}) \cdot \frac{f(t) - 49.9Hz}{-0.4Hz}, & \text{if } 49.9Hz \geq f(t) \text{ and } 5s \geq t_0 \geq 30s \\ P_{IndCon}[MW] \cdot \frac{f(t) - 49.9Hz}{-0.4Hz}, & \text{if } 49.9Hz \geq f(t) \text{ and } 30s \geq t_0 \end{cases} \tag{22}$$

Where $t_0 = 0$ when the frequency drops below 49.9Hz and P_{IndCon} is the rated power of the industrial consumer.

Centralized reserves - Generators

The centralized generators will be represented by VSCs emulating large hydro-powered generators. If they were to be modeled as the other generators with a given droop setting, their primary frequency control would contribute at all frequencies (making them provide both FCR-N and FCR-D downwards), which would make it difficult to correctly emulate the specific requirements for providers of FCR-D as specified in Chapter 2.2.2.

In order to correctly emulate a hydro-powered generator's response to a drop in frequency, a small simulation has been performed. Figure 30 shows the response of generator G5120-1 (located in NO1) to the frequency drop shown in Figure 31. In this case, as only FCR-N is activated, there is a total frequency bias in the EPS of only about 3000MW/Hz, but the nature of the generator response is still considered representative of a large generator providing FCR-D.

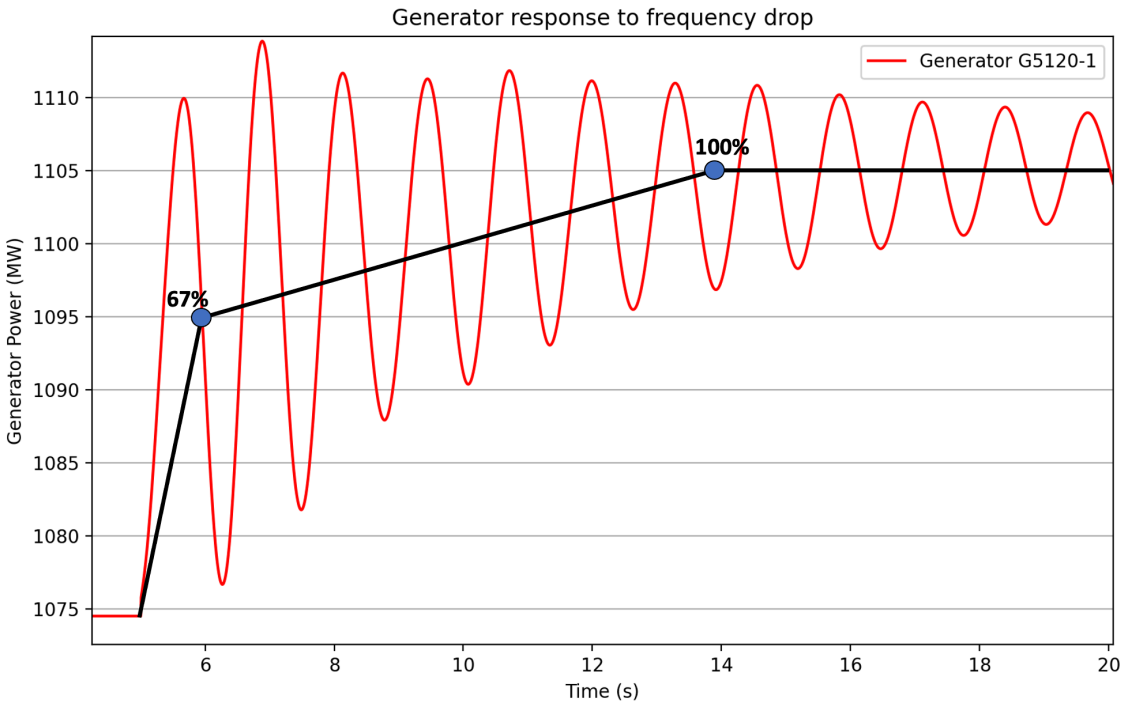

Figure 30: Generator response with linear approximation

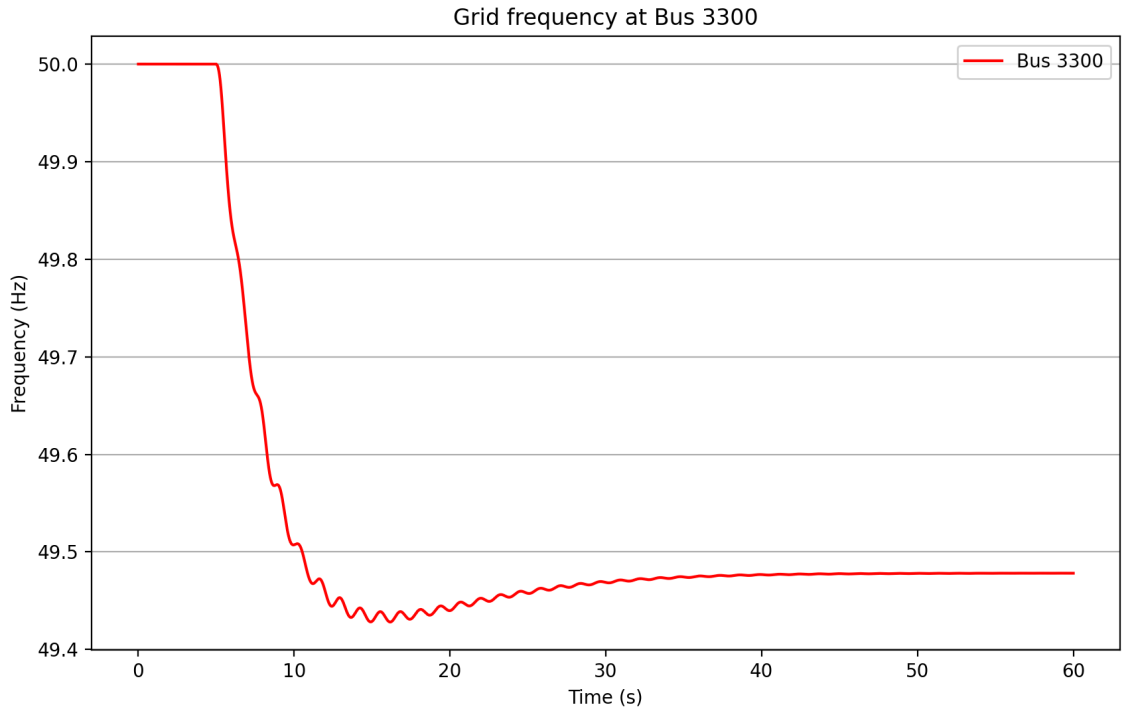

Figure 31: Frequency response to a fault (only FCR-N activated)

Using the approximated linear response of the generator in Figure 30 as well as the fact that FCR-D upwards shall be activated only when the frequency drops below 49.9 Hz, the centralized generators as providers of FCR-D upwards will have their power production modeled as shown in Eq. 23.

$$P(f) = \begin{cases} 67\% \cdot P_{Gen}[MW] \cdot \frac{t_0}{1s} \cdot \frac{f(t) - 49.9Hz}{-0.4Hz}, & \text{if } 49.9Hz \geq f(t) \text{ and } t_0 \leq 1s \\ P_{Gen}[MW] \cdot (67\% + 33\% \cdot \frac{t_0 - 1s}{9s}) \cdot \frac{f(t) - 49.9Hz}{-0.4Hz}, & \text{if } 49.9Hz \geq f(t) \text{ and } 1s \geq t_0 \geq 9s \\ P_{Gen}[MW] \cdot \frac{f(t) - 49.9Hz}{-0.4Hz}, & \text{if } 49.9Hz \geq f(t) \text{ and } 9s \geq t_0 \end{cases} \tag{23}$$

Where $t_0 = 0$ when the frequency drops below 49.9Hz and P_{Gen} is the rated power of the centralized generator.

Distributed reserves - EV Fleet

The distributed reserves used as providers of FCR-D upwards will be represented by an EV fleet placed on each bus in the system. The EV fleets will be distributed evenly between buses based on the number of buses and level of procurement capacity in each area.

In Chapter 3.1.1, it was assumed a total EV fleet capacity in the Nordic EPS of 1200MW, distributed between the Nordic countries as follows:

- Norway: 600MW
- Sweden: 300MW
- Finland: 200MW
- Denmark: 100MW
- Total: 1200MW

It will be assumed that the EV fleets will have a time delay of 1 second. The EV fleet as a provider of FCR-D upwards will be modeled as follows:

$$P(f) = P_{Fleet}[MW] \cdot \frac{f(t - t_{delay}) - 49.9Hz}{-0.4Hz}, \text{if } 49.9Hz \geq f(t-1) \tag{24}$$

Where $t = 0$ at the instant of the occurrence of the fault, $t_{delay} = 1s$ and P_{Fleet} is twice the rated charging/discharging power of the EV fleet.

When modeling the EV fleet as a provider of FFR, it will be assumed that in the future, as explained in Chapter 3.1.3, the time delay of charging equipment and measurement tools will be greatly reduced, which would allow the use of EV fleets as FFR providers. Further, a long support duration of 45 seconds will be used, altering the FFR scheme from Eq. 21 as used in the K2A simulations.

The EV fleet as an FFR provider will therefore be modeled as follows:

$$P(f) = \begin{cases} \frac{P_{Fleet}[MW]}{0.7s} \cdot t, & \text{if } f \leq 49.7Hz \text{ and } t \leq 0.7s, \text{ (Activation time)} \\ P_{Fleet}[MW], & \text{if } f \leq 49.7Hz \text{ and } t \leq 45s, \text{ (1st support duration)} \\ P_{Fleet} - \frac{P_{Fleet}[MW]}{10s} \cdot t_{d1}, & \text{if } f \leq 49.7Hz \text{ and } t_{d1} \leq 5s, \text{ (1st deactivation time)} \\ \frac{P_{Fleet}}{2}[MW], & \text{if } f \leq 49.7Hz, \text{ (2nd support duration)} \\ \frac{P_{Fleet}}{2} - \frac{P_{Fleet}[MW]}{10s} \cdot t_{d2}, & \text{if } f \leq 49.7Hz \text{ and } t_{d2} \leq 5s, \text{ (2nd deactivation time)} \end{cases} \tag{25}$$

Where $t = 0$ at the instant of the occurrence of the fault, $t_{d1} = 0$ at the instant when the frequency reaches 49.7Hz the first time (when rising), and $t_{d2} = 0$ at the instant when the frequency reaches 49.7Hz the second time (when rising). P_{Fleet} is twice the rated charging/discharging power of the EV fleet.

As explained in Chapter 3.3.1, this power output control function of the EV fleet represents its response to an FFR event. First, the EV fleet switches from charging its EVs to discharging them, which makes up the first support duration. Then, when a frequency of 49.7Hz is reached after the frequency nadir has been reached, the EV fleet switches off the discharging of the EVs, which makes up the second support duration. Then, following the second deactivation time, the EV fleet goes back to charging its EVs, which in practice is a recovery period of the fleet as an FFR-providing entity. Figure 58 from Appendix D and Figure 38 from Chapter 4.1.5 shows this power output control function in action on the K2A system.

3.4.3 Procurement of frequency reserves

FCR-N

A total of 600MW of FCR-N is procured at all times (Figure 13). These reserves shall be delivered within a frequency ranging from 49.9 to 50.1Hz. It is possible that 600MW shall be procured in both directions, i.e. both from 50 to 49.9Hz and from 50 to 50.1Hz. However, for this thesis, it will be assumed that 300MW shall be procured in each direction. This means that without including the procurement of FCR-D, the Nordic EPS shall have a total frequency bias of:

$$K_f = \frac{600MW}{0.2Hz} = 3000MW/Hz \tag{26}$$

These 3000MW/Hz will lay the foundation of the frequency control of the power system. The centralized and distributed reserves will be added on top of this frequency bias. In order to obtain a simulated frequency bias of 3000MW/Hz, no nuclear power plants were contributing to primary frequency control, and the droop of the hydropower plants was set to 80%.

Realistically, the droop settings of the turbine governors of hydropower plants are usually set to a value between 2 and 12% [37]. Therefore, if only 3000MW/Hz of frequency bias were to be delivered in the Nordic EPS, it would probably be delivered by

fewer generators with a much lower droop setting. However, for the sake of simplicity, and since it does not affect the performance of the units providing FCR-D upwards and FFR, all hydropower generators will be given the same droop value in the simulations of this thesis.

Figure 31 shows the frequency response to the disconnection of Olkiluoto 3 when only FCR-N is activated.

FCR-D

In Chapter 3.1.2, the procurement of FCR-D capacity in the Nordic EPS was assumed to be 1500MW. The given initial distribution key of FCR demands the following procurement from each of the Nordic countries:

- Norway: 575MW
- Sweden: 575MW
- Finland: 300MW
- Denmark: 50MW
- Total: 1500MW

FFR

In Chapter 3.1.2, the procurement of FFR capacity in the Nordic EPS was assumed to be 385MW. The given initial distribution key of FFR demands the following procurement from each of the Nordic countries:

- Norway: 150MW
- Sweden: 135MW
- Finland: 70MW
- Denmark: 30MW
- Total: 385MW

3.4.4 Cases

The system frequency is measured at the slack bus (Bus 3300) for all cases.

Case 6 - Effect of centralized vs. distributed reserves

In this case, the effect of providing FCR-D using centralized vs. distributed power reserves will be compared and analyzed.

Case 7 - Removing the time delay of the EV fleet

One can assume that the time delay in measuring and charging equipment decreases in the future. Therefore, this case will test the performance of the EV fleet without any time delay.

Case 8 - Using fast fault detection to counteract time delay of EV fleets

In this case, it will be analyzed whether or not fast fault detection could be used to counteract the effect of the time delay of the EV fleets. By being able to detect faults very rapidly after they occur, one could activate FCR-D and FFR reserves before the frequency has dropped below 49.9Hz (activation level for FCR-D upwards) or 49.7Hz (earliest activation level for FFR). As can be seen from Figure 32, FCR-D upwards is activated about 0.64 seconds after the occurrence of a fault. Being able to activate frequency reserves earlier gives valuable extra time for the reserves to counteract the frequency drop.

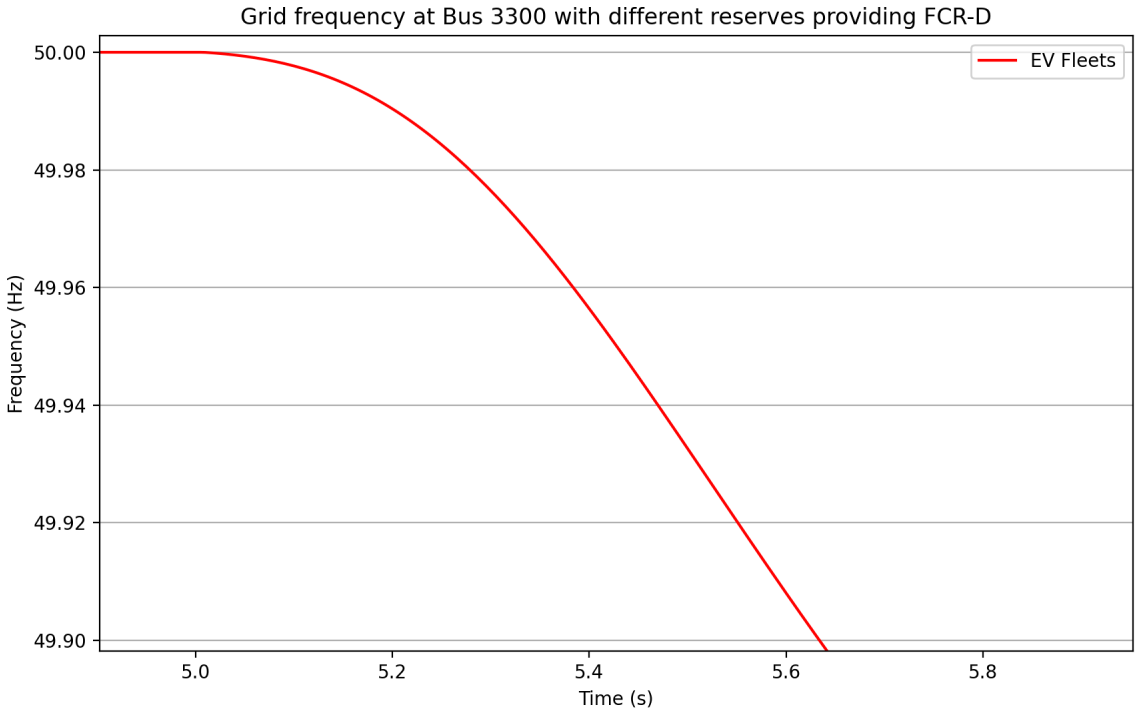

Figure 32: Frequency response from Case 1 (Zoomed)

Being able to detect faults immediately after they occur has been proven to be difficult though. One could think that the ROCOF could be measured, and depending on how large it is, one could estimate the frequency nadir of the following frequency drop. However, due to noise from measuring equipment and over-harmonic frequencies in the frequency signal, one would have to filter the frequency signal over the course of some time, at which point the frequency would probably already have fallen below 49.9 or 49.7Hz.

For the sake of investigating what effect fast fault detection would have on the performance of the EV fleets, the control signals for the three frequency reserves as

providers of FCR-D upwards will be activated at 49.99Hz instead of 49.9Hz, with a linear activation rate down to 49.5Hz.

Case 9 - High and low amounts of system inertia

In this case, the total amounts of inertia in the EPS will be varied. This is done in order to analyze the performance of the three types of reserves under varying amounts of IRES penetration and HVDC import in the EPS. As previously explained, intermittent renewable energy sources like solar- and wind power and HVDC import has no contribution of traditional inertia in the EPS, which leads to less kinetic energy available for breaking changes in the system frequency.

Two simulations will be performed:

- Low inertia simulation: 119.2GWs of kinetic energy
- High inertia simulation: 250.8GWs of kinetic energy

The base case simulation has a total amount of 183.5GWs of kinetic energy. The choice behind this value is explained in Chapter 3.2.3.

Case 10 - Realistic case with the provision of FCR-D and FFR in the Nordic EPS using EVs

In this scenario, the contribution and responses of all three frequency reserve services (FCR-N, FCR-D and FFR) will be analyzed in what could be a realistic future scenario where EVs are included as a primary frequency control reserve.

As explained in Chapter 3.4.3, a total of 600MW of FCR-N is procured from the 34 hydropower stations of the Nordic 45 model, producing a total frequency bias of about 3000MW/Hz.

For this case, 50% of the required provision of FCR-D shall be provided by EV fleets, while the remaining 50% shall be provided by the centralized generators. Further, 100% of the required provision of FFR shall be provided by EV fleets. This means that the total EV fleet capacity in the Nordic EPS of 1200MW (as calculated in Chapter 3.1.1) must cover 750MW of FCR-D reserves and 385MW of FFR reserves.

The FFR reserves delivered by the EV fleets will have a long support duration of 45 seconds, giving enough time for the secondary frequency control in the EPS to be activated. According to Statnett [38], the automatic secondary frequency reserves (aFRR) must be activated at a maximum delay of 30 seconds after they obtain a signal for activation, which is sent by the TSO at the occurrence of a fault. Then, after a maximum of 120s, the reserves must be fully activated. It is therefore assumed that after 35 seconds of simulation (30 seconds after the occurrence of the fault), the secondary frequency reserves will take over the frequency containment process, and the power response from the FCR-D reserves can slowly be reduced.

The extreme scenario, as explained in Chapter 3.4.1, is a plausible (though unlikely) event that could occur in the Nordic EPS. Therefore, this scenario will also be used in this case.

4 Results

In this chapter, the results from all cases will be presented. Supplementary results, such as voltage magnitudes and power responses, can be found in Appendix D.

4.1 K2A

4.1.1 Case 1 - FCR-D without time delay

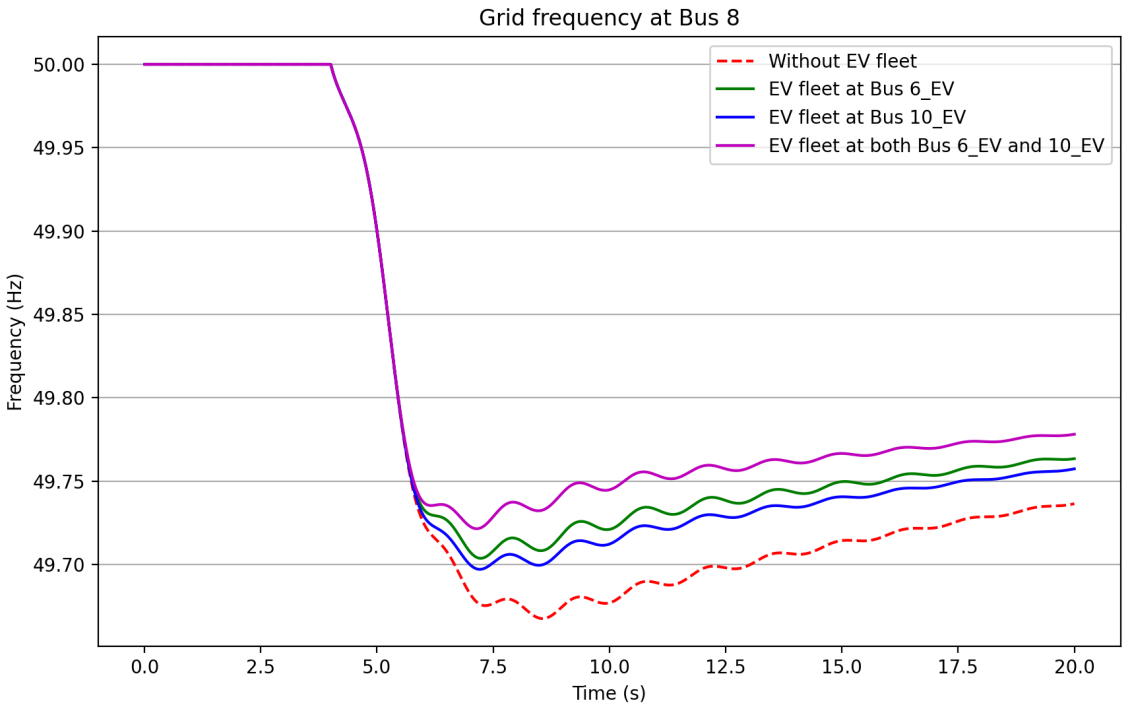

Figure 33: All scenarios - Frequency response

4.1.2 Case 2 - FCR-D with time delay

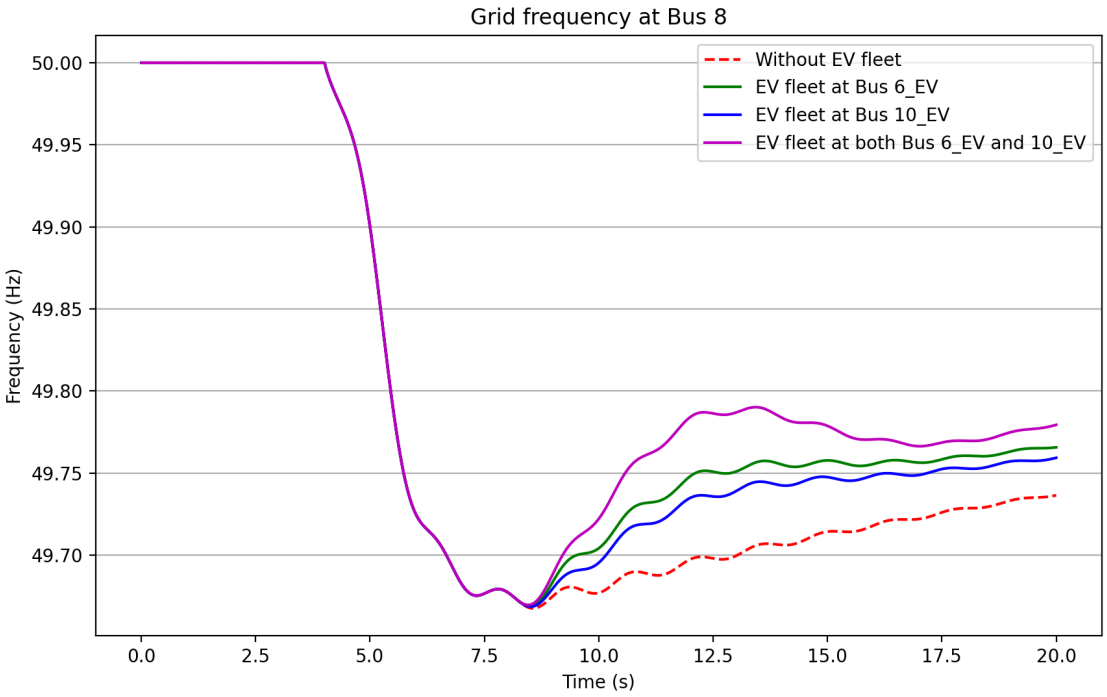

Figure 34: All scenarios - Frequency response ($t_{delay} = 3s$)

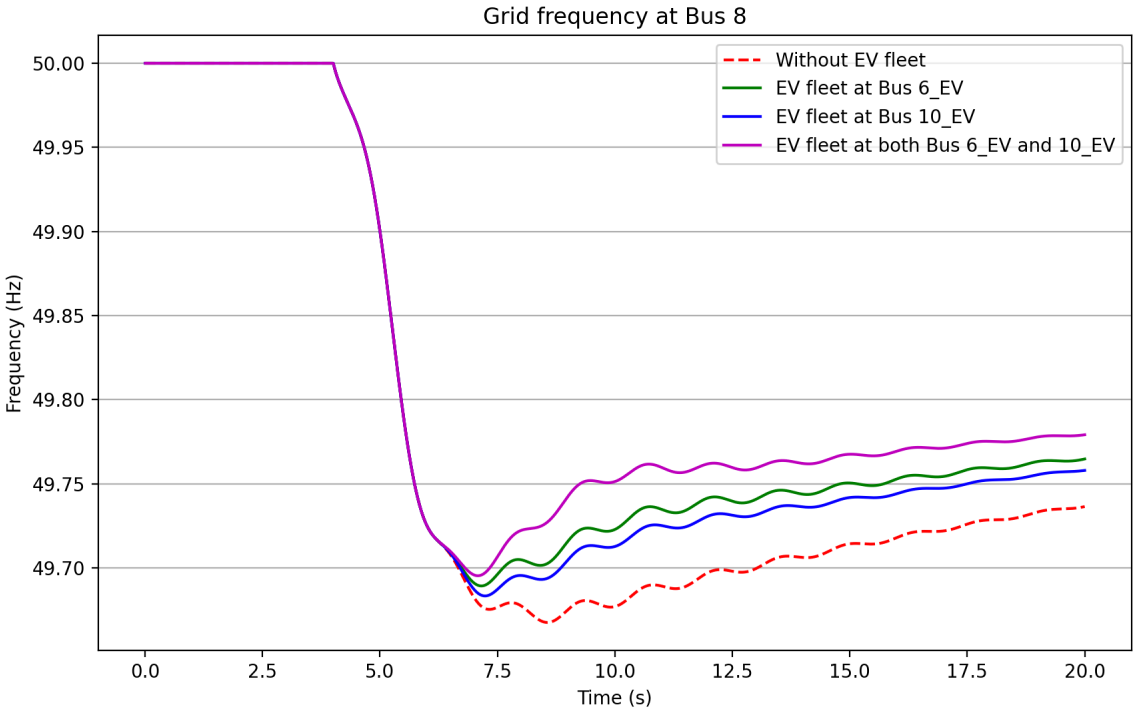

Figure 35: All scenarios - Frequency response ($t_{delay} = 1s$)

4.1.3 Case 3 - FFR with short deactivation time

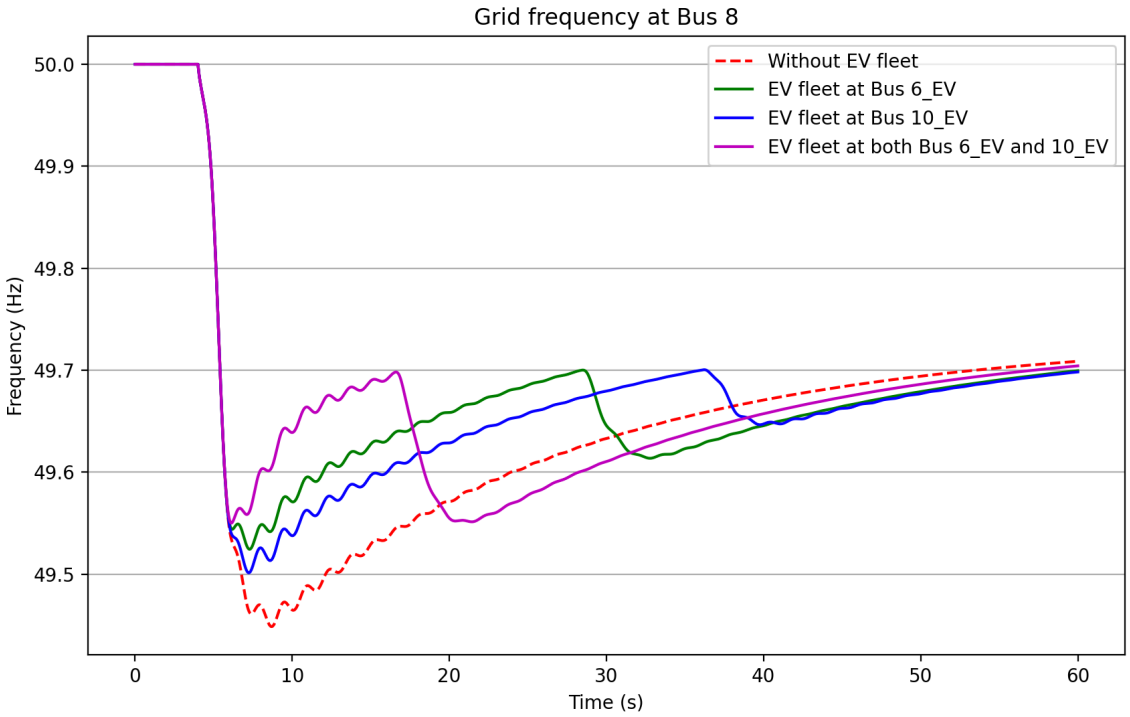

Figure 36: All scenarios - Frequency response

4.1.4 Case 4 - FFR with long deactivation time

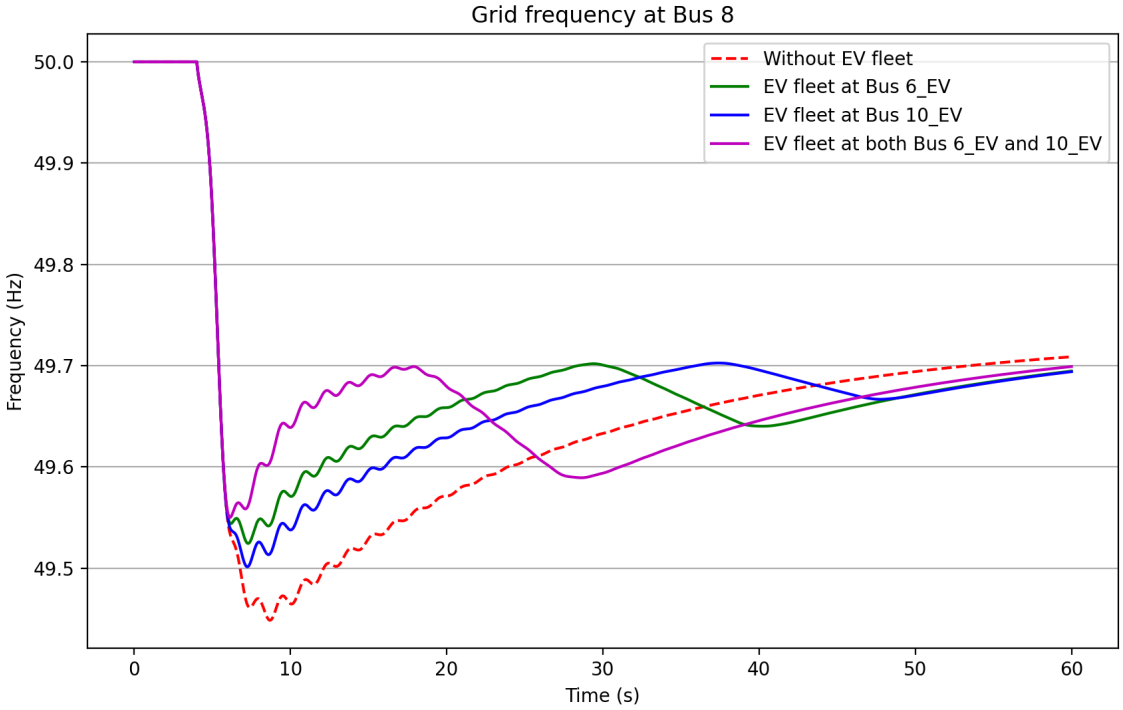

Figure 37: All scenarios - Frequency response ($t_d = 10s$)

4.1.5 Case 5 - FFR with step-wise deactivation

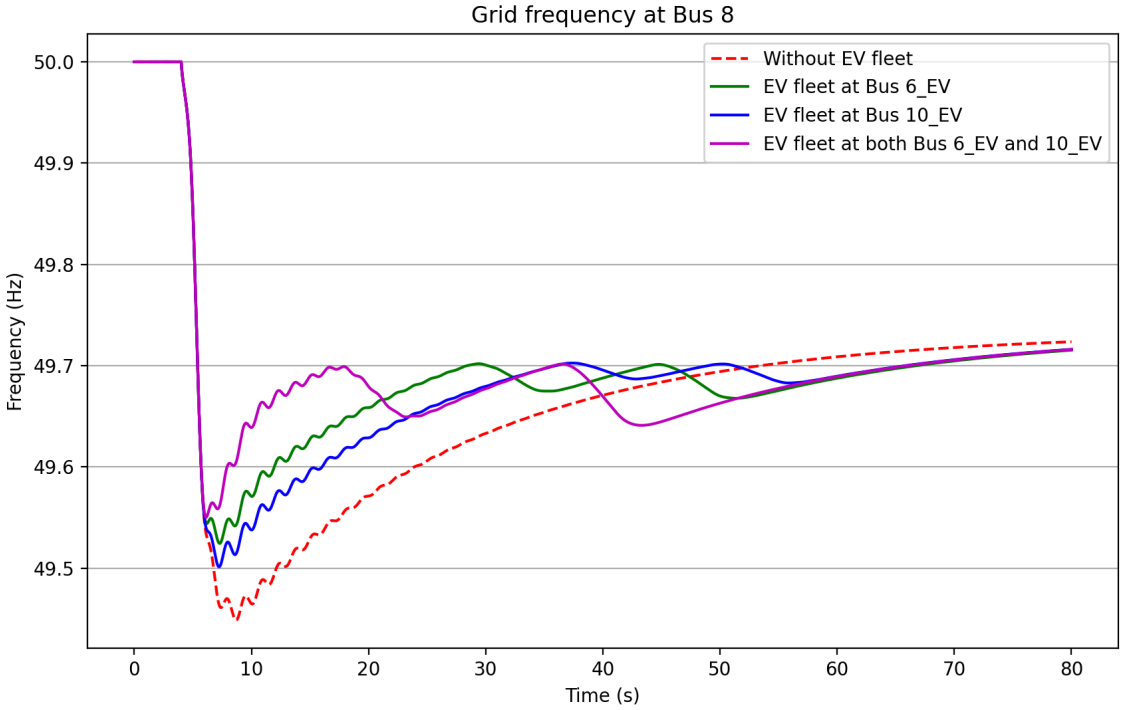

Figure 38: All scenarios - Frequency response (New control function)

4.2 N45

4.2.1 Case 6 - Effect of centralized vs. distributed reserves

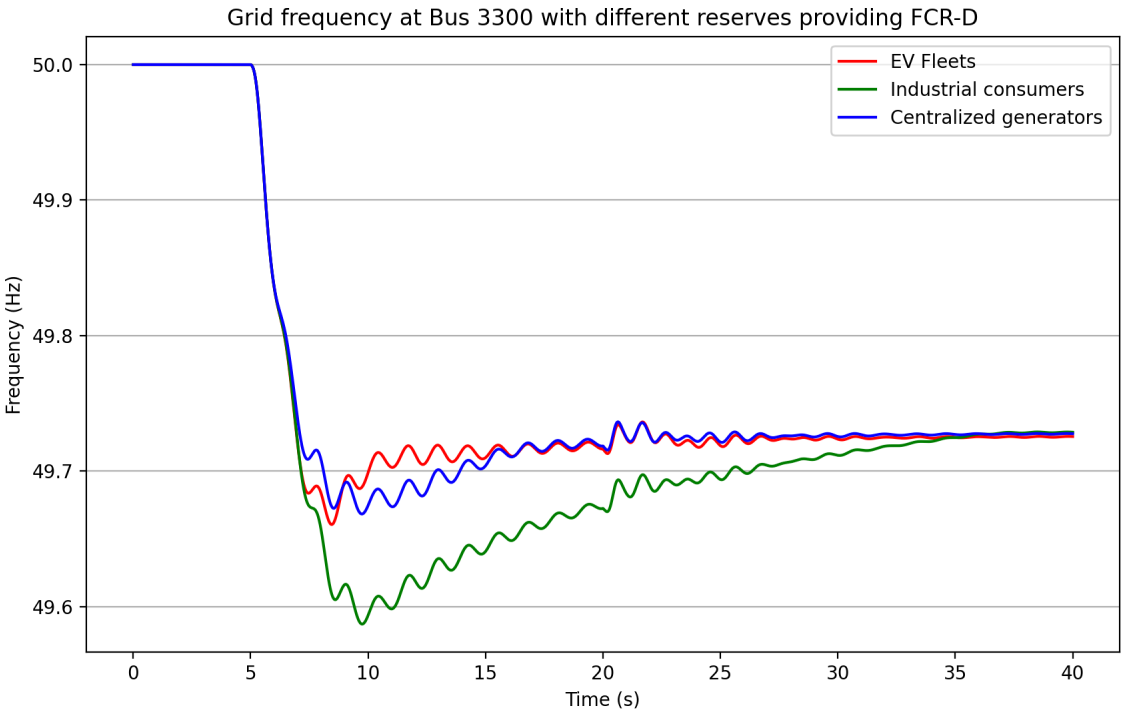

Figure 39: Frequency response

Table 10: Transmission line losses

	EV Fleets	Industrial consumers	Centralized generators
Before disturbance	1585	1585	1585
Before line disconnection	2347	2373	2385
After line disconnection	2388	2415	2414

Table 11: Load losses and total losses after line disconnection

	EV Fleets	Industrial consumers	Centralized generators
Total load losses	44499	44503	44502
Total losses	46887	46918	46916

Table 12: Transmission line flow before line disconnection

	EV Fleets	Industrial consumers	Centralized generators
NO4 - SE1	883	847	841
NO3 - SE2	589	565	559
NO1 - SE3 (Line 1)	856	883	886
NO1 - SE3 (Line 2)	844	871	873
NO - SE (Total)	3172	3166	3159

Table 13: Transmission line flow after line disconnection

	EV Fleets	Industrial consumers	Centralized generators
NO4 - SE1	918	878	877
NO3 - SE2	604	577	577
NO1 - SE3 (Line 1)	0	0	0
NO1 - SE3 (Line 2)	1720	1772	1771
NO - SE (Total)	3242	3226	3225

4.2.2 Case 7 - Removing the time delay of the EV fleet

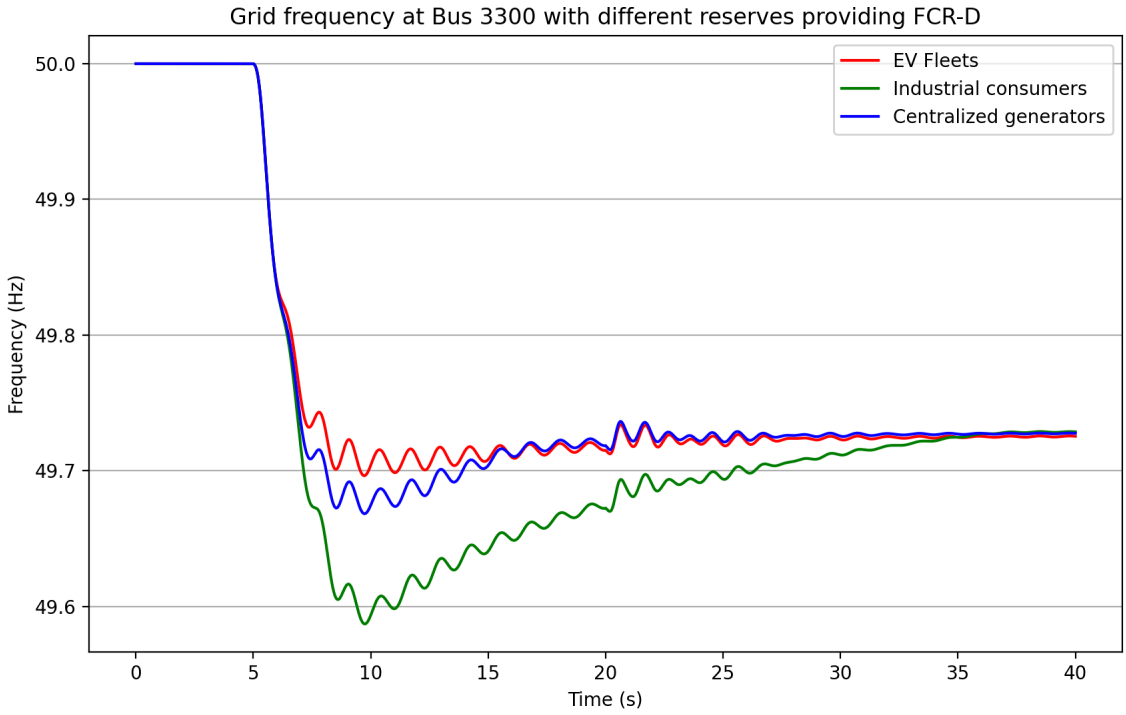

Figure 40: Frequency response (no time delay)

4.2.3 Case 8 - Using fast fault detection to counteract time delay of EV fleets

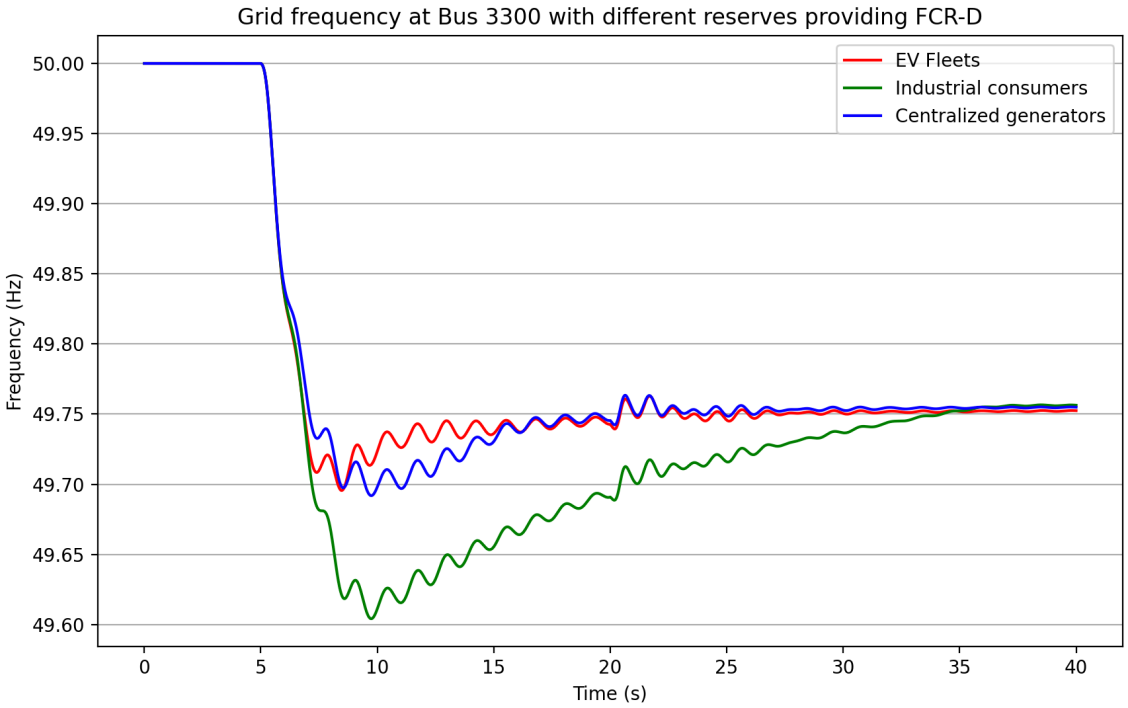

Figure 41: Frequency response (with fast fault detection)

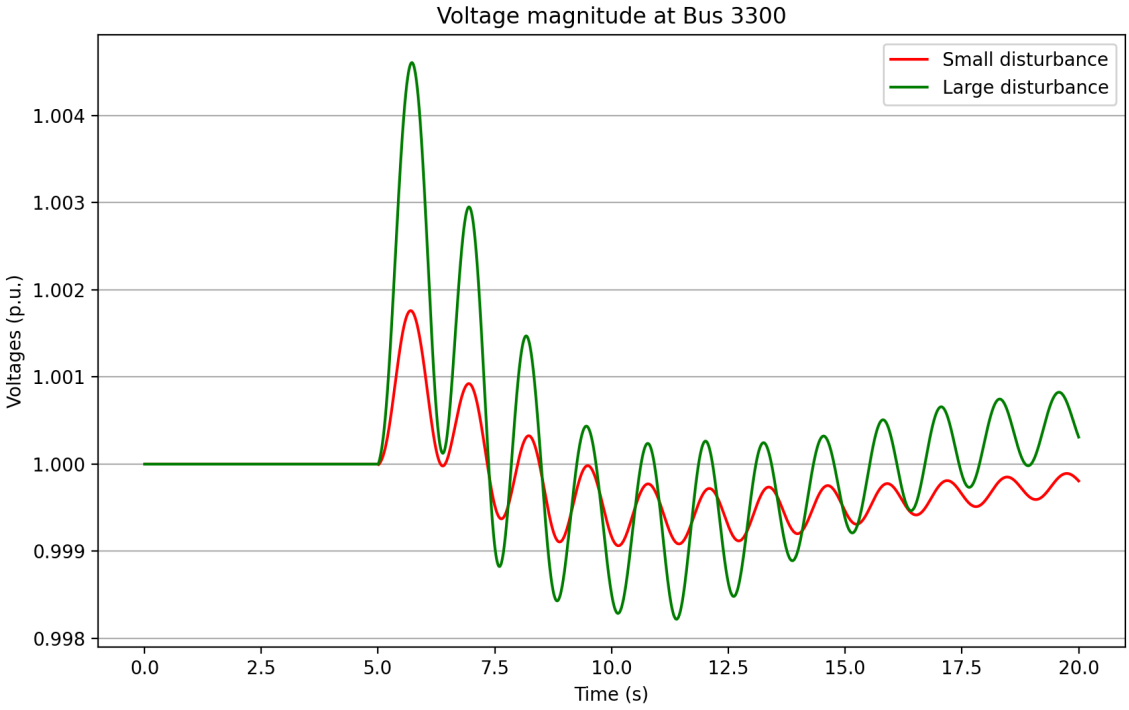

Figure 42: Difference in voltage magnitude for small (500MW) and large (1000MW) disturbance

4.2.4 Case 9 - High and low amounts of system inertia

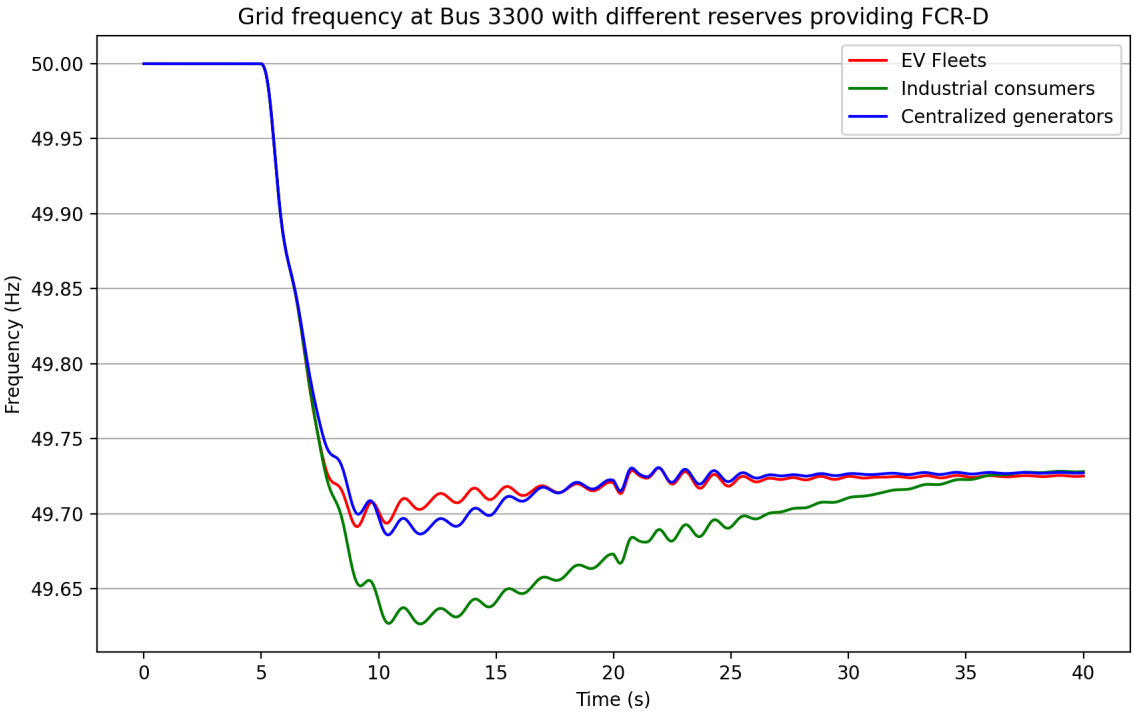

Figure 43: Frequency response (High inertia)

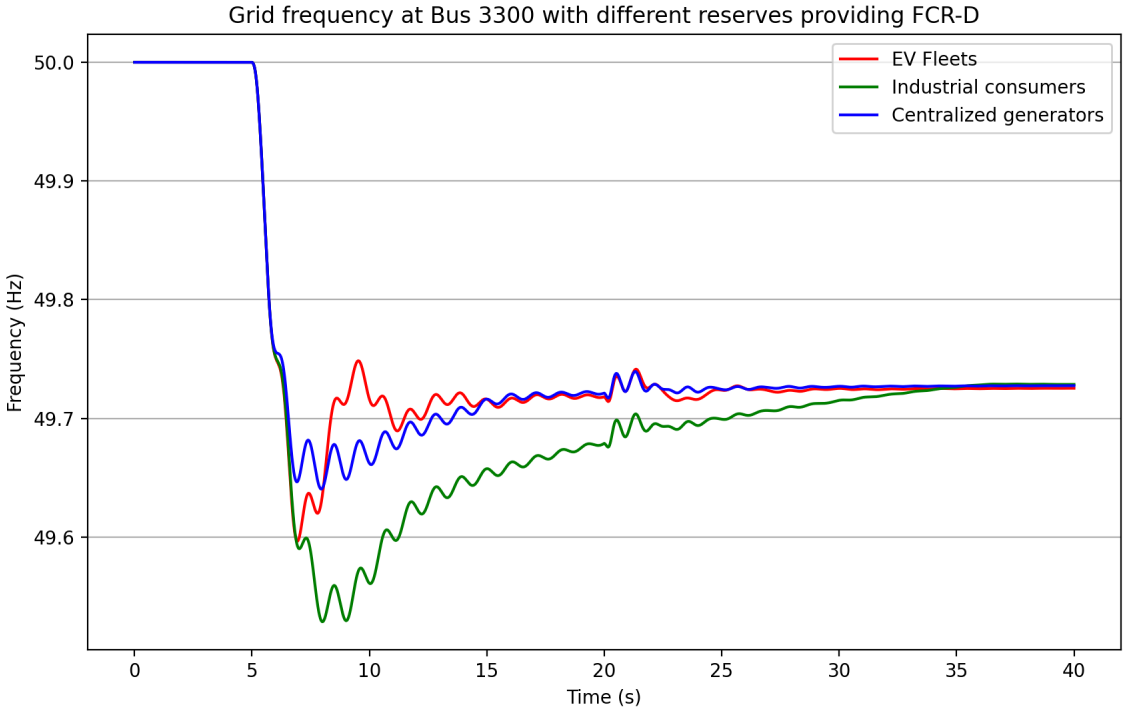

Figure 44: Frequency response (Low inertia)

4.2.5 Case 10 - Realistic case with the provision of FCR-D and FFR in the Nordic EPS using EVs

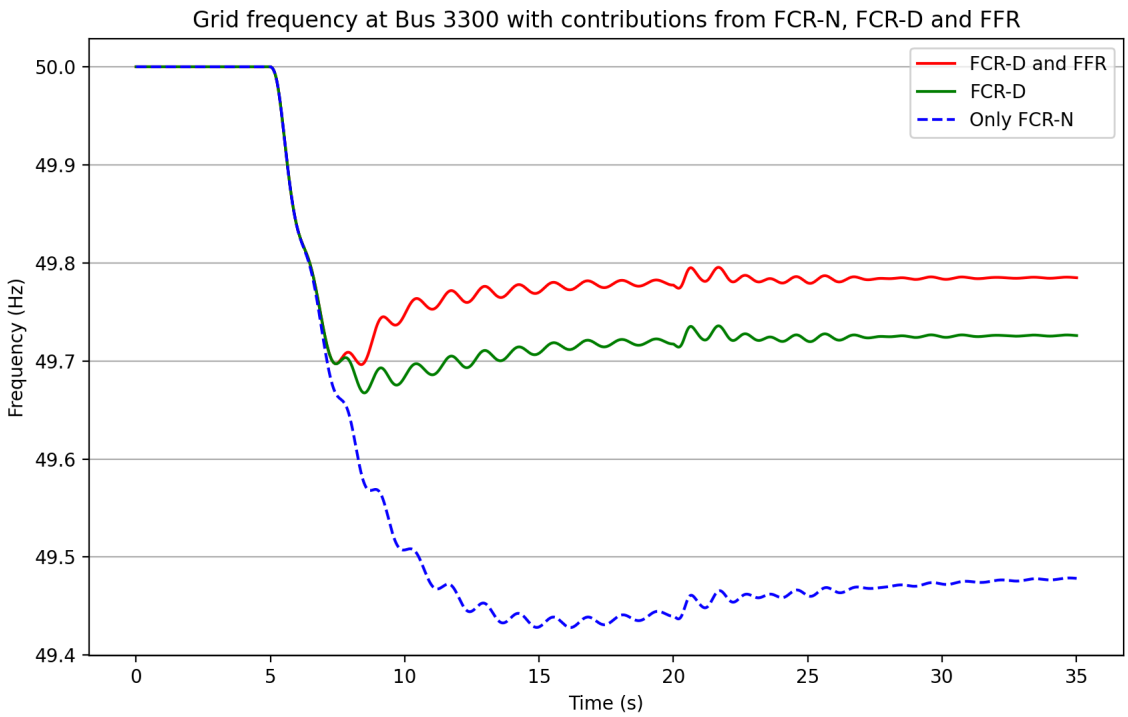

Figure 45: Frequency response

5 Discussion

5.1 K2A

5.1.1 Case 1 - FCR-D without time delay

From Figure 33, one can see that the scenario with the lowest frequency nadir (the lowest point of the frequency deviation) is Scenario 2. The reason why the frequency of Scenario 2 drops further than the frequency of Scenario 1, even though the increase in load is locally compensated in Scenario 2, is most likely due to the voltage dependency of the loads. Explained shortly, the inherent voltage dependency of the loads leads to higher load values in Scenario 2, which again results in a larger frequency drop than in Scenario 1.

The more detailed explanation is that in Scenario 1, the increased load in Area 2 was partly compensated by using an EV fleet located in Area 1. In Scenario 2, however, the increased load and the EV fleet were located in the same area. The voltage magnitudes were higher in Scenario 2 than in Scenario 1 since the increased amount of transmitted power between the areas in Scenario 1 led to a decrease in voltage magnitude (compared to the voltage magnitudes of Scenario 2). For Scenario 3, the voltage magnitudes were even higher due to a further decrease in transmitted power between the areas.

The frequency drop of Scenario 3 is smaller than the frequency drops of the other two scenarios. This is to be expected as the two EV fleets of Scenario 3 help the system regain its power balance faster than the scenarios with only one EV fleet. Other than the differences in frequency nadir, the frequency responses are very similar for the three scenarios, and all scenarios provide an improved frequency response compared to the base scenario where no EV fleets are present.

From this simple case, one can see how the provision of FCR-D upwards helps reduce the frequency deviation at the occurrence of large network disturbances. Additionally, the provision of FCR-D decreases the required increase in power production from generators. The provision of FCR-D from EV fleets could therefore be an important contribution to future power systems with limited amounts of spinning reserves available.

5.1.2 Case 2 - FCR-D with time delay

In this case, where the EV fleet is modeled with a time delay, the delay causes the peak power delivery from the fleet to occur 3 seconds after the frequency nadir. This causes a large fluctuation in both the power output, voltage and speed (frequency) of the generators, which potentially could be damaging to some equipment.

Further, if a large percentage of the total reserves providing FCR-D upwards in an EPS came from EV fleets with large time delays, this effect would be amplified.

If EV fleets are going to be used as providers of FCR-D upwards in the future, some measures should probably be done in order to compensate for this effect. Most likely, the inherent delay in communication and frequency measurement devices will be re-

duced significantly in the future. However, if some sort of fast fault detection device were to be developed, it could be possible to detect faults and activate frequency containment reserves faster. The effect of utilizing such a fast fault detection device is investigated in Case 8.

Figure 35 shows the frequency results when the EV fleet is modeled with a time delay of 1 second instead of 3 seconds. The results are significantly better than the frequencies from Figure 34, so one can conclude that the lower the time delays of the EV fleets are, the more of the total FCR-D reserves can be procured from them.

5.1.3 Case 3 - FFR with short deactivation time

In this case, Scenarios 1 and 2 have rather different results in their power generation and frequency response. The reason for this is most likely the same reason why Scenarios 1 and 2 gave rather different results when providing FCR-D, namely the voltage dependency of the loads in the system. When providing FFR however, this effect is amplified due to the EV fleet providing its full rated power throughout its whole FFR duration time and due to a larger fault in the system. The FCR-D-controlled EV fleet on the other hand is frequency-dependent, which means it won't provide its full rated power unless the frequency surpasses 49.5Hz.

Regarding the effect of the EV fleet as an FFR provider, one can clearly see how the frequency nadir is significantly increased. As expected, having two EV fleets at buses 6 and 10 gives the best result. Also, as one can see from the relatively large difference in results for Scenarios 1 and 2, the location of the EV fleet has a larger effect on the provision of FFR than it has on the provision of FCR-D.

From Figure 36 one can see that the frequency drops quite dramatically following the deactivation of the FFR reserves. Similarly to how the time delay could cause issues for stability and equipment in the EPS when providing FCR-D, this could potentially cause the same issues. One way to tackle this issue is quite simply to reduce the deactivation time of the FFR reserves, which would cause more gentle deactivation slopes than what is seen in Figure 55. Even though it is preferred to have a rather short deactivation time so that the FFR recovery time can start as early as possible (see Figure 9), the recovery time is not that important for a large EV fleet due to its large battery capacity. If the EV fleet has to provide FFR reserves continuously for several minutes, however, recharging of the total battery capacity may be needed. This would however be a very rare situation as FFR reserves are procured with the main goal of increasing the frequency nadir of the frequency response, which is reached within a couple of seconds after the occurrence of the fault.

5.1.4 Case 4 - FFR with long deactivation time

Figure 37 shows the frequency response when the FFR reserves are modeled with a deactivation time of 10 seconds instead of 0.35 seconds. As can be seen when comparing this frequency response to the one in Case 3, the effect of increasing the deactivation time is quite simply a less abrupt change of frequency in the EPS and a less abrupt change of power output of the EVs providing FFR. This may be beneficial both for the stability of the EPS and for the charging equipment and battery life of the EVs.

5.1.5 Case 5 - FFR with step-wise deactivation

In this case, using step-wise deactivation as a method of reducing the frequency drop after deactivation of the FFR provision is analyzed.

As one can see from Figure 38, having more than one support- and deactivation time leads to a much more acceptable frequency drop after the deactivation of the FFR reserves. In theory, one could probably have as many steps as one would like for an EV fleet, which would improve this deactivation phase even more. As previously mentioned in Chapter 2.2.1, the Nordic SOA has specified that the deactivation of FFR reserves may be step-wise and non-linear, so there is no reason not to do this.

5.2 N45

5.2.1 Case 6 - Effect of centralized vs. distributed reserves

Figure 39 shows the frequency responses for the extreme scenario with FCR-D provision from the three different types of reserves. Some interesting characteristics of each of the three types can be seen.

Firstly, the industrial consumers perform rather poorly as a provider of FCR-D upwards. Its frequency response had the largest nadir and its power response had the slowest activation rates. This is to be expected as the industrial consumer only needs to follow the minimum requirements for the provision of FCR-D set by the TSO unless there is any extra compensation for delivering better performance.

Secondly, the response of the EV fleets and the centralized generators are rather comparable, as they both have good qualities. The EV fleet has by far the fastest activation rate, leading it to be able to provide the highest peak of power out of the three reserve types. At its peak production, it is able to provide about 200MW more than the centralized generators, leading to a fast reestablishment of power balance in the EPS. The centralized generators, on the other hand, have an adequate activation rate and zero time delay, which leads to the highest frequency nadir out of the three reserve types.

Typically, the quality of the provision of FCR-D upwards can be determined based on the frequency nadir. This means that from these simulations, one could argue that the centralized generators perform better as a provider of FCR-D upwards than the distributed EV fleets.

Transmission flows and losses

Tables 10 - 13 can be used in order to assess how the choice of centralized vs. distributed reserves affects the flows and losses in the EPS.

Table 10 shows how the total transmission line losses in the EPS change during three points of simulation; before the disturbance occurs ($t = 0s$), before the line is disconnected ($t = 19s$) and after the line has been disconnected and the system has reestablished the power balance. ($t = 40s$). As can be seen from the table, and as would be expected, using distributed reserves leads to lower transmission line losses compared to when using centralized reserves.

Table 11 shows total load losses and total losses (from loads and lines) after line disconnection, i.e. at the end of the simulation. There is a total reduction of about 30MW of losses in the EPS when using distributed reserves compared to when using centralized reserves. This is to be expected as the distributed reserves will produce a more optimized power flow and better utilization of the whole transmission network.

The total load losses are also an indicator of the voltage levels in the EPS since the loads are voltage-dependent. Since the total load losses are almost identical for the three types of reserves, one can conclude that the choice of distributed or centralized reserves has little effect on the voltage levels following a disturbance or line disconnection.

Tables 12 and 13 show the power flows from Norway to Sweden for the three types of reserves before and after the line disconnection. It can be seen that generally, when using distributed reserves, more of the power flow is transmitted from the northern parts of Norway to Sweden compared to when centralized reserves are being used. This is to be expected since the Norwegian centralized reserves lie in the southernmost point of Norway (bus 5220), which causes higher transmission through the southernmost line from Norway to Sweden. Both after and before the line disconnection, there is about 50MW less power flowing from NO1 to SE3 when using distributed reserves compared to centralized reserves.

5.2.2 Case 7 - Removing the time delay of the EV fleet

Without a time delay, the power response of the EV fleet is quite simply identical to how it would be with a time delay, but it is activated 1 second earlier, which leads to a faster break of the frequency drop. This lifts the frequency nadir greatly, as can be seen from Figure 40.

From this case, one can conclude that with no time delay, the distributed EV fleet has the best performance out of the three reserves providing FCR-D upwards.

5.2.3 Case 8 - Using fast fault detection to counteract time delay of EV fleets

As shown in Figure 32 in Chapter 3.4.4, a total of 0.64s elapses before the frequency drops below 49.9 Hz, which is valuable time where frequency reserves could have been activated.

As can be seen from the frequency response in Figure 41, the frequency nadir when using distributed EV fleets is now higher than for the centralized generators, proving that the use of fast fault detection and earlier activation of the frequency reserves counteracts the effect of the time-delay of the EV fleets, making distributed EV fleets a better alternative for the provision of FCR-D than the centralized reserves.

Comparing the power responses from this case to the one from Case 6, which can both be found in Appendix D, one can see that with earlier activation levels, the power response from the EV fleets catches up with the power response from the centralized generators earlier, enhancing the frequency response when using EV fleets. Of course, with earlier activation levels, the frequency- and power responses of the centralized generators and the industrial consumers are also improved, though not as much as for the EV fleets.

Additionally, it can be seen that the level at which the frequency stabilizes increases with earlier activation rates, which is to be expected as the power response increases when the area of linear activation (previously 49.9 - 49.5Hz) is increased to 49.99 - 49.5Hz. This demands more from the frequency reserves, but also improves the frequency bias of the system.

As explained in Chapter 3.4.4, using the measured ROCOF as a tool for fast fault detection is not currently possible. However, as seen in Figure 42, the voltage in the system fluctuates at a certain amplitude following the disturbance in an EPS, which is found to be dependent on the size of the fault that occurred. This is easily observable

in this simulation, and estimating the frequency nadir by measuring the amplitude of the voltage fluctuations could have potential as a fast fault detection method, but it might not be as easily observable using real-life measuring equipment.

5.2.4 Case 9 - High and low amounts of system inertia

Figures 43 and 44 show the frequency responses for the two simulations. Interestingly enough, the most noticeable effect of the amount of inertia in the system, other than the fact that with more inertia the frequency nadir will generally increase, is the effect of the time delay on the performance of the EV fleet.

One can see that with high amounts of inertia, the frequency nadir for the distributed EV fleets is higher than for the two other reserve types. However, with low amounts of inertia, i.e. with higher amounts of IRES in the EPS, the frequency nadir for the distributed EV fleets is substantially lower than for the centralized generators.

The reason behind this is the fact that with higher amounts of inertia, the ROCOF, i.e. the speed at which the frequency drops, is smaller than with low amounts of inertia. With low amounts of inertia, the time delay of the EV fleets causes the frequency to be able to drop substantially before the EV fleet is able to respond with its power response, leading to a low frequency nadir. On the other hand, with high amounts of inertia, the frequency drops slower, giving the EV fleets more time to respond with its power response, leading to a higher frequency nadir.

From this case, one can conclude that the time delay of EV fleets has a large effect on their performance as providers of FCR-D upwards when there are low amounts of inertia in the system, i.e. large amounts of IRES and/or HVDC import. Vice versa, when there are high amounts of inertia in the system, the time delay of the EV fleets has less effect on their performance as providers of FCR-D upwards.

5.2.5 Case 10 - Realistic case with the provision of FCR-D and FFR in the Nordic EPS using EVs

As can be seen from the frequency response in Figure 45, when only FCR-N is activated, the frequency nadir drops and stabilizes below 49.45Hz (as can also be seen from Figure 31), which gives the very poor total frequency bias of 3000MW/Hz.

When adding FCR-D reserves, the power response seen from the green graph in Figure 61 helps lift the frequency nadir up to about 49.67Hz, and the frequency stabilizes at about 49.73Hz, giving a total frequency bias of about 6300MW/Hz (Calculated using Eq. 13).

When also adding FFR reserves, the power response seen from the red graph in Figure 61 helps lift the frequency nadir up to about 49.7Hz, and the frequency stabilizes at about 49.78Hz, giving a total frequency bias of about 6430MW/Hz (Calculated using Eq. 13). The isolated contribution and power response from the FFR reserves of each country can be found in Figures 61 and 62 in Appendix D.

From this realistic simulation, one can see the major importance of the FCR-D reserves. The FFR reserves also help lift the frequency nadir, but will have bigger importance for larger faults or when there is less inertia in the EPS.

5.3 Viability of using EVs as providers of FCR-D upwards and FFR

If EV fleets are to be used as providers of FCR-D upwards and FFR in the future, one must take into account some real-life issues that do not have to be assessed when performing simulations [23]:

- Failure of Frequency Measurement Equipment (FME)
- Failure of communication links between FME and charging stations
- Failure of a charging station or an EV to respond
- EVs driving away
- Security against hacking
- Threat analysis of system and all components

Further, the Nordic TSOs would of course have to pay for the provision of FCR-D upwards and FFR. Therefore, in order to make the provision of these services more acceptable for EV owners, one could decrease the cost of charging the cars at public charging stations where these types of services are enabled. One could also give the owners an option of either charging on frequency service-enabled chargers or regular chargers, in case they do not want to have their EV at the disposal of the TSOs. For the provision of FCR-N, there could also be an option of setting a desired point in time when the owner wants their EV to be fully charged, leaving it as a provider of FCR-N for several hours if, for example, their EV is charging while they're at work. Also, since the amount of inertia in the system plays a large role in the importance of the provision of FCR-D upwards and FFR, one could add a function where there are lower prices for charging when there is less inertia in the system.

6 Conclusion

In this thesis, the use of EVs as providers of FCR-D upwards and FFR in the Nordic power system has been analyzed. The Nordic 45 test model was created, which is a new and improved version of the Nordic 44 test model. An EV fleet was modeled both as a provider of FCR-D upwards and as a provider of FFR according to the current rules and regulations set by the Nordic TSOs. Various aspects of the performance of the EV fleets were analyzed through 10 simulation cases, performed in the simple Kundur's two-area power system model and the larger Nordic 45 test model.

In cases 1 to 5, the basic effects of providing FCR-D and FFR from an EV fleet in a power system was shown. In cases 6 to 10 however, some more intricate observations were made. Cases 7, 8 and 9 revolved around the inherent time delay of EVs, case 6 compared the use of distributed versus centralized reserves and case 10 was a realistic case where both FCR-D upwards and FFR were provided by EVs in the Nordic power system.

In case 6, the effect of using large centralized reserves (hydro-powered generators and industrial consumers) versus small distributed reserves (EV fleets) was analyzed, revealing an improved power flow when using the distributed EV fleets. However, as the centralized generators obtained a slightly higher frequency nadir, they barely outperformed the distributed EV fleets. In case 7, it was found that with no time delay, the EV fleets greatly outperformed the centralized reserves, highlighting its effect on the EVs' performance as providers of FCR-D upwards. In case 8, it was found that when using fast fault detection, which activates frequency reserves earlier, the EV fleets were able to barely outperform the centralized reserves as the effect of their time delay was reduced. In case 9, it was found that when there are low amounts of inertia in the power system, the effect of the time delay of the EVs is enhanced quite dramatically. In case 10, a realistic case with the provision of both FCR-D upwards and FFR in the Nordic power system was simulated, showing what a frequency response could look like if EVs with short time delays were used as providers of these services today.

Ultimately, from the work of this thesis, it can be concluded that using EVs as providers of FCR-D upwards is currently not a viable option. The reason for this is the inherent time delay of charging equipment and measurement devices, which according to the Parker project could be up to 5-6 seconds when including communication delays, or down to 3 seconds when controlling the car and charger directly [23]. Additionally, as shown in Case 9, when the amount of inertia in the power system decreases as the green transition moves forward, the importance of reducing the time delay also increases quite dramatically.

However, if the time delay of charging equipment and measurement devices is sufficiently reduced, making it possible to activate the frequency response of the EVs almost instantaneously after the occurrence of a fault, the EVs could potentially perform just as well as the hydro-powered generators, if not better.

It can similarly be concluded that the provision of FFR from EVs is not a viable option until the time delay is reduced. However, for the simulations of the provision of FFR in this thesis (cases 3-5 in particular), where the time delay was ignored, the EVs performed very well. It was found that one should probably provide long-support duration with a step-wise deactivation though, as this may be beneficial both for the

stability of the EPS and for the charging equipment and battery life of the EVs.

6.1 Further work

By updating and improving the grid topology of the Swedish, Finnish and Danish parts of the Nordic 45 test model, it would be possible to perform much more accurate simulations on the Nordic EPS. Additionally, by updating all line data and transformer data in the model, one could potentially achieve realistic power flows in the model when inserting generation and load data directly from Nordpool, allowing for live simulations performed on real-time data.

A study could certainly be performed on the development of a method for achieving fast fault detection as a way of counteracting the time delay of EVs. One could for example investigate whether or not the use of optical current transformers (CTs) could accurately measure the amplitude of the voltage fluctuations following a fault, making it possible to estimate the frequency nadir and thereby activate frequency reserves if needed. The CT could be placed as close to the EVs as possible, reducing the time delay of communication equipment. Other interesting ideas to investigate could be the use of quantum entanglement as a way of sending data at the speed of light, completely removing the time delay of communication equipment. Alternatively, one could try to come up with some mechanical device which is directly affected by the system frequency or voltage, removing the signal noise that comes with electric measuring equipment. Then, one would possibly not have to spend time filtering the frequency signal, making it possible to use the measured ROCOF as a signal for the activation of frequency reserves.

New technical requirements regarding the provision of FCR in the Nordic EPS will soon be published [18]. It could be interesting to check whether these new requirements affect the ability of EVs to provide FCR-D upwards.

Before using EVs as providers of FCR-D or FFR, it should probably be investigated how the provision of these services affects the battery life and charging equipment of an EV.

Ultimately, considering the fact that the inertia of power systems worldwide decreases as the green transition moves forward, it will be hard to ignore the enormous potential of the millions of rolling batteries in EVs as providers of frequency-stabilizing services. Therefore, performing further work on this subject could potentially improve the frequency stability of future power systems worldwide.

Bibliography

[1] *Statistikk elbil*, Dec. 2022. [Online]. Available: https://elbil.no/om-elbil/elbilstatistikk/.

[2] M. Teigenes, 'Primary frequency control in the nordic power system', Department of Electric Power Engineering, NTNU – Norwegian University of Science and Technology, Project report in TET4900, Dec. 2022.

[3] J. Shair, H. Li, J. Hu and X. Xie, 'Power system stability issues, classifications and research prospects in the context of high-penetration of renewables and power electronics', *Renewable and Sustainable Energy Reviews*, vol. 145, 2021, ISSN: 1364-0321. DOI: https://doi.org/10.1016/j.rser.2021.111111. [Online]. Available: https://www.sciencedirect.com/science/article/pii/S1364032121003993.

[4] T. Lee, *A Market for Primary Frequency Response? The Role of Renewables, Storage, and Demand*. Jun. 2018. [Online]. Available: https://kleinmanenergy.upenn.edu/paper/market-primary-frequency-response.

[5] K. Porter, *Measuring grid inertia accurately will enable more efficient frequency management*, en-GB, Sep. 2017. [Online]. Available: https://watt-logic.com/2017/10/12/inertia/ (visited on 3rd Jun. 2023).

[6] G. Ódor and B. Hartmann, *Power-law distributions of dynamic cascade failures in power-grid models*, May 2020. [Online]. Available: https://www.researchgate.net/publication/341231325_Power-law_distributions_of_dynamic_cascade_failures_in_power-grid_models.

[7] J. Machowski, Z. Lubosny, J. W. Bialek and J. R. Bumby, *Power System Dynamics: Stability and Control*, Third. John Wiley; Sons, Inc., 2020.

[8] P. Tumino, *Frequency control in a power system - technical articles*, Oct. 2020. [Online]. Available: https://eepower.com/technical-articles/frequency-control-in-a-power-system/#.

[9] *Fast frequency reserves - ffr*, Dec. 2022. [Online]. Available: https://www.statnett.no/for-aktorer-i-kraftbransjen/systemansvaret/kraftmarkedet/reservemarkeder/ffr/.

[10] *Fast frequency reserve – solution to the nordic inertia challenge*, Dec. 2019. [Online]. Available: https://www.statnett.no/globalassets/for-aktorer-i-kraftsystemet/utvikling-av-kraftsystemet/nordisk-frekvensstabilitet/ffr-stakeholder-report_13122019.pdf.

[11] *Nordic system operation agreement (soa) – annex load-frequency control & reserves (lfcr)*, Jan. 2022. [Online]. Available: https://eepublicdownloads.entsoe.eu/clean-documents/SOC%20documents/LFC/210624_Nordic_SOA_Annex_LFCR__version_4_approved_by_RGN.pdf.

[12] *Nordic synchronous area proposal for the dimensioning rules for fcr in accordance with article 153 of the commission regulation (eu) 2017/1485 of 2 august 2017 establishing a guideline on electricity transmission system operation*, May 2018. [Online]. Available: https://consultations.entsoe.eu/markets/nordic-tsos-proposals-for-frequency-quality-and-fc/supporting_documents/Nordic%20FCR%20dimensioning%20proposal.pdf.

[13] *Nordic system operation agreement (soa) – annex load-frequency control & reserves (lfcr) appendix 1: Regularly changing parameters 2023*, Nov. 2022. [Online]. Available: https://www.fingrid.fi/globalassets/dokumentit/fi/kantaverkko/sahkonsiirto/nordic-soa_appendix-1-to-annex-lfcr_regularly-changing-parameters_2023.pdf.

[14] R. Eriksson, N. Modig and K. Elkington, 'Synthetic inertia versus fast frequency response: A definition', *IET Renewable Power Generation*, vol. 12, Sep. 2017. DOI: 10.1049/iet-rpg.2017.0370.

[15] P. Denholm, T. Mai, R. W. Kenyon, B. Kroposki and M. O'Malley, *Inertia and the Power Grid: A Guide Without the Spin*, May 2020. [Online]. Available: https://www.nrel.gov/docs/fy20osti/73856.pdf.

[16] *Nordisk frekvensstabilitet*, Jun. 2022. [Online]. Available: https://www.statnett.no/for-aktorer-i-kraftbransjen/utvikling-av-kraftsystemet/prosjekter-og-tiltak/nordisk-frekvensstabilitet/.

[17] *Technical requirements for frequency containment reserve provision in the nordic synchronous area*, Jun. 2022. [Online]. Available: https://www.statnett.no/globalassets/for-aktorer-i-kraftsystemet/marked/reservemarkeder/fcr-technical-requirements-2022-06-27.pdf.

[18] *Primærreserver - FCR*, Apr. 2023. [Online]. Available: https://www.statnett.no/for-aktorer-i-kraftbransjen/systemansvaret/kraftmarkedet/reservemarkeder/primarreserver/ (visited on 3rd Jun. 2023).

[19] *Explanatory document for the amended nordic synchronous area methodology for additional properties of fcr in accordance with article 154(2) of the commission regulation (eu) 2017/1485 of 2 august 2017 establishing a guideline on electricity transmission system operation*, Feb. 2023. [Online]. Available: https://www.statnett.no/globalassets/for-aktorer-i-kraftsystemet/marked/reservemarkeder/fcr/explanatory-document-for-the-amended-nordic-synchronous-area-methodology-for-additional-properties-of-fcr.pdf.

[20] *Pilot for nye fcr-krav*, May 2021. [Online]. Available: https://www.statnett.no/for-aktorer-i-kraftbransjen/utvikling-av-kraftsystemet/prosjekter-og-tiltak/nordisk-frekvensstabilitet/pilot-for-nye-fcr-krav/.

[21] D. Thai, *Which electric cars have bidirectional charging (v2l, v2g, v2h)?*, Nov. 2022. [Online]. Available: https://zecar.com/resources/which-electric-cars-have-bidirectional-charging.

[22] *"bidirectional charging": This is how volkswagen wants to earn money by storing electricity*, Apr. 2021. [Online]. Available: https://www.handelsblatt.com/mobilitaet/elektromobilitaet/elektromobilitaet-bidirektionales-laden-so-will-volkswagen-am-speichern-von-strom-verdienen/27052182.html?ticket=ST-1932499-X1gulRmA6zm34i93qirA-cas01.example.org.

[23] P. B. Andersen, S. Hashemi Toghroljerdi, T. M. Sørensen, B. E. Christensen, J. C. M. L. Høj and A. Zecchino, 'The Parker Project: Final Report', Technical University of Denmark, Report, 2019, Publication Title: The Parker Project: Final Report. [Online]. Available: https://backend.orbit.dtu.dk/ws/portalfiles/portal/201164295/Parker_Final_report_v1.1_2019.pdf.

[24] *What is fast charging?* [Online]. Available: https://www.chademo.com/technology.

[25] *Ladestasjoner*, Apr. 2023. [Online]. Available: https://elbil.no/om-elbil/elbilstatistikk/ladestasjoner/.

[26] S. H. Jakobsen, L. Kalemba and E. H. Solvang, *The nordic 44 test network*, 2018. [Online]. Available: https://www.sintef.no/en/publications/publication/1701481/.

[27] E. Henningsson, H. Olsson and L. Vanfretti, 'Dae solvers for large-scale hybrid models', Feb. 2019, pp. 491–502. DOI: 10.3384/ecp19157491.

[28] S. M. Hamre, *Inertia and fcr in the present and future nordic power system - inertia compensation*, 2015. [Online]. Available: https://ntnuopen.ntnu.no/ntnu-xmlui/handle/11250/2368231.

[29] *Nettutviklingsplan 2021 - statnett*, Sep. 2021. [Online]. Available: https://www.statnett.no/globalassets/for-aktorer-i-kraftsystemet/planer-og-analyser/nup-2021/nettutviklingsplan_2021_samandrag.pdf.

[30] *Market data | nord pool*. [Online]. Available: https://www.nordpoolgroup.com/en/Market-data1/#/nordic/map.

[31] *Future system inertia 2*, Feb. 2018. [Online]. Available: https://www.statnett.no/globalassets/for-aktorer-i-kraftsystemet/utvikling-av-kraftsystemet/nordisk-frekvensstabilitet/future-system-inertia-phase-2.pdf.

[32] *Kinetic energy of the nordic power system - real time data - fingridin avoin data*. [Online]. Available: https://data.fingrid.fi/en/dataset/kinetic-energy-nordic-realtime.

[33] P. Kundur, *Power System Stability and control*. McGraw Hill, 1994.

[34] C. Konstantinou, 'A study on the impact of wind generation on the stability of electromechanical oscillations', Feb. 2015. [Online]. Available: https://www.researchgate.net/publication/271771513_A_Study_on_the_Impact_of_Wind_Generation_on_the_Stability_of_Electromechanical_Oscillations.

[35] *Requirement for minimum inertia in the nordic power system*, Jun. 2021. [Online]. Available: https://www.epressi.com/media/userfiles/151043/1634122821/requirement-for-minimum-inertia-in-the-nordic-power-system.pdf.

[36] *Ol3 production*, 2023. [Online]. Available: https://www.tvo.fi/en/index/production/plantunits/ol3/ol3production.html.

[37] *Statnett - nvf 2022*, Jul. 2022. [Online]. Available: https://www.statnett.no/globalassets/for-aktorer-i-kraftsystemet/systemansvaret/retningslinjer-fos/systemansvaret---vedlegg-til-retningslinjer-fos--14---nvf.pdf.

[38] *Appendix 1: Technical product and interface specification for delivery of automatic frequency restoration reserves (afrr) to statnett*, Sep. 2021. [Online]. Available: https://www.statnett.no/contentassets/7baf5f39abcc4e6288e9c505741620de/technical-product-and-interface-specification-for-delivery-of-afrr-to-statnett.pdf.

A K2A Model Data - Base Version

Generator data

Each generator has a rating of 900MVA and 20kV.

$X_d = 1.8$ $X_q = 1.7$ $X_l = 0.2$ $X'_d = 0.3$ $X'_q = 0.55$
$X''_d = 0.25$ $X''_q = 0.25$ $R_a = 0.0025$ $T'_{d0} = 8.0$ s $T'_{q0} = 0.4$ s
$T''_{d0} = 0.03$ s $T''_{q0} = 0.05$ s $A_{Sat} = 0.015$ $B_{Sat} = 9.6$ $\psi_{T1} = 0.9$
$H = 6.5$ (for G1 and G2) $H = 6.175$ (for G3 and G4) $K_D = 0$

Figure 46: Generator data in p.u. [33]

The generators have the following base case production scheme:

Table 14: Generator production

Generator	Area	P [MW]	Q [MVAr]
G1	1	700	185
G2	1	700	235
G3	2	719	176
G4	2	700	202

Load data

Table 15: Load data

Load	Area	P [MW]	Q_L [MVAr]	Q_C [MVAr]
L7	1	967	100	200
L9	2	1767	100	350

Transformer data

Table 16: Transformer data

Transformer	From bus	To bus	S_n	$V_{n\ from}$	$V_{n\ to}$	R	X
T1	B1	B5	900	20	230	0	0.15
T2	B2	B6	900	20	230	0	0.15
T3	B3	B11	900	20	230	0	0.15
T4	B4	B10	900	20	230	0	0.15

Line data

Table 17: Line data

Line	From bus	To bus	length	S_n	V_n	unit	R	X	B
L5-6	B5	B6	25	100	230	p.u.	0.0001	0.001	0.00175
L6-7	B6	B7	10	100	230	p.u.	0.0001	0.001	0.00175
L7-8-1	B7	B8	110	100	230	p.u.	0.0001	0.001	0.00175
L7-8-2	B7	B8	110	100	230	p.u.	0.0001	0.001	0.00175
L8-9-1	B8	B9	110	100	230	p.u.	0.0001	0.001	0.00175
L8-9-2	B8	B9	110	100	230	p.u.	0.0001	0.001	0.00175
L9-10	B9	B10	10	100	230	p.u.	0.0001	0.001	0.00175
L10-11	B10	B11	25	100	230	p.u.	0.0001	0.001	0.00175

B K2A Model Data - Modified Version

Generator data

Each generator has a rating of 720MVA and 20kV.

$X_d = 1.8$ $X_q = 1.7$ $X_l = 0.2$ $X'_d = 0.3$ $X'_q = 0.55$
$X''_d = 0.25$ $X''_q = 0.25$ $R_a = 0.0025$ $T'_{d0} = 8.0$ s $T'_{q0} = 0.4$ s
$T''_{d0} = 0.03$ s $T''_{q0} = 0.05$ s $A_{Sat} = 0.015$ $B_{Sat} = 9.6$ $\psi_{T1} = 0.9$
$H = 6.5$ (for G1 and G2) $H = 6.175$ (for G3 and G4) $K_D = 0$

Figure 47: Generator data in p.u. [33]

The generators have the following base case production scheme:

Table 18: Generator production

Generator	Area	P [MW]	Q [MVAr]
G1	1	560	185
G2	1	560	235
G3	2	575	176
G4	2	560	202

Load data

Table 19: Load data

Load	Area	P [MW]	Q_L [MVAr]	Q_C [MVAr]
L7	1	967	100	200
L9	2	1767	100	350

Transformer data

Table 20: Transformer data

Transformer	From bus	To bus	S_n	$V_{n\ from}$	$V_{n\ to}$	R	X
T1	B1	B5	720	20	230	0	0.15
T2	B2	B6	720	20	230	0	0.15
T3	B3	B11	720	20	230	0	0.15
T4	B4	B10	720	20	230	0	0.15
T5	$B6_{EV}$	B6	720	20	230	0	0.15
T6	$B10_{EV}$	B10	720	20	230	0	0.15

Line data

Table 21: Line data

Line	From bus	To bus	length	S_n	V_n	unit	R	X	B
L5-6	B5	B6	25	100	230	p.u.	0.0001	0.001	0.00175
L6-7	B6	B7	10	100	230	p.u.	0.0001	0.001	0.00175
L7-8-1	B7	B8	50	100	230	p.u.	0.0001	0.001	0.00175
L7-8-2	B7	B8	50	100	230	p.u.	0.0001	0.001	0.00175
L8-9-1	B8	B9	50	100	230	p.u.	0.0001	0.001	0.00175
L8-9-2	B8	B9	50	100	230	p.u.	0.0001	0.001	0.00175
L9-10	B9	B10	10	100	230	p.u.	0.0001	0.001	0.00175
L10-11	B10	B11	25	100	230	p.u.	0.0001	0.001	0.00175

C Nordic 45 Model Data - Base Case Scenario

The base case scenario is taken from 01.06.2022 between 11:00AM and 12:00PM.

Table 22: Production, net export and consumption in scenario 1

[MW]	NO1	NO2	NO3	NO4	NO5	SE1	SE2	SE3	SE4	FI
Production	1929	5218	3703	3152	3914	3680	5840	7243	859	6787
Net Export	-1357	1421	610	906	2157	2596	4238	-2108	-1680	-1111
Consumption	3286	3797	3093	2246	1757	1084	1602	9351	2539	7898

Generators:

Table 23: Overview of generators in the Norwegian part of N45

Description	Area	Generator	Bus	P [MW]
Oslo	NO1	G5120-1	5120	964.50
Oslo	NO1	G5120-2	5120	964.50
Tonstad	NO2	G5230-1	5230	870.00
Tonstad	NO2	G5230-2	5230	870.00
Kvilldal/Holen	NO2	G5240-1	5240	870.00
Kvilldal/Holen	NO2	G5240-2	5240	870.00
Kvilldal/Holen	NO2	G5240-3	5240	870.00
Sauda	NO2	G5250-1	5250	870.00
Sunnmøre	NO3	G5310-1	5310	925.75
Trondheim	NO3	G5320-1	5320	925.75
Trondheim	NO3	G5320-2	5320	925.75
Trondheim	NO3	G5320-3	5320	925.75
Nedre Røssåga	NO4	G5420-1	5420	1050.67
Nedre Røssåga	NO4	G5420-2	5420	1050.67
Nedre Røssåga	NO4	G5420-3	5420	1050.67
Samnanger	NO5	G5510-1	5510	652.33
Samnanger	NO5	G5510-2	5510	652.33
Sima	NO5	G5520-1	5520	652.33
Sima	NO5	G5520-2	5520	652.33
Indre Sogn	NO5	G5551-1	5551	652.33
Bergen	NO5	G5560-1	5560	652.33

Loads:

Table 24: Overview of loads in the Norwegian part of N45

Description	Area	Load	Bus	P [MW]	Q [MW]
Oslo	NO1	L5120-1	5120	1046	25
Oslo	N01	L5120-2	5120	1095	25
Oslo	NO1	L5120-3	5120	1095	25
Skagerrak 1-4	NO2	L5210-1	5210	990	50
Kristiansand	NO2	L5210-2	5210	1099	50
NorNed	NO2	L5220-1	5220	0	0
NordLink	NO2	L5230-1	5230	1436	50
Stavanger	NO2	L5231-1	5231	1099	50
North Sea Link	NO2	L5240-1	5240	637	50
Kvilldal/Holen	NO2	L5240-2	5240	1099	50
Kårstø	NO2	L5270-1	5370	461	50
Sunnmøre	NO3	L5310-1	5310	779	250
Trondheim	NO3	L5320-1	5320	773	250
Trondheim	NO3	L5320-2	5320	773	250
Nyhamna	NO3	L5321-1	5321	773	250
Nedre Røssåga	NO4	L5420-1	5420	749	50
Ofoten	NO4	L5430-1	5430	627	50
Hammerfest	NO4	L5431-1	5431	749	50
Indre Vestland	NO5	L5530-1	5530	500	100
Bergen	NO5	L5560-1	5560	615	400
Bergen	NO5	L5560-2	5560	629	400

D Supplementary results

D.1 K2A

D.1.1 Case 1 - FCR-D without time delay

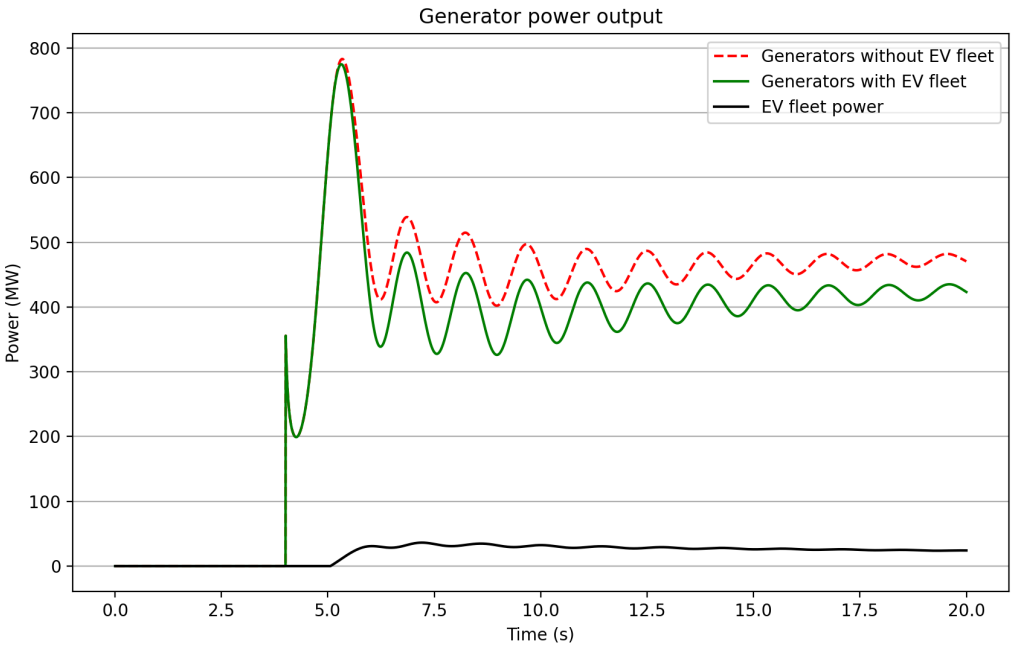

Figure 48: Scenario 1 - Power generation

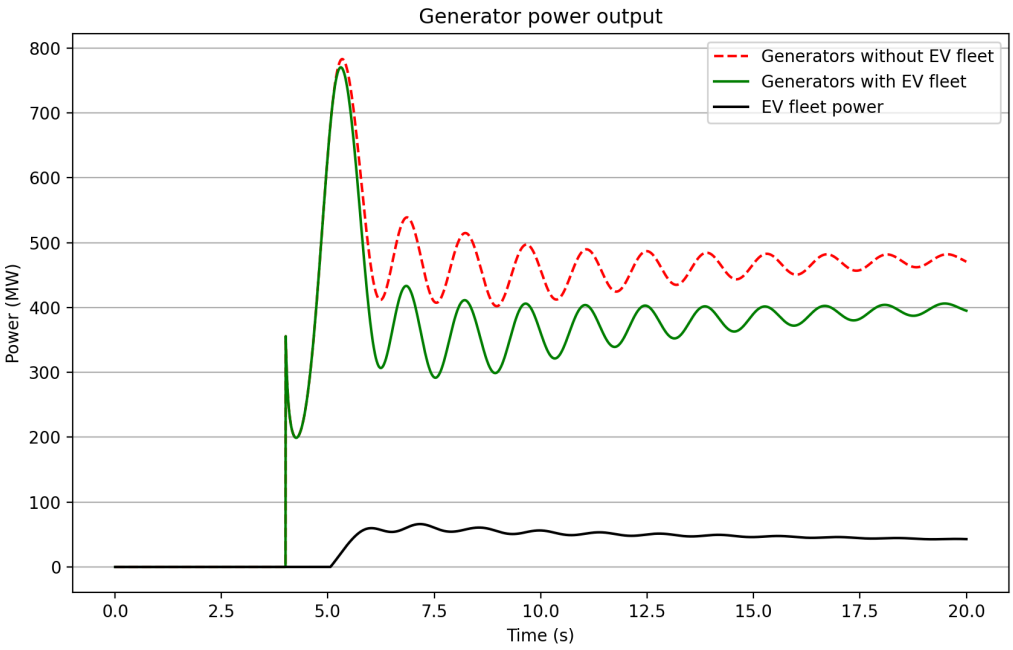

Figure 49: Scenario 3 - Power generation

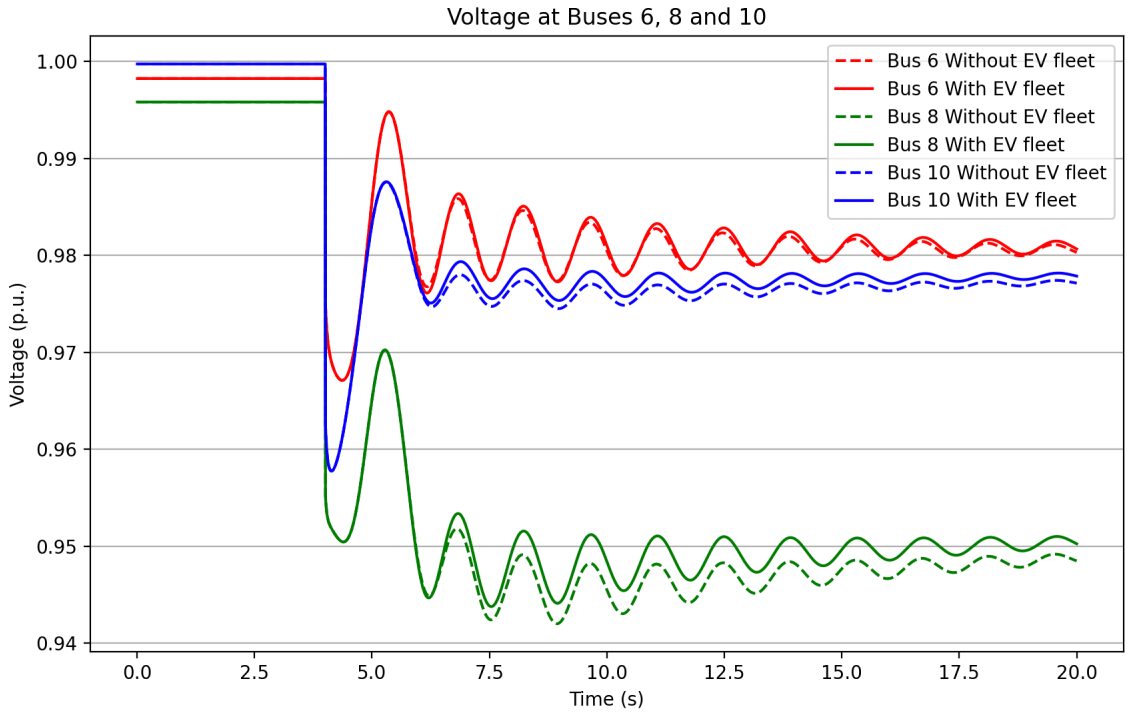

Figure 50: Scenario 1 - Voltage magnitudes

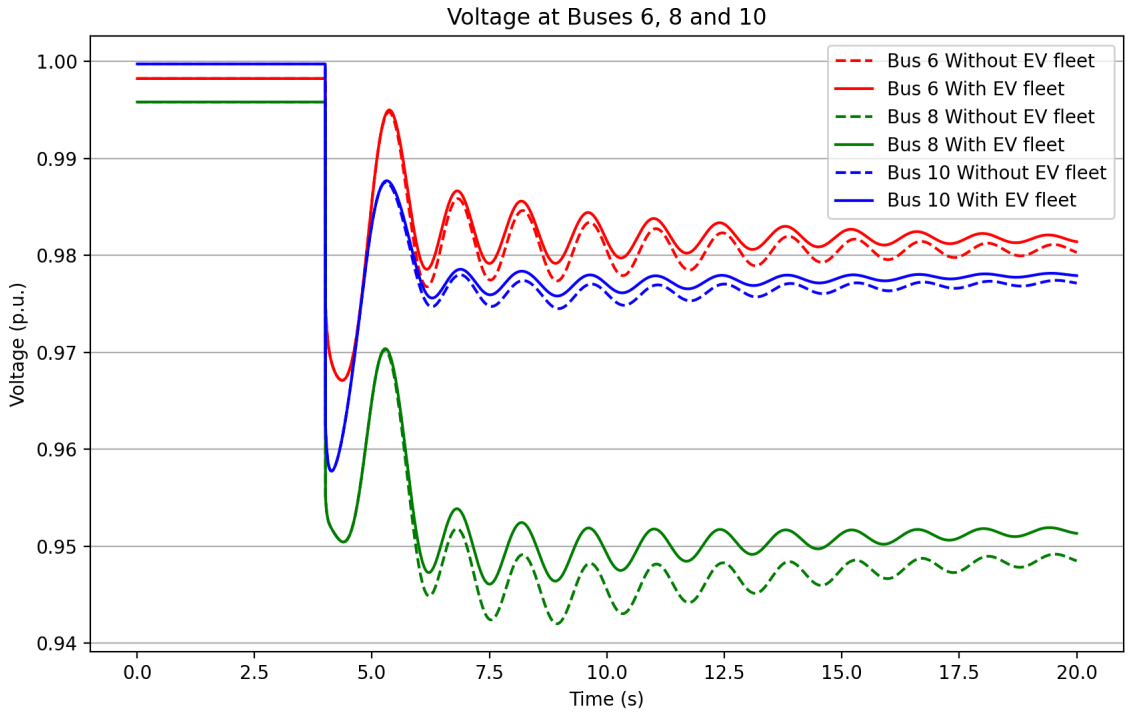

Figure 51: Scenario 2 - Voltage magnitudes

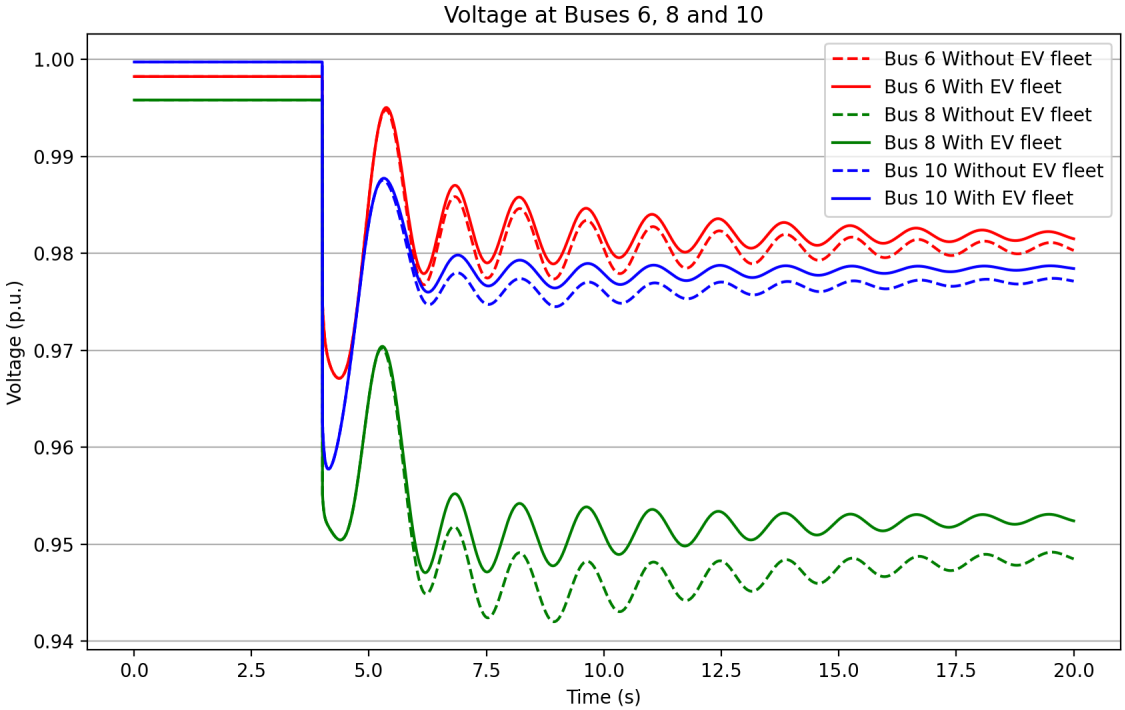

Figure 52: Scenario 3 - Voltage magnitudes

D.1.2 Case 2 - FCR-D with time delay

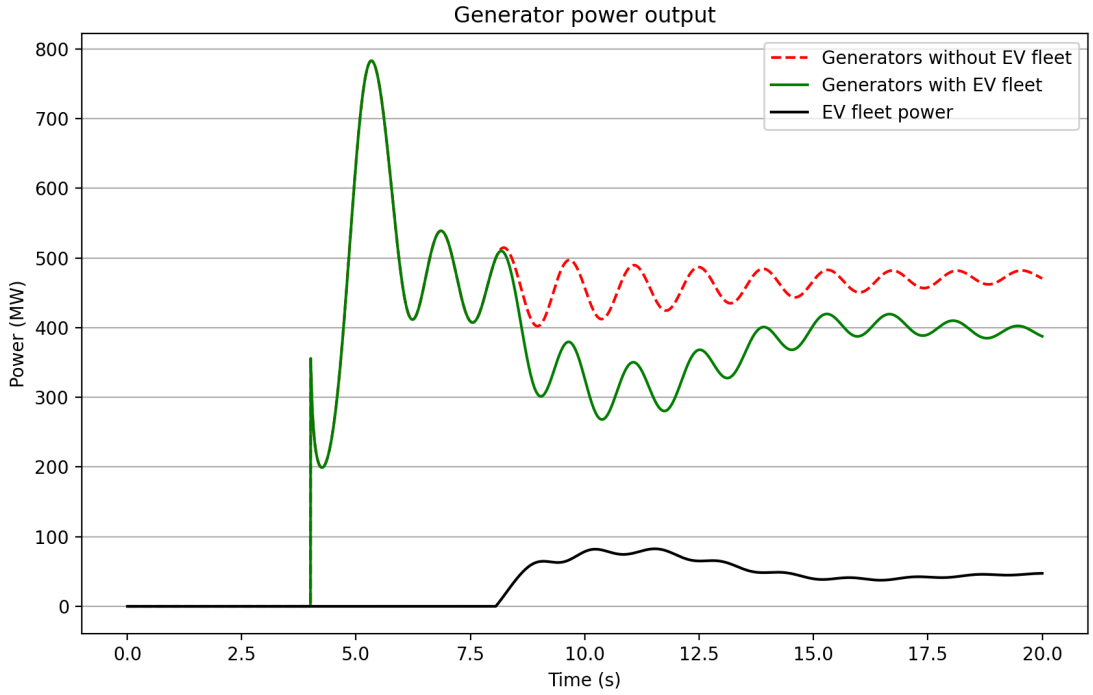

Figure 53: Scenario 3 - Power generation

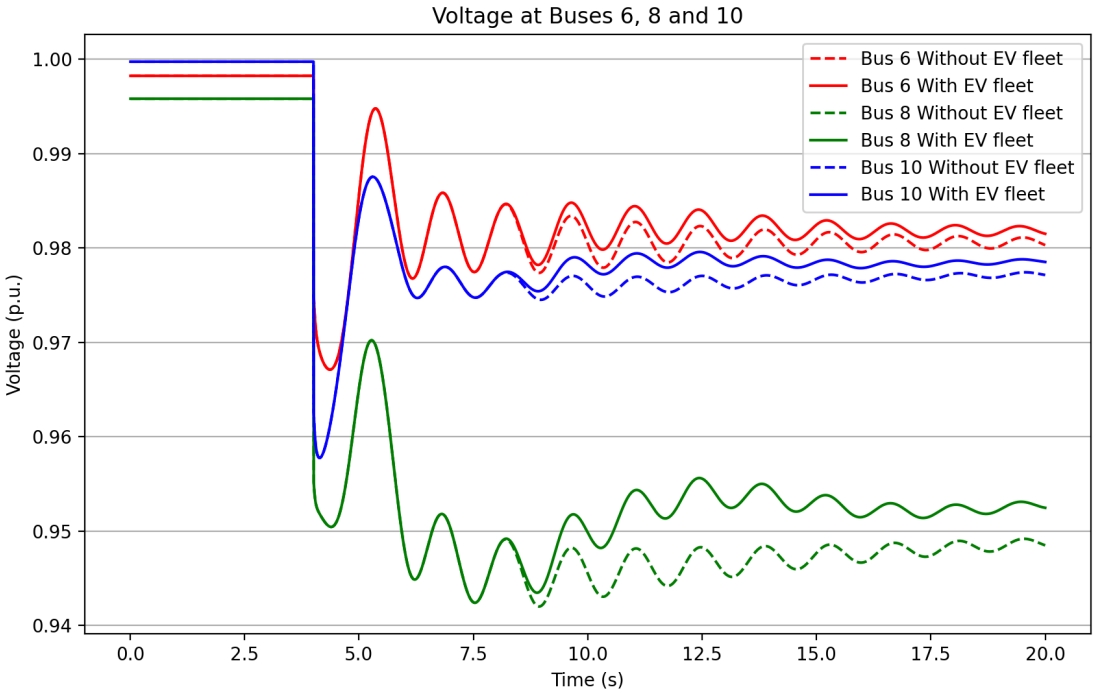

Figure 54: Scenario 3 - Voltage magnitudes

D.1.3 Case 3 - FFR with short deactivation time

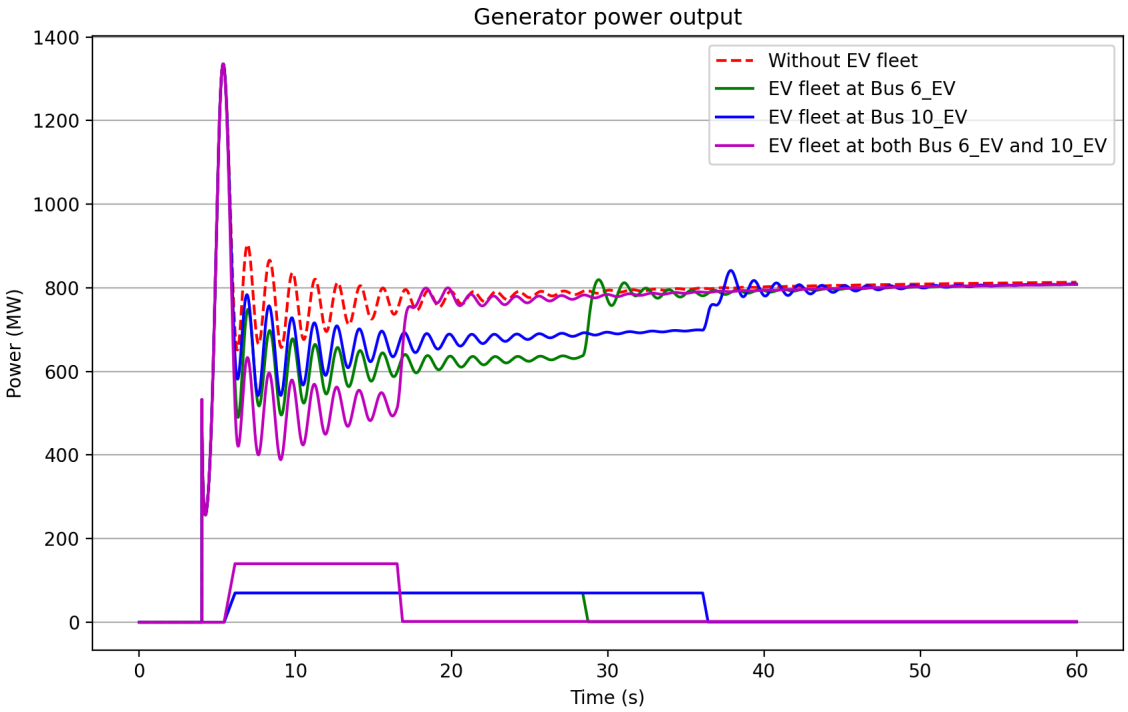

Figure 55: All scenarios - Power generation

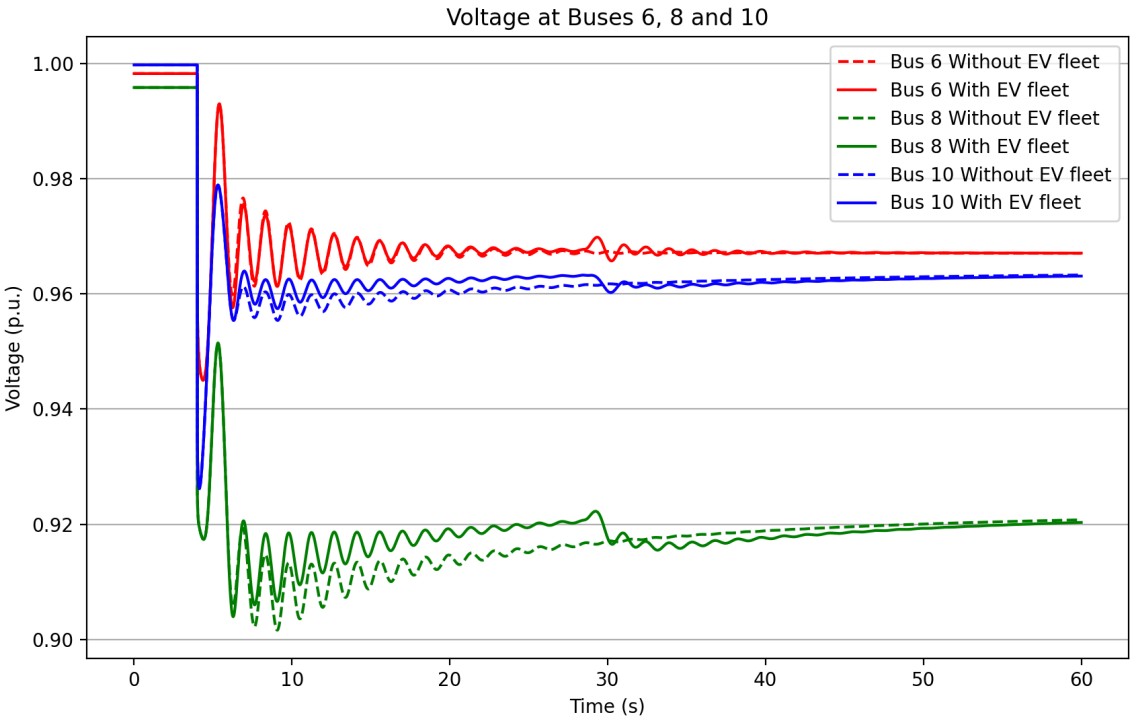

Figure 56: Scenario 1 - Voltage magnitudes

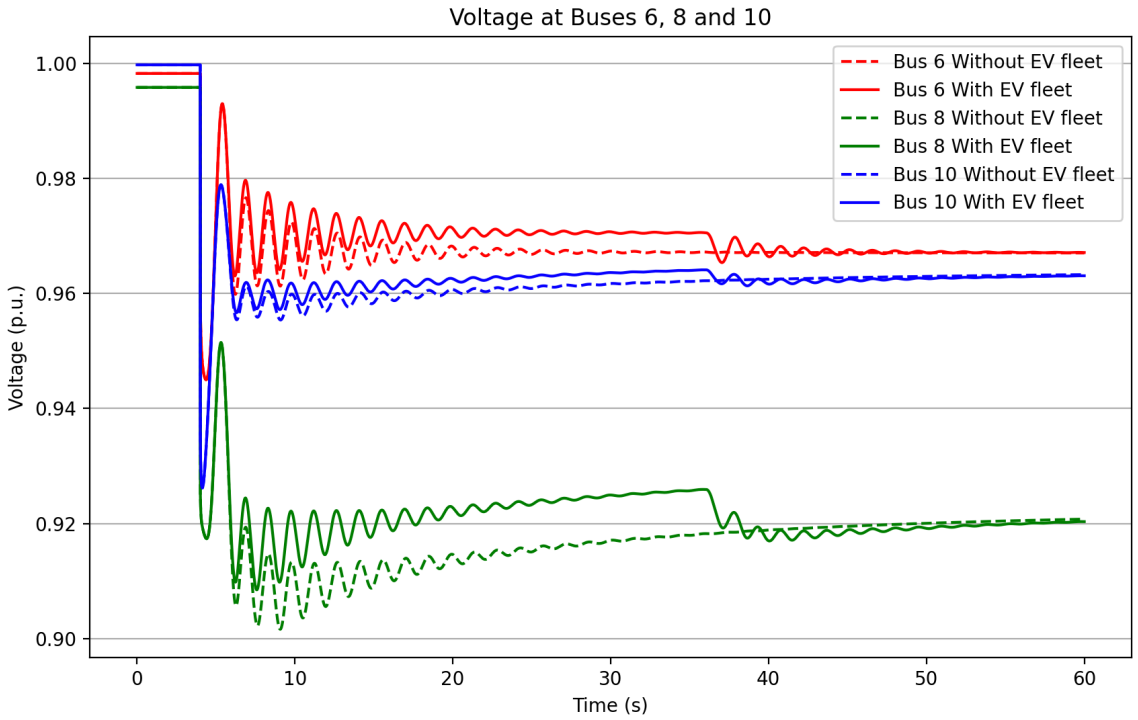

Figure 57: Scenario 2 - Voltage magnitudes

D.1.4 Case 5 - FFR with step-wise deactivation

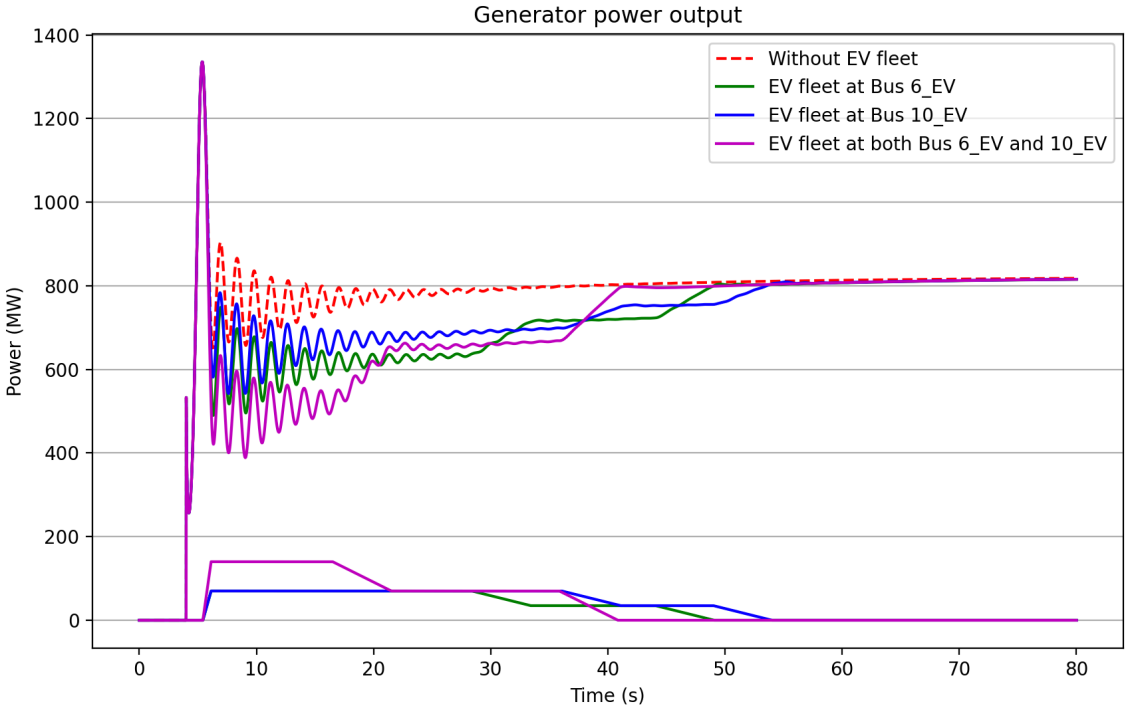

Figure 58: All scenarios - Power generation (New control function)

D.2 N45

D.2.1 Case 6 – Effect of centralized vs. distributed reserves

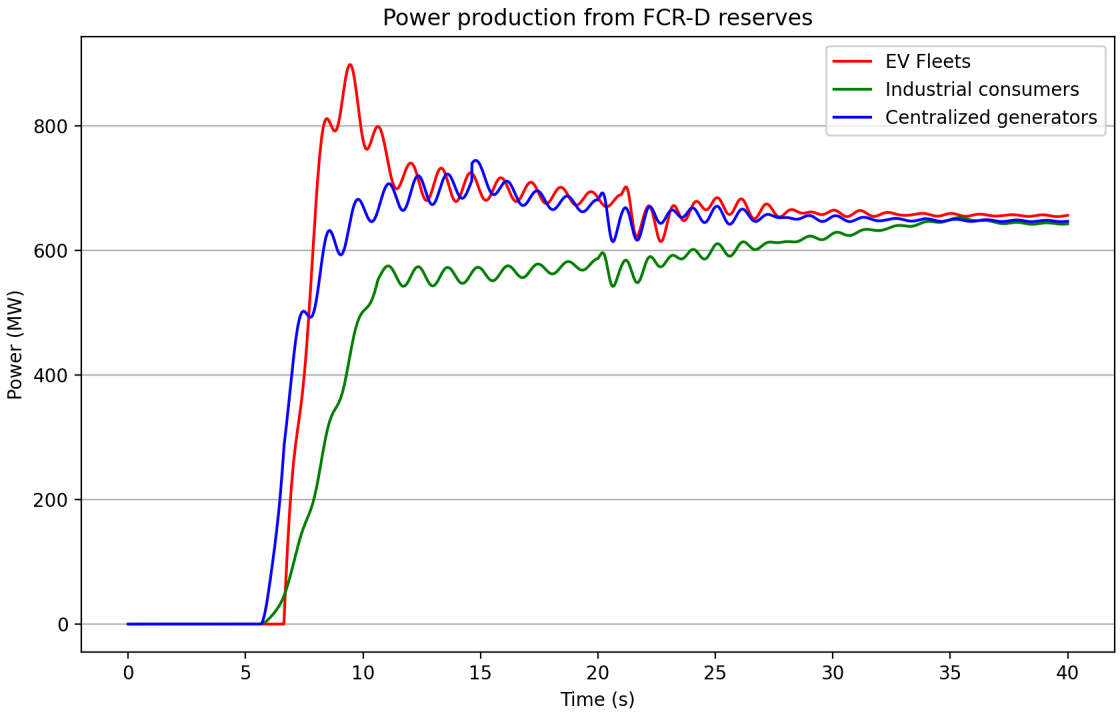

Figure 59: Power response

D.2.2 Case 8 - Using fast fault detection to counteract time delay of EV fleets

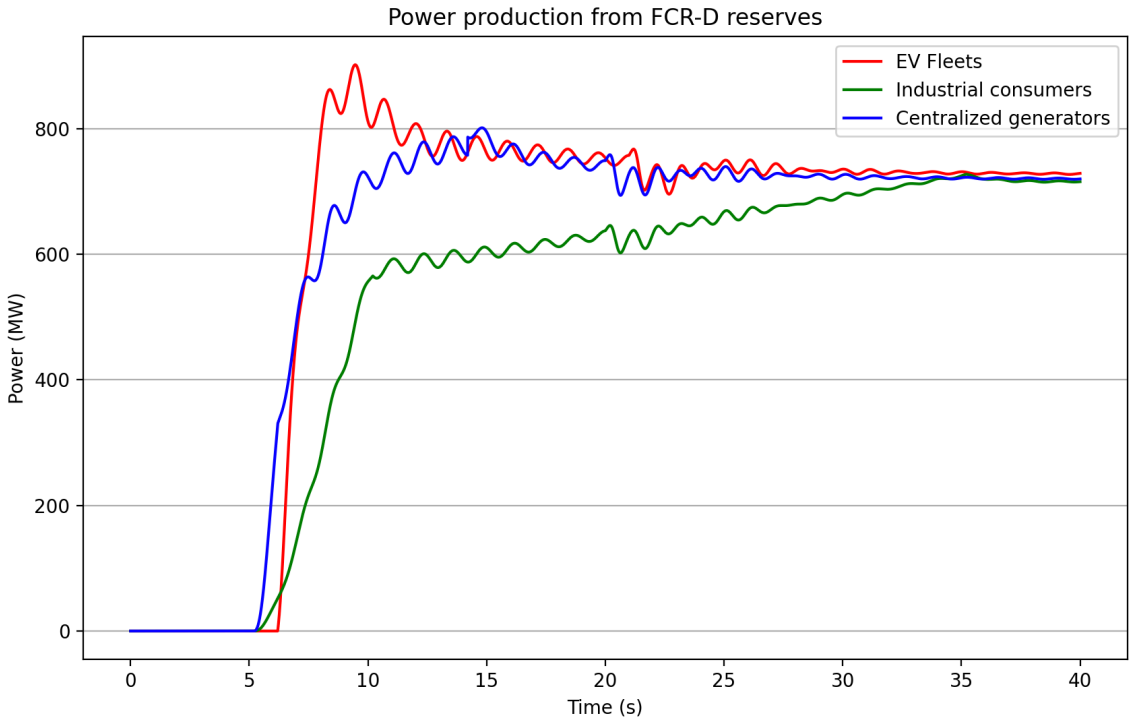

Figure 60: Power response (with fast fault detection)

D.2.3 Case 10 - Realistic case with provision of FCR-D and FFR in the Nordic power system using EVs

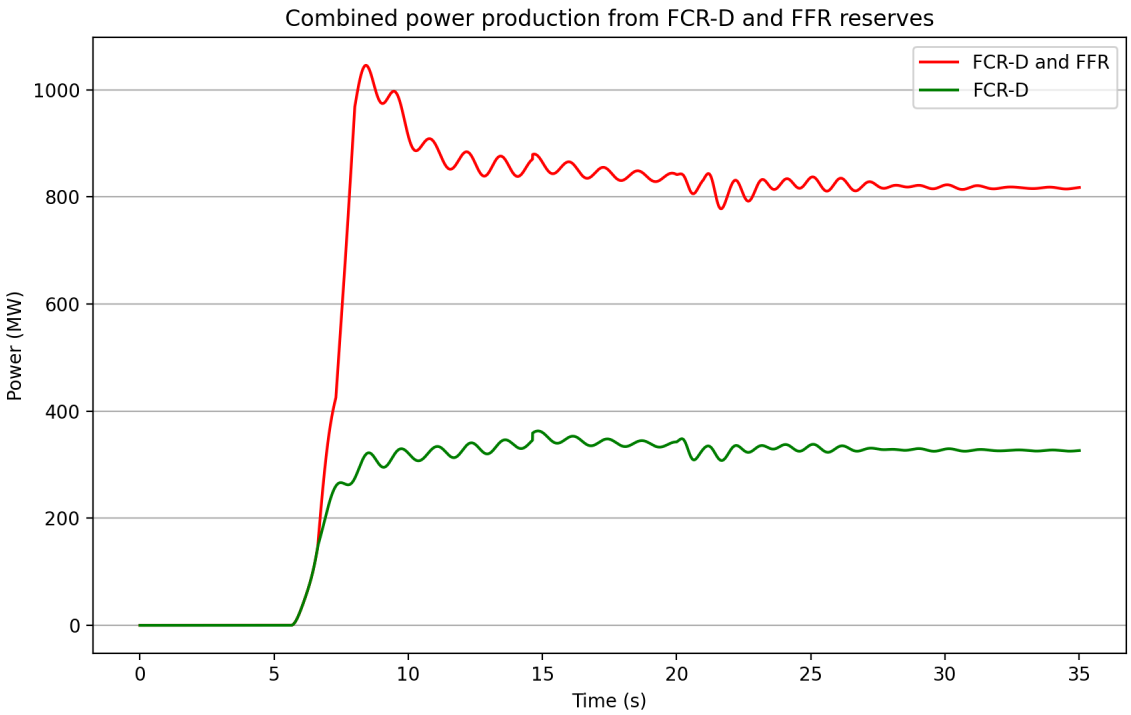

Figure 61: Power response

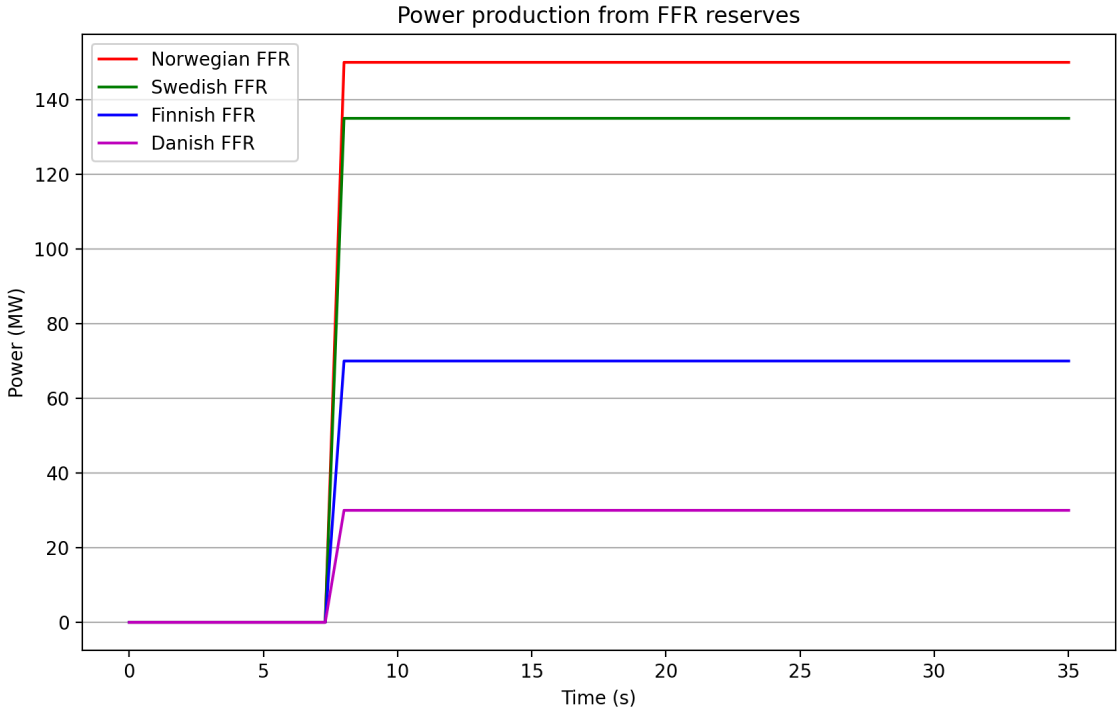

Figure 62: Power response of FFR reserves

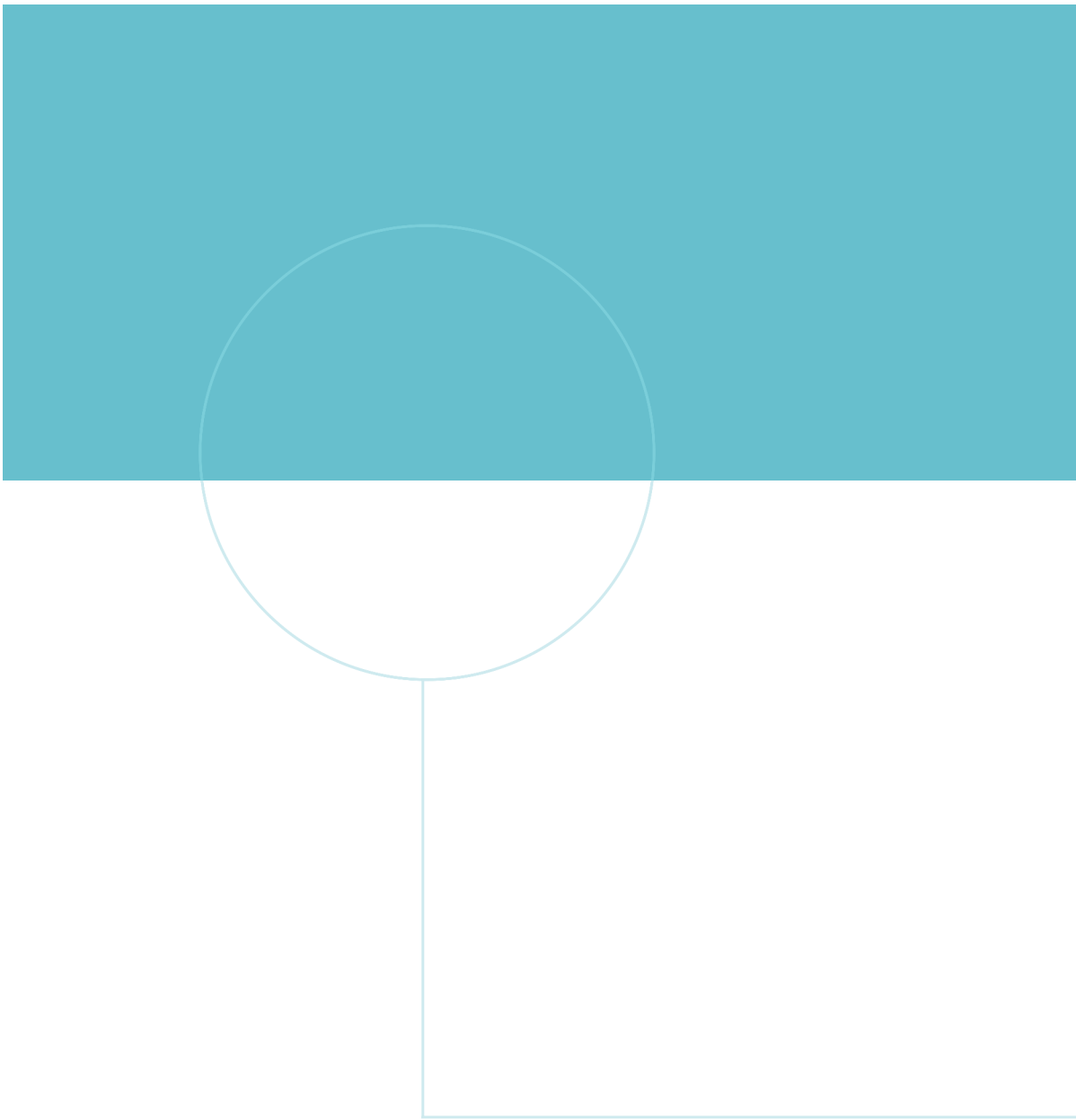

NTNU

Norwegian University of
Science and Technology